

A11101 725912

NAT'L INST OF STANDARDS & TECH R.I.C.



A11101725912

Larson, Wilbur/The rotary-vane attenuato  
QC100 .U556 V144;1975 C.2 NBS-PUB-R 1975

REFERENCE



NBS MONOGRAPH 144

U.S. DEPARTMENT OF COMMERCE/National Bureau of Standards

# The Rotary-Vane Attenuator as an Interlaboratory Standard

QC

100

.U556

no.144

1975







# The Rotary-Vane Attenuator as an Interlaboratory Standard

---

*to Monograph no. 144.*

Wilbur Larson

Institute for Basic Standards  
National Bureau of Standards  
Boulder, Colorado 80302

JAN 27 1976  
761546-Ref  
QC100  
.U556  
no.144  
1975



---

U.S. DEPARTMENT OF COMMERCE, Rogers C. B. Morton, Secretary

James A. Baker, III, Under Secretary

Dr. Betsy Ancker-Johnson, Assistant Secretary for Science and Technology

U.S. NATIONAL BUREAU OF STANDARDS, Ernest Ambler, Acting Director

Issued November 1975

**Library of Congress Cataloging in Publication Data**

Larson, Wilbur.

The Rotary-Vane Attenuator as an Interlaboratory Standard.

(National Bureau of Standards Monograph; 144)

Bibliography: p.

1. Attenuators, Rotary-Vane. 2. Microwave Measurements. I.

Title. II. Series: United States. National Bureau of Standards. Monograph; 144.

QC100.U556 No. 144 [TK7871.65]

389'.08s [621.381'37]  
75-619099

**National Bureau of Standards Monograph 144**

Nat. Bur. Stand. (U.S.), Monogr. 144, 70 pages (Nov. 1975)

CODEN: NBSMA6

U.S. GOVERNMENT PRINTING OFFICE  
WASHINGTON: 1975

---

For sale by the Superintendent of Documents, U.S. Government Printing Office, Washington, D.C. 20402  
(Order by SD Catalog No. C13.44:149). Price \$5.05. (Add 25 percent additional for other than U.S. mailing)  
Stock Number 003-003-01416-8



# Contents

	Page		Page
1. Introduction.....	1	7.1.2. Angular resettability of attenuator.....	25
2. Theory of operation.....	1	7.2. Mounting the gear drive.....	25
2.1. Zero setting.....	2	7.3. Optical rotary-vane attenuator.....	26
2.2. Stator alignment.....	2	7.3.1. Measurements on optical rotary-vane attenuator.....	26
2.3. Transmission error or insufficient attenuation in the rotor.....	4	7.3.2. Measurement after rotor repair.....	27
3. Dial readout of rotary-vane attenuator.....	5	8. Resolution and resettability.....	27
4. The measurement of the rotary-vane attenuator by different methods.....	8	9. Resolution of rotary-vane attenuator in percent of dial setting.....	28
4.1. NBS developed attenuation systems.....	8	10. Frequency sensitivity of the rotary-vane attenuator.....	28
4.2. Comparison of modulated sub-carrier and dc substitution methods.....	10	10.1. Spectrum of microwave attenuation calibration systems 2.6 to 40 GHz.....	29
4.3. Comparison of modulated sub-carrier and <i>i-f</i> substitution methods.....	10	10.2. Statistical analysis of the frequency sensitivity from calibration data at 30, 40, and 50 dB.....	33
4.4. Simultaneous measurement by modulated sub-carrier and dc substitution methods.....	11	10.3. Frequency sensitivity of rotary-vane attenuators for eight waveguide frequency ranges.....	35
4.5. Measurement of precision optical rotary-vane attenuator by dc and <i>i-f</i> substitution methods.....	11	11. Evaluation of the rotary-vane attenuator by "bootstrapping" and check standards.....	35
4.6. Power ratio (dc) versus off-null measurements.....	11	11.1. Errors in attenuation for the initial and the final setting of the rotary-vane attenuator for an attenuation difference measurement.....	36
5. Procedures for evaluating the rotary-vane attenuator.....	14	11.2. Graphical presentation.....	36
5.1. Determination of average vane angle error and eccentricity from calibration data.....	15	11.2.1. Deviations in attenuation due to rotor-vane alignment error.....	36
5.1.1. Analysis of calibration data.....	15	11.2.2. Attenuation versus $\theta$ in degrees.....	36
5.1.2. Cyclic pattern of angular displacement.....	15	11.2.3. $\epsilon'_0$ and $\epsilon'_l$ versus dial setting (in degrees and decibels).....	38
5.2. Gearing errors related to rotary-vane attenuator.....	16	11.2.4. Minimal value of $\epsilon'$ .....	38
5.2.1. Effects of $\alpha$ on $\epsilon\gamma'$ .....	17	12. Evaluation of precision rotary-vane attenuator with waveguide fixed-step attenuator.....	40
5.2.2. Effects of pitch diameter on error of attenuation... ..	19	13. Attenuation measurement with the rotary-vane attenuator as the standard.....	40
6. Compensation for transmission error of rotary-vane attenuator.....	21	13.1. Introduction.....	40
6.1. Transmission error versus dial setting in decibels.....	21	13.2. The Measurement system.....	40
6.2. Stator realignment.....	21	13.3. Errors of microwave measurement system.....	42
6.3. Illustration of transmission error and compensation for 110-dB maximum.....	22	13.3.1. Systematic and random errors.....	42
6.4. Mechanical compensation and measured results.....	24	13.3.2. Insertion point of the device under test.....	42
7. Measurement of precision rotary-vane attenuators with high resolution readouts.....	24		
7.1. Measurement of rotary-vane attenuator with a gear driven readout.....	24		
7.1.1. Measurements of precision gear driven rotary-vane attenuator.....	25		

13.3.3. Mismatch error in attenuation measurement.....	42
13.4. External leakage.....	44
14. Conclusion.....	50

15. References.....	50
16. Appendices	
A. Definitions and Terms.....	51
B. Machine Drawings for Optical Rotary-Vane Attenuators.....	51

## List of Figures

Figure 1. Pictorial diagram of the rotary-vane attenuator .....	1	Figure 15. Illustrated deviation of the rotor vane of an attenuator calibrated by different methods: power ratio (1960), off-null, and power ratio (1968) .....	13
Figure 2. Illustration of the determination of $b'$ with measured distances $b_1$ and $b_2$ from the reference plane as viewed from the rectangular waveguide input flange .....	3	Figure 16. Apparent deviation of rotor vane in degrees from nominal at each dial setting in degrees. The indicated vane angle correction has been applied to each result ..	13
Figure 3. Rotor index or zero coincident with first (or second) stator .....	3	Figure 17. Graphs of deviations in attenuation from nominal versus dial setting in decibels and degrees.	
Figure 4. Rotor index or zero coincident with average position of stators ..	3	a. Measured deviation (circles) and computed deviation for $+0.064^\circ$ vane-angle error ..	16
Figure 5. Type <i>B</i> alignment: first attenuation maximum, $M_1$ , at $\theta'/2$ prior to $90^\circ$ ; saddle minimum, $M_s$ , at $90^\circ$ ; and second maximum, $M_2$ , at $\theta/2$ beyond $90^\circ$ .....	4	b. Measured values after applying $-0.064^\circ$ vane angle correction .....	16
Figure 6. Type <i>A</i> alignment, rotor advanced to $\theta'/2$ : first attenuation maximum, $M_1$ , at $90^\circ - \theta'$ ; saddle minimum, $M_s$ , at $90^\circ - \theta'/2$ ; and the second maximum, $M_2$ , at $90^\circ$ .....	4	Figure 18. Graphs of the cyclic pattern of angular displacement curve, $\theta'_r$ , with average vane-angle error of $+0.064^\circ$ and $\theta'_r$ with $-0.064^\circ$ correction .....	16
Figure 7. Type <i>A</i> alignment, rotor retarded: first attenuation maximum, $M_1$ , at $90^\circ$ ; saddle minimum, $M_s$ , at $90^\circ + \theta'/2$ ; and the second maximum at $90^\circ + \theta'$ .....	4	Figure 19. Variations in gear eccentricity error .....	17
Figure 8. Rotary-vane attenuator dial readout in decibels—spiral—3 cycle ..	5	Figure 20. Attenuation as a function of vane angle, variation in the indexing error for the three cycles, and the error in attenuation from nominal for the dial settings of 0 to $90^\circ$ .....	17
Figure 9. Rotary-vane attenuator dial readout in decibels—cylindrical—6 cycle .....	6	Figure 21. Errors in attenuation at the dial setting of 10 dB versus the angle $\alpha$ for different pitch diameters ..	18
Figure 10. Rotary-vane attenuator dial readout in decibels—cylindrical—9 cycle .....	6	Figure 22. Errors in attenuation at the dial setting of 20 dB versus the angle $\alpha$ for different pitch diameters ..	18
Figure 11. Graph of the deviation in attenuation from nominal versus dial setting in degrees which corresponds to a linear deviation of $0.020''$ for three rotary-vane attenuators .....	6	Figure 23. Errors in attenuation at the dial setting of 30 dB versus the angle $\alpha$ for different pitch diameters ..	18
Figure 12. Dial readout in units, tenths, hundredths and thousandths of degrees for rotary-vane attenuator .....	7	Figure 24. Errors in attenuation at the dial setting of 40 dB versus the angle $\alpha$ for different pitch diameters ..	18
Figure 13. Pictorial view of drive unit for rotary-vane attenuator .....	8	Figure 25. Errors in attenuation at the dial setting of 50 dB versus the angle $\alpha$ for different pitch diameters ..	19
Figure 14. Machine drawing of drive unit gearing for rotary-vane attenuator .....	9	Figure 26. Errors in attenuation at the dial setting of 10 dB versus pitch	



	diameter for the angular displacement error.....	19		after precise machining was applied .....	26
Figure 27.	Errors in attenuation at the dial setting of 20 dB versus pitch diameter for the angular displacement error.....	20	Figure 39.	Deviation in decibels and degrees versus dial setting in degrees.....	26
Figure 28.	Errors in attenuation at the dial setting of 30 dB versus pitch diameter for the angular displacement error.....	20	Figure 40.	Deviation in decibels and degrees versus dial setting in degrees, after repair of the rotor section..	27
Figure 29.	Errors in attenuation at the dial setting of 40 dB versus pitch diameter for the angular displacement error.....	20	Figure 41.	(a) Deviation of measured attenuation and equivalent angular deviation from theoretical values for a vane angle correction of $-0.033^\circ$ versus dial setting of 0 to $45^\circ$ .....	27
Figure 30.	Errors in attenuation at the dial setting of 50 dB versus pitch diameter for the angular displacement error.....	20		(b) Deviation of measured attenuation and equivalent angular deviation from theoretical values for a vane angle correction of $-0.033^\circ$ versus dial setting of 45 to $87.5^\circ$ .....	27
Figure 31.	Estimate of the transmission error versus dial setting in decibels for maximum attenuation values of 60 to 160 dB .....	21	Figure 42.	Resolution error in decibels versus dial setting in decibels.....	28
Figure 32.	Illustration of stator rotation and rotor alignment to induce the type <i>B</i> error .....	21	Figure 43.	Resolution of the dial in percent of attenuation versus dial setting in decibels for an attenuator with angular resolution of $0.01^\circ$ .....	28
Figure 33.	Estimated angular displacement of stators in degrees versus the maximum attenuation value of rotor vane in decibels for the compensation required to approach theoretical $\cos^2 \theta$ law.....	22	Figure 44.	Deviation of attenuation for average vane-angle errors of 0.098, 0.080, and $0.036^\circ$ versus dial setting in decibels at 9.0, 9.8, and 11.2 GHz .....	29
Figure 34.	Deviation in attenuation caused by misalignment of the stators, $\theta'$ equals $0.2^\circ$ , and insufficient maximum attenuation of 110 dB for the dial setting of 20 to 70 dB .....	23	Figure 45.	Deviation of attenuation for average vane-angle errors of $-0.032$ , $-0.042$ and $-0.054^\circ$ versus dial setting in decibels at 9.0, 9.8, and 11.2 GHz .....	30
Figure 35.	Deviation of attenuation from nominal versus dial setting in decibels for rotary-vane attenuator with 72-dB maximum: (a) Curve of calibration points, (b) Curve of correction induced by misaligning the stator $0.87^\circ$ , and (c) Plot of calibrated values after stator misalignment.....	24	Figure 46.	Deviation of attenuation for average vane-angle errors of 0.024, 0.035 and $0.049^\circ$ versus dial setting in decibels at 29, 33, and 37 GHz .....	30
Figure 36.	Angular error, $\theta'_r$ , in degrees from nominal (theory) versus the dial setting, $\theta$ , in degrees, determined from measurements by the power ratio, modulated subcarrier, and <i>i-f</i> substitution methods .....	25	Figure 47.	Deviation of attenuation for average vane-angle errors of 0.008, $-0.014$ , and $-0.042^\circ$ versus dial setting in decibels at 29, 33, and 37 GHz .....	31
Figure 37.	Angular error caused by binding effect between the drive gear and the driven gear (concentric to the rotor section).....	26	Figure 48.	Deviation of attenuation for average vane-angle errors of $-0.031$ , $-0.010$ , and $0.013^\circ$ versus dial setting in decibels at 2.85, 3.25, 3.55 GHz .....	31
Figure 38.	Angular error, $\theta'$ , in degrees versus dial setting in degrees, $\theta$ ,		Figure 49.	Deviation of attenuation for average vane-angle errors of 0.128, 0.105, and $0.120^\circ$ versus dial setting in decibels at 2.85, 3.25, and 3.55 GHz .....	32
			Figure 50.	Deviation of attenuation for average vane-angle errors of $-0.070$ ,	

			-0.067, and -0.032° versus dial setting in decibels at 2.85, 3.25, and 3.55 GHz -----				
Figure 51.	Limits of magnitude of one-sigma error in attenuation versus frequency in GHz for twenty WR284 rotary-vane attenuators at 30, 40, and 50-dB dial settings -----	32		Figure 61.	(a) $\epsilon'$ error from nominal (6 dB) increments versus dial setting in decibels for rotor misalignment, $\theta'_i$ , equal to 0.100, 0.200, and 0.300° -----	38	
Figure 52.	Limits of magnitude of one-sigma error in attenuation versus frequency in GHz for twenty-one WR187 rotary-vane attenuators at 30, 40, and 50-dB dial settings -----	33			(b) Attenuation in decibels versus $\theta$ in degrees, and angular limits in degrees for attenuation difference of 6 dB -----	39	
Figure 53.	Limits of magnitude of one-sigma error in attenuation versus frequency in GHz for eighteen WR137 rotary-vane attenuators at 30, 40, and 50-dB dial settings --	33		Figure 62.	$\epsilon'$ error in decibels versus $\theta'_i$ from 0 to +0.300° for 6-dB increments as follows: 0 to 6 dB, 3 to 9 dB, 6 to 12 dB, 9 to 15 dB, 12 to 18 dB, 15 to 21 dB, and 18 to 24 dB -----	39	
Figure 54.	Limits of magnitude of one-sigma error in attenuation versus frequency in GHz for twenty-three WR112 rotary-vane attenuators at 30, 40, and 50-dB dial settings -----	33		Figure 63.	(a) $\epsilon'$ error from nominal (3 dB) increments versus dial setting in decibels for rotor misalignment, $\theta'_i$ , equal to 0.100, 0.200, and 0.300° -----	40	
Figure 55.	Limits of magnitude of one-sigma error in attenuation versus frequency in GHz for fifty-one WR90 rotary-vane attenuators at 30, 40, and 50-dB dial settings --	33			(b) Attenuation in decibels versus $\theta$ in degrees, and angular limits in degrees for attenuation difference of 3 dB -----	41	
Figure 56.	Limits of magnitude of one-sigma error in attenuation versus frequency in GHz for seven WR62 rotary-vane attenuators at 30, 40, and 50-dB dial settings -----	34		Figure 64.	$\epsilon'$ error in decibels versus $\theta'_i$ from 0 to +0.300° for 3-dB increments as follows: 0 to 3 dB, 2 to 5 dB, 3 to 6 dB, 6 to 9 dB, 9 to 12 dB, 15 to 18 dB, 18 to 21 dB, and 21 to 24 dB -----	41	
Figure 57.	Limits of magnitude of one-sigma error in attenuation versus frequency in GHz for seven WR42 rotary-vane attenuators at 30, 40, and 50-dB dial settings -----	34		Figure 65.	(a) $\epsilon'$ error from nominal (1 dB) increments versus dial setting in decibels for rotor misalignment $\theta'_i$ , equal to 0.100, 0.200, and 0.300° -----	42	
Figure 58.	Limits of magnitude of one-sigma error in attenuation versus frequency in GHz for seven WR28 rotary-vane attenuators at 30, 40, and 50-dB dial settings -----	34			(b) Attenuation in decibels versus $\theta$ in degrees, and angular limits in degrees for attenuation difference of 1 dB -----	43	
Figure 59.	(a) $\epsilon'$ error from nominal (10 dB) increments versus dial setting in decibels for rotor misalignment, $\theta'_i$ equal to 0.100, 0.200, and 0.300° -----	35		Figure 66.	$\epsilon'$ error in decibels versus $\theta'_i$ from 0 to +0.300° for 1-dB increments as follows: 0 to 1 dB, 5 to 6 dB, 9 to 10 dB, 29 to 30 dB, and 39 to 40 dB -----	43	
	(b) Attenuation in decibels versus $\theta$ in degrees, and angular limits in degrees for attenuation difference of 10 dB -----	37		Figure 67.	$\epsilon'$ error from nominal (0.1 dB) increments versus dial setting in decibels for rotor misalignment, $\theta'_i$ , equal to 0.100, 0.200, and 0.300° -----	44	
Figure 60.	$\epsilon'$ error in decibels versus $\theta'_i$ from 0 to $\pm 0.300^\circ$ for 10-dB increments as follows: 0 to 10	37			(b) Attenuation in decibels versus $\theta$ in degrees, and angular limits in degrees for attenuation difference of 0.1 dB -----	45	
				Figure 68.	$\epsilon'$ error in decibels versus $\theta'_i$ from 0 to +0.300° for 0.1-dB increments as follows: 0 to 0.1	45	



	dB, 6.0 to 6.1 dB, 10 to 10.1 dB, 30 to 30.1 dB, and 50 to 50.1 dB	46	Figure 74. Photo of the open rectangular waveguide at the insertion point for devices under test	49
Figure 69.	Deviations in attenuation from nominal in decibels versus dial setting in degrees and decibels, for $\theta'_i$ equal 0.100, 0.200, and 0.300°, and $\theta'_o$ equal $\pm 0.010^\circ$	46	Figure 75. Photo of a fixed waveguide attenuator under test being inserted into the rectangular waveguide at the insertion point	49
Figure 70.	Deviations in attenuation from nominal in decibels versus dial setting in degrees and decibels (for 5 to 6 dB) when $\theta'_i$ equal $\pm 0.100$ , $\pm 0.200$ , and $\pm 0.300^\circ$ , and $\theta'_o$ equal $\pm 0.010^\circ$	47	Figure 76. Photo of the rectangular waveguide with adapters to admit coaxial devices at the insertion point	50
Figure 71.	Block diagram of microwave attenuation measurement system	48	Figure 77. Photo of a fixed coaxial attenuator under test being inserted into the line at the coaxial insertion point	50
Figure 72.	Detailed block diagram of microwave attenuation measurement system	48	Figure 78-87. Machine drawings for optical rotary-vane attenuator	52-61
Figure 73.	A recording showing the system stability at a 30-dB measurement level	49	Figure 88. Exploded view of a rotary-vane attenuator utilizing a Spiroid gear set in WR15 waveguide	62

### List of Tables

Table 1.	Angular displacement of rotor corresponding to a linear displacement of 0.020 inches on the readout scale for 3, 6, and 9 cycle readouts	6	Table 10.	Summary of data for determining average vane-angle error of a rotary-vane attenuator	15
Table 2.	Comparison of measurements obtained by modulated subcarrier and dc substitution methods	10	Table 11.	Angular values of $\alpha$ for maximum and minimum $\epsilon'_v$ at 10, 20, 30, 40, and 50-dB dial settings	17
Table 3.	Comparison of measurements obtained by modulated subcarrier and <i>i-f</i> substitution methods	10	Table 12.	Angular values of $\theta$ where maximum (+ or -) deviations of attenuation occur due to indexing error in 3-cycle drive and the corresponding theoretical attenuation values	19
Table 4.	Differences between measurements made simultaneously by modulated subcarrier and dc substitution methods	11	Table 13.	The angular correction required for different values of maximum attenuation and the distance $b'$ necessary to produce the angular correction for various waveguide sizes	22
Table 5.	Calibration data of optical rotary-vane attenuator in power ratio and <i>i-f</i> substitution systems at 9.0 GHz	12	Table 14.	Limits of magnitude of one-sigma error in attenuation in decibels per GHz for rotary-vane attenuators in WR28, WR42, WR62, WR90, WR112, WR137, WR187, and WR284 waveguide at 30, 40, and 50-dB dial settings	35
Table 6.	Comparison of calibration data for the same attenuator at 9.39 GHz using two independent methods (power ratio 1960 versus off-null)	12	Table 15.	Deviations from nominal 1-dB increment of attenuation (dial setting changed from 5 to 6 dB) for $\theta'_o = \pm 0.010^\circ$ and $\theta'_i = 0, \pm 0.100^\circ, \pm 0.200^\circ$ , and $\pm 0.300^\circ$	47
Table 7.	Comparison of calibration data for the same attenuator at 9.39 GHz using two independent methods (power ratio 1968 versus off-null)	12	Table 16.	Attenuation difference measurements of a waveguide step attenuator at 10 GHz with initial dial settings of the standard RVA from 0 to 60 dB	47
Table 8.	Comparison of deviation from the average values with vane-angle correction applied	14			
Table 9.	Comparison of calibration data with average vane-angle error correction applied	14			



# The Rotary-Vane Attenuator as an Interlaboratory Standard

Wilbur Larson

This paper presents a comprehensive report on the measurement and the use of the rotary-vane attenuator as an interlaboratory standard.

Methods of attenuation measurement developed at NBS are used to supply data for the evaluation of the deviations from theoretical  $\cos^2$  law due to rotor misalignment, gear eccentricity, resettability, resolution, and insufficient maximum attenuation.

A precision rotary-vane attenuator with an optical readout capable of 1 second of arc angular resolution has an effective attenuation resolution of 0.00005 dB at a 3-dB dial setting, and 0.0005 dB at a 30-dB dial setting. This type of precision attenuator is an effective standard for use in the dual detection microwave bridge measurement system.

Key words: Attenuation; interlaboratory standard; measurement; rotary-vane attenuator.

## 1. Introduction

In the past decade a considerable amount of material has been published on use of the rotary-vane attenuator for attenuation measurements in the microwave region. During this period an effort has been made to establish an improved standard for attenuation that would be useful and adaptable to calibration of commercial attenuators over the entire microwave frequency range.

The dial readout of the rotary-vane attenuator indicates either the angular displacement in degrees or the corresponding value of attenuation in decibels.

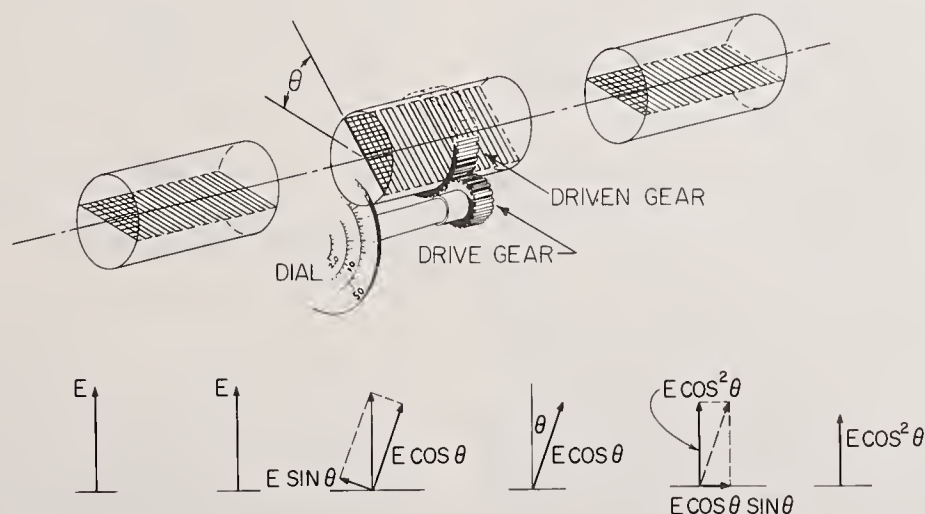
The purpose of this report is to discuss the work and experiments employed in the development and evaluation of the rotary-vane attenuator as an interlaboratory standard.

## 2. Theory of Operation

The rotary-vane attenuator has the properties essential for a standard attenuator. This type of attenuator is a device that has a dissipative resistive vane which can be rotated in a circular section of waveguide. The attenuation produced follows very nearly the cosine squared  $\theta$  law where  $\theta$  is the angular displacement of the vane from the polarization of the  $TE_{1,1}$  mode of the waveguide.

Intrinsically, the rotary-vane attenuator consists of three sections of waveguide, two ends which are rectangular/circular transitions and the circular center section. These three sections are placed in tandem on the longitudinal axis as shown in figure 1. A resistive vane is mounted across the center of each circular section of waveguide. In the minimum

### ROTARY VANE ATTENUATOR



$$\text{ATTENUATION} = -20 \log_{10} \cos^2 \theta = -40 \log_{10} \cos \theta$$

FIGURE 1. Pictorial diagram of the rotary-vane attenuator.



attenuation position, the vanes in the three sections are parallel to each other and the wide side of the rectangular waveguide (i.e., perpendicular to the electric  $E$  field). The entire center section, the rotor, can be rotated about the longitudinal axis of the waveguide, thus putting the vane parallel to a portion ( $E \sin \theta$ ) of the  $E$  field. The resistive film absorbs the component  $E \sin \theta$ , while the component  $E \cos \theta$ , normal to the center vane, passes through unattenuated to the vane in the second stator. The  $E \cos \theta$  component upon entering the second stator splits into two components. The resistive film absorbs the  $E \cos \theta$  component, and the  $E \cos \theta^2$  component emerges in a plane normal to the original.

Thus, the attenuation,  $A$ , stipulated from this relationship can be written as

$$A = -20 \log_{10} \cos^2 \theta + C \quad (1)$$

where  $\theta$  is the angle of the rotating vane relative to the stator vane of the input section,  $C$  is the residual attenuation, and  $A$  is the corresponding attenuation in decibels [1].<sup>1</sup>

The center section is mounted concentrically with either a driven gear mechanism, an optical device [3], or an electrical transducer [4] for translation of angular rotation to a suitable display. Each of the above methods of displaying the angular rotation will be discussed later in detail, which will include their respective desirable features or disadvantages.

## 2.1. Zero Setting

The variable attenuator can be used for attenuation difference with a known reference level. Usually, this reference is zero dial setting, corresponding to minimum insertion loss. The value of minimum insertion loss appears to be the most logical position to align the rotor and the stator vanes to correspond to zero dial setting. However, if achieved electrically, the angular displacement of the rotor section from  $0^\circ$  requires more than  $0.6^\circ$  to correspond to a 0.001 dB in attenuation. But, when the rotor vane approaches a right angle with the stator vane, the same  $0.6^\circ$  of angular rotation corresponds theoretically to a change greater than 100 dB. Although the maximum attenuation is much less than the theoretical value (approaches a limit of 110 to 120 dB) the loss of sensitivity in measuring such large values of attenuation more than offsets the advantage of high angular resettability for a given value of attenuation. Therefore, an equal angle technique of approximately  $10^\circ$  either side of  $90^\circ$  appears to be a good compromise. Using this technique, the attenuator is set to an angle of approximately  $100^\circ$  so that its output is equal to the output

at  $80^\circ$ . The midpoint of these two angles represents the true electrical plane of the attenuation vane. This technique is only valid for direct driven dial mechanisms, where the angular displacement due to gear eccentric or run out is not present [5]. The misalignment encountered by eccentric gearing has been evaluated at NBS [6].

Some commercially available attenuators have stops to prevent angular rotation beyond zero, and/or  $90^\circ$  the theoretical maximum for attenuation. This type of mechanical stop makes it impossible to align the rotor vane by the equal angle technique. In addition, striking the stop a severe blow during rotation at either end could reorient the center rotor vane due to gear or shaft slippage and cause undesirable deviation from the  $\cos^2$  law at the high angle setting.

## 2.2. Stator Alignment

In the fabrication of a precision rotary-vane attenuator it is not only essential that the zero of the dial readout be oriented with the reference plane of the vane in the rotor section, but the vanes of the end sections or stators should lie in the same plane. If the end vanes are not parallel the insertion loss will increase slightly, but more important, the rotor to stator alignment will be impaired, and cause an angular misalignment about the longitudinal axis, as shown in figure 2. Here, the distances to the stator vanes from the reference plane are indicated as  $b_1$  and  $b_2$ , and the difference as  $b'$ .

Figures 3 and 4 illustrate two methods of initially aligning the rotor vane with reference to the stator vanes. Two types (Type  $A$  and Type  $B$ ) of errors are possible for rotary-vane attenuator with rotationally misaligned stators [6]. The Type  $A$  occurs when the rotating section index or zero is coincident to the first (or second) stator vane, and the Type  $B$  occurs when the rotating section index or zero is coincident to the average position (or bisection) of the stator vanes.

The error, in decibels, for Type  $A$  misalignment is

$$\epsilon_a = -20 \log_{10} \frac{\cos(\theta + \theta')}{\cos \theta} \quad (2)$$

and the error, in decibels, for the Type  $B$  misalignment is

$$\epsilon_b = -20 \log_{10} \frac{\cos(\theta + \frac{\theta'}{2}) \cos(\theta - \frac{\theta'}{2})}{\cos^2 \theta} \quad (3)$$

With the use of trigonometric identities the Type  $B$  error can be written [7] as

$$\epsilon_b = -20 \log \left( \cos^2 \frac{\theta'}{2} - \tan^2 \theta \sin^2 \frac{\theta'}{2} \right) \text{ dB} \quad (4)$$

<sup>1</sup> Figures in brackets indicate the literature references on page

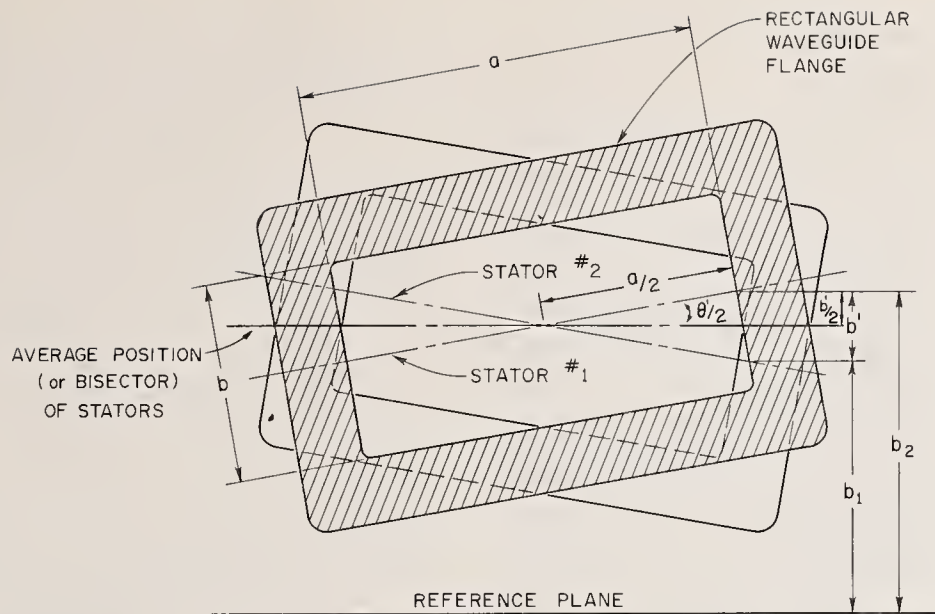


FIGURE 2. Illustration of the determination of  $b'$  with measured distances  $b_1$  and  $b_2$  from the reference plane as viewed from the rectangular waveguide input flange.

- TYPE "A" ERROR -

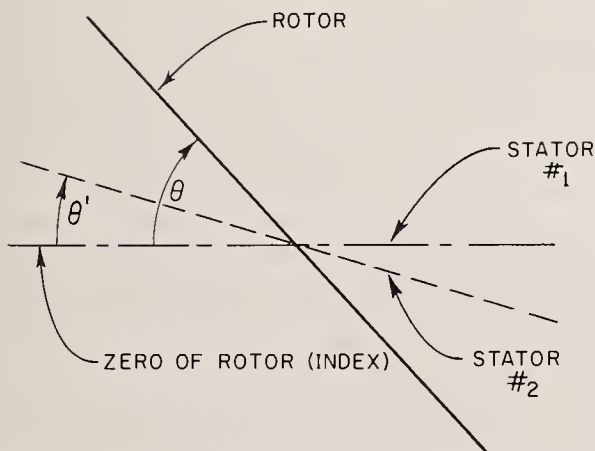


FIGURE 3. Rotor index or zero coincident with first (or second) sector.

- TYPE "B" ERROR -

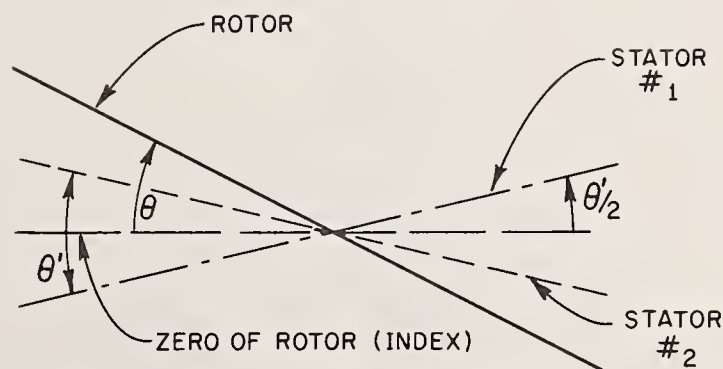


FIGURE 4. Rotor index or zero coincident with average position of stators.

Regardless of the type of alignment with reference to the dial zero, the entire range of attenuation is affected by any misalignment of the stators. For example, in a Type *B* alignment, a  $90^\circ$  rotation of the rotor vane will coincide with the saddle portion of a double hump maximum attenuation, figure 5. Figure 5 shows that the first maximum attenuation will be reached to coincide with  $\theta'/2$  prior to  $90^\circ$  on the dial,

while the second maximum will occur at  $\theta'/2$  beyond  $90^\circ$  on the dial. However, the Type *A* alignment gives rise to two possible situations, an advanced rotor vane or a retarded rotor vane with reference to either stator vane. In figure 6, the rotor vane is assumed to be advanced  $\theta'/2$ . The first maximum attenuation occurs at  $90^\circ - \theta'$ , the saddle minimum at  $90^\circ - \theta'/2$ , and the second maximum attenuation at  $90^\circ$  of the

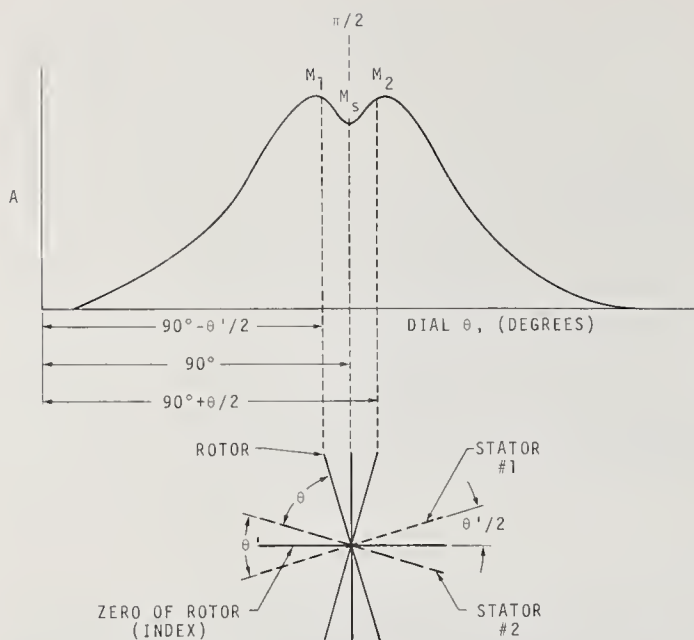


FIGURE 5. *Type B alignment: first attenuation maximum,  $M_1$ , at  $\theta'/2$  prior to  $90^\circ$ ; saddle minimum,  $M_s$ , at  $90^\circ$ ; and second maximum,  $M_2$ , at  $\theta'/2$  beyond  $90^\circ$ .*

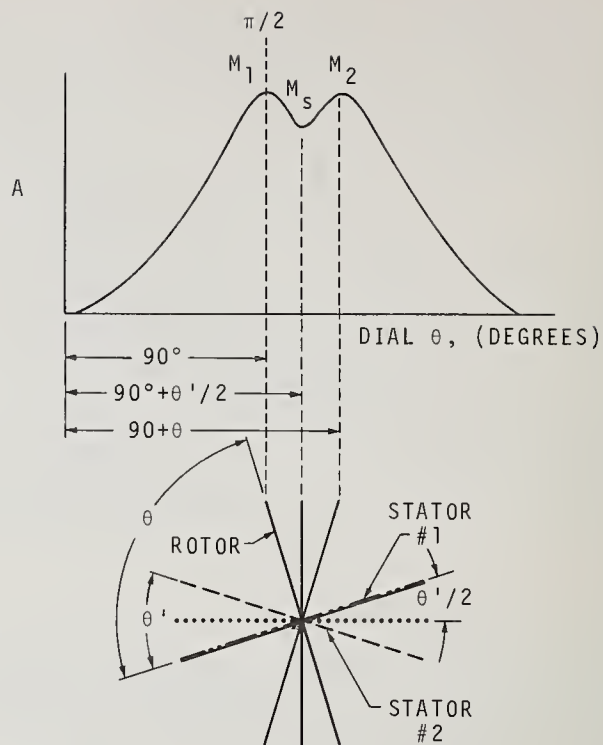


FIGURE 7. *Type A alignment, rotor retarded: first attenuation maximum,  $M_1$ , at  $90^\circ$ ; saddle minimum,  $M_s$ , at  $90^\circ + \theta'/2$ ; and the second maximum at  $90^\circ + \theta'$ .*

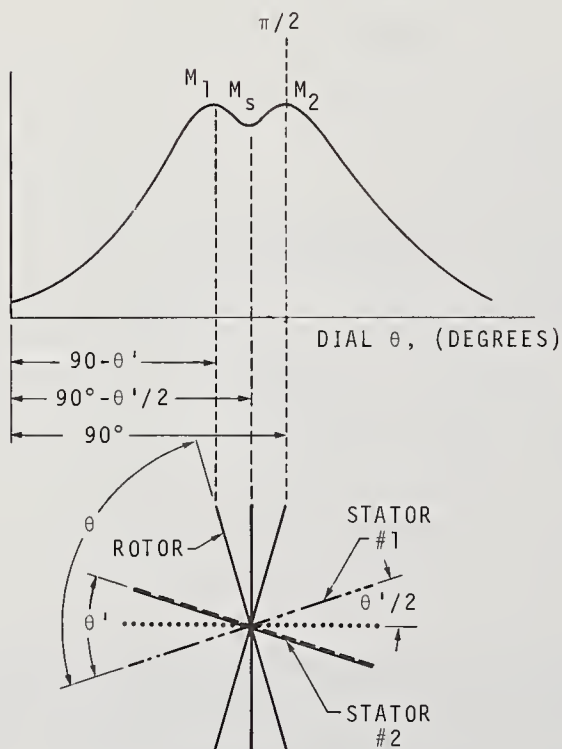


FIGURE 6. *Type A alignment, rotor advanced to  $\theta'/2$ : first attenuation maximum,  $M_1$ , at  $90^\circ - \theta'$ ; saddle minimum,  $M_s$ , at  $90^\circ - \theta'/2$ ; and the second maximum,  $M_2$ , at  $90^\circ$ .*

dial setting. To observe the conditions for a retarded rotor vane of  $\theta'/2$  refer to figure 7. In this case the first maximum attenuation occurs at  $90^\circ$ , the saddle minimum at  $90^\circ + \theta'/2$ , and the second maximum attenuation at  $90^\circ + \theta'$  of the dial setting.

The double-humped attenuation curves shown in figure 5, 6, and 7 only occur when end vane misalignment and insufficient attenuation are simultaneously present. With perfect vanes, attenuation would tend to infinity at two angles.

### 2.3. Transmission Error or Insufficient Attenuation in the Rotor

The ideal characteristics of the  $\cos^2$  law is not obtainable with the rotary-vane attenuator at the high setting of  $\theta$  due to the transmission error. Although one may argue that any error occurring during transmission of a wave through a rotary-vane attenuator could be called transmission error, the author here follows the common practice of many writers on the subject and assigns the transmission error entirely to the error resulting from insufficient maximum attenuation in the center vane. Of course, the theoretical  $\cos^2 \theta$  law assumes infinite attenuation in the center vane. In addition to large transmission error, the lack of sufficient maximum attenuation shows increased phase shift and frequency sensitivity at the higher setting of  $\theta$ .



The error related to the transmission error and phase shift of the rotary-vane attenuator has been treated by James [8], Otoshi [7], and Mariner [5].

The transmission error is given by

$$\epsilon_t = -20 \log (1 + e^{-\alpha l} \tan^2 \theta) \text{ dB} \quad (5)$$

where the term  $e^{-\alpha l}$  can be determined experimentally by setting  $\theta$  to  $90^\circ$  and then measuring  $A$  (maximum attenuation)

$$e^{-\alpha l} = \frac{1}{\log_{10}^{-1} \frac{A'}{20}} = 10 \left( \frac{-A'}{20} \right) \quad (6)$$

Where  $l$  is the distance the wave travels in the rotor section of the attenuator and  $\alpha$  is equal to the difference between the attenuation constants of the tangential and normal electric field components in the rotor.

The calculated error from eq (5) and a measured value of 90 dB for  $\theta = \pi/2$ , shows that  $\epsilon_t = 0.086$  dB at a dial setting of 50 dB.

The phase shift of the transmitted signal as a function of  $\theta$  is given by

$$\phi_t = \tan^{-1} \frac{e^{-\alpha l} \sin \beta l \sin^2 \theta}{\cos^2 \theta + e^{-\alpha l} \sin^2 \theta \cos \beta l} \quad (7)$$

where  $\beta = \beta_0 - \beta_1$ . The quantity  $\beta l$  can be found experimentally. Where  $\beta$  is equal to the difference between the phase shift constants of the tangential and normal electric field components in the rotor. If  $\beta l$  equals  $90^\circ$ , the phase shift  $\phi$  will be less than  $0.2^\circ$  between 0 to 40 dB.

For use in the deep space project a compact rotary-vane attenuator was developed. Any compactness, especially in the rotor section of the attenuator would affect its  $\cos^2$  response in relation to maximum attenuation, phase shift and frequency sensitivity. However, at a fixed frequency and low values of attenuation, this device can be a standard.

A shorter rotor section provides less maximum attenuation, thus increasing transmission error. A modified law derived by Otoshi [9] corrects for this effect of transmission error. His treatment of the transmission error is similar to James [8] but does not assume that the transmission error signal effect is of a known magnitude or phase.

The attenuator's physical length need not be long as the modified law does not require a zero transmission error. This permits a marked decrease in physical length where this is a physical factor.

In addition, the modified law can be used for corrections, that are necessary to extend the dynamic attenuation range of the present precision rotary-vane attenuator. A mechanical technique for compensating for insufficient attenuation will be discussed in a later section of the text.

### 3. Dial Readout of Rotary-Vane Attenuator

The readout scale indicates the value of attenuation in decibels for most rotary-vane attenuators. Let us consider several of the methods that can be used for presenting a decibel scale of the attenuation, such as the 3 cycle spiral, and 6 and 9 cycle cylindrical readouts as illustrated in figures 8, 9, and 10 respectively.

X-band (WR90) rotary-vane attenuators were used in the evaluation of 3 and 6 cycle readouts and an S-band (WR284) attenuator was used to evaluate a 9 cycle readout. It is estimated that setting the indicator line of the readout on either edge of a given mark on the scale corresponds to a linear deviation of about  $0.020''$ . The angular displacement of the rotor section, that is equivalent to  $0.020''$  linear displacement on the dial, was calculated for each of three types of scales. The results of these calculations are summarized in table 1. Column five in the table shows the calculated angular displacement of the rotor in degrees which corresponds to a linear deviation of  $0.020''$  (the nominal width of a scale line) on the scale readout. Note that the value of angular displacement of the rotor changes with each spiral in the 3 cycle readout for a given linear deviation, but remains constant for all parts of the cylindrical readouts. Graphs of the deviation of attenuation from nominal in decibels versus the dial setting in degrees, 0 to  $86.5$  (0 to 50 dB), are shown for each of the three types of readouts in figure 11. The devia-

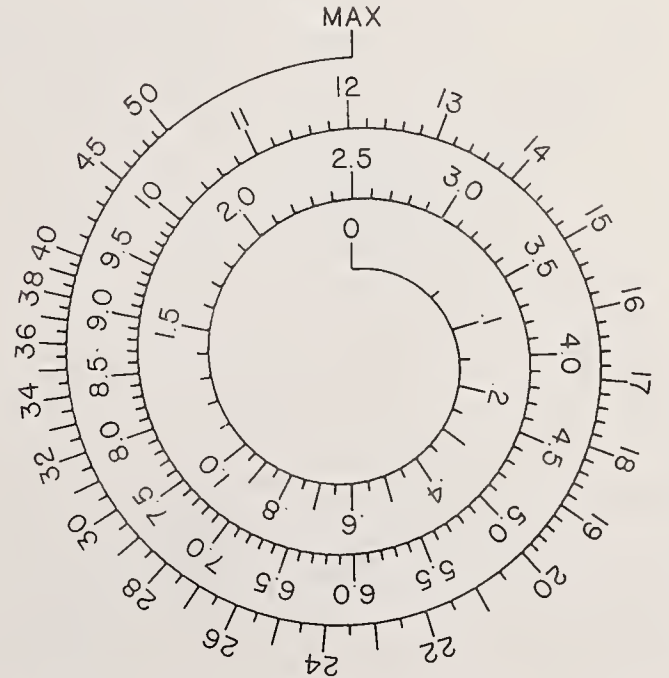


FIGURE 8. Rotary-vane attenuator dial readout in decibels—spiral—3 cycle.

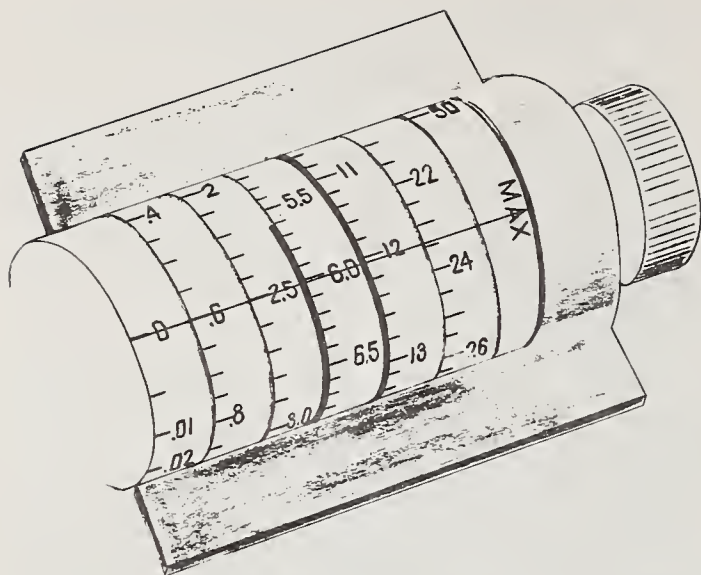


FIGURE 9. Rotary-vane attenuator dial readout in decibels—Cylindrical—6 cycle.

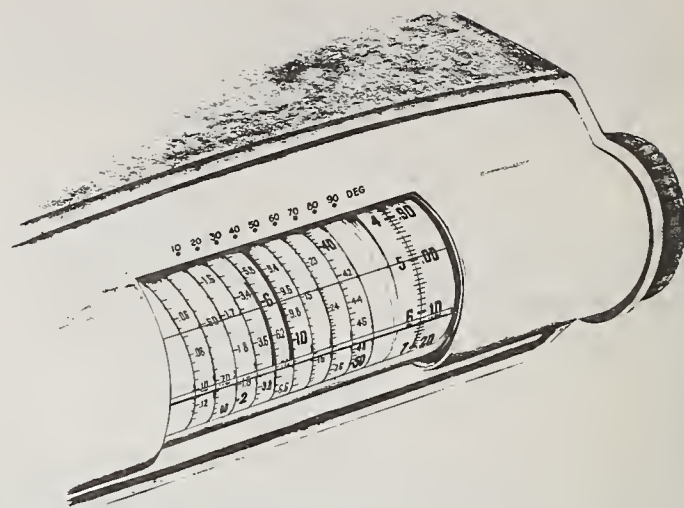


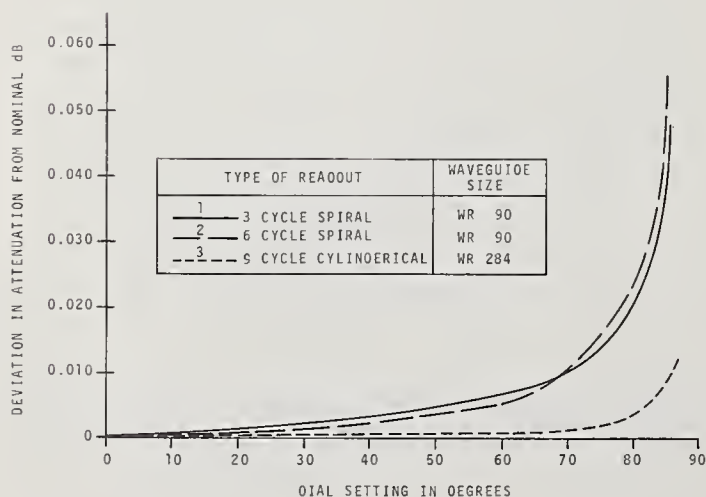
FIGURE 10. Rotary-vane attenuator dial readout in decibels—cylindrical—9 cycle.

tion of attenuation from nominal in decibels is very nearly the same for the 3 cycle spiral, and the 6 cycle cylindrical readout, in WR90 waveguide. However, the deviations are considerable less for the 9 cycle cylindrical readout in WR284 waveguide.

NBS has designed a drive unit for a commercial rotary-vane attenuators that have a gear mechanism ratio of 12. The use of the drive unit modifies the attenuator to give the angular rotation of the rotor section in decimal parts of a degree. Figure 12 shows

TABLE 1. Angular displacement of rotor corresponding to a linear displacement of 0.020 inches on the readout scale for 3, 6, and 9 cycle readouts

Type of scale	Gear ratio	Diameter of scale readout	Diameter of driven rotor gear	Rotor angular displacement degree
3 cycle (spiral)	12:1	1.75'' (0–2.5 dB)	1.59''	0.021°
		2.75'' (2.5–12 dB)	1.59''	.014°
		3.80'' (12–max)	1.59''	.009°
6 cycle (cylindrical)	24:1	1.27''	2.17''	.010°
9 cycle (cylindrical)	36:1	2.25''	4.5''	.002°



the three dial readout of the rotor in units, tenths, hundredths and thousandths of a degree. The use of a three dial readout is an appropriate method to increase the resolution of the angular displacement dial to thousandths of a degree. In order to convert an angular displacement to decibels for increments of 0.001° refer to NBS Technical Note 229. Figure 13 and 14 show the machine drawings of the drive mechanism and scale used to display the angular displacement of the gear driven rotor (ratio of 12)

FIGURE 11. Graph of the deviation in attenuation from nominal versus dial setting in degrees which corresponds to a linear deviation of 0.020 inch for three rotary-vane attenuators.



in  $0.001^\circ$  increments from 0 to  $90^\circ$ . A simplified gear drive for rotary-vane attenuators was developed recently at NBS in WR15 waveguide size [10]. This one-step drive consists of a 180:1 precision spiroid gear set which provides an accurate and repeatable readout an order of magnitude better than commercial attenuators. This drive mechanism permits readout of  $0.01^\circ$  increments of vane angle displacement. To convert this readout to decibels, refer to NBS Technical Note 229.

A rotary-vane attenuator with an optical readout [3] was designed at NBS, Boulder, that provides an angular displacement and readout with a resolution of  $\pm 1$  second of arc. A table is very useful for determining the attenuation in decibels for angular displacements in degrees, minutes, and seconds as

would be obtained from the above attenuator readout. Three computer tapes have been run off for the function ( $A = -40 \log_{10} \cos \theta$ ) versus degrees, minutes, seconds as follows:

Tape	Attenuation	$\theta$
(1)	(0.000000–2.498726 dB)	( $0^\circ 0' 0''$ to $29^\circ 59' 59''$ )
(2)	(2.498775–12.041054 dB)	( $30^\circ 0' 0''$ to $59^\circ 59' 59''$ )
(3)	(12.041200–212.577005 dB)	( $60^\circ 0' 0''$ to $89^\circ 59' 59''$ )

The computer tapes provide 324,000 values of attenuation to six decimal places from 0 to 212.577005 dB for every second of arc from 0 to  $89^\circ 59' 59''$ .

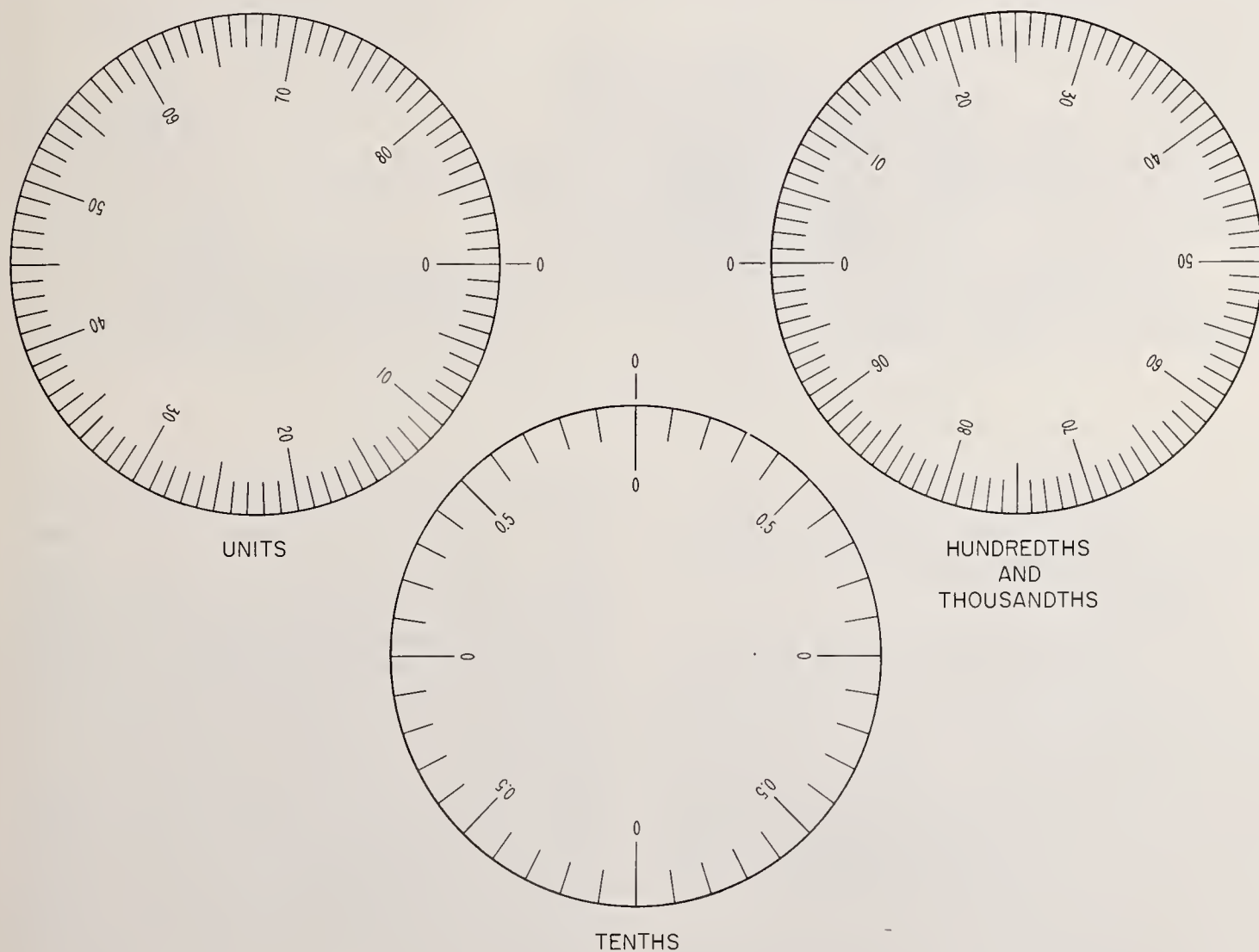


FIGURE 12. Dial readout in units, tenths, hundredths and thousandths of degrees for rotary-vane attenuator.

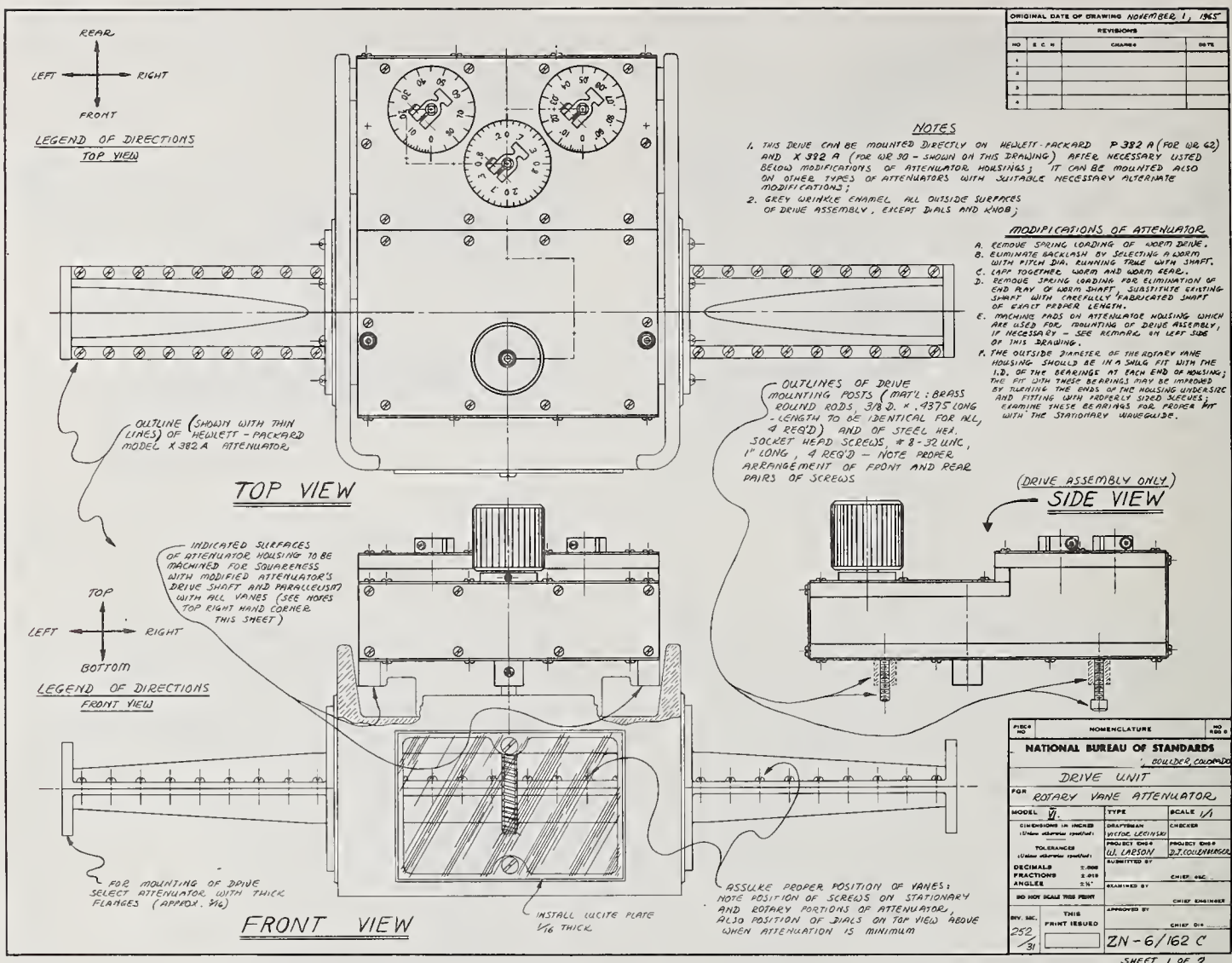


FIGURE 13. Pictorial view of drive unit for rotary-vane attenuator.

## 4. The Measurement of the Rotary-Vane Attenuator by Different Methods

In most of the microwave standards laboratories several methods are available for the measurement of waveguide attenuation devices. At NBS several excellent methods were developed to calibrate rotary-vane attenuators. The inherent properties of the rotary-vane attenuator make this device an excellent standard for intercomparison of calibration systems. In order to obtain the best results from any measurement data, it is essential that the interlaboratory standard used meets the criteria of a desirable standard [11].

The purpose of this section of the report will show that the calibration data of the rotary-vane attenuator used in several systems enables one to evaluate both the systems and the interlaboratory standard, simultaneously.

### 4.1. NBS Developed Attenuation Systems

The power ratio method was developed in 1959 at NBS/Boulder for microwave attenuation measurements and the error affiliated with this technique has been carefully evaluated [12]. The application of this method resulted in a significant improvement in the resolution and stability of attenuation difference measurements, especially for small attenuation values, over a broad frequency range. Other systems were developed at NBS in the microwave attenuation measurement area, namely, the modulated sub-carrier [13] and off-null [14] methods. In addition to these highly accurate and precise measurement systems, the *i-f* substitution method for attenuation measurement has been developed to a high degree of excellence [15, 16]. The *i-f* substitution method is the most commonly used in both waveguide and coaxial systems at NBS. At present the *i-f* substitution waveguide systems are used over the frequency



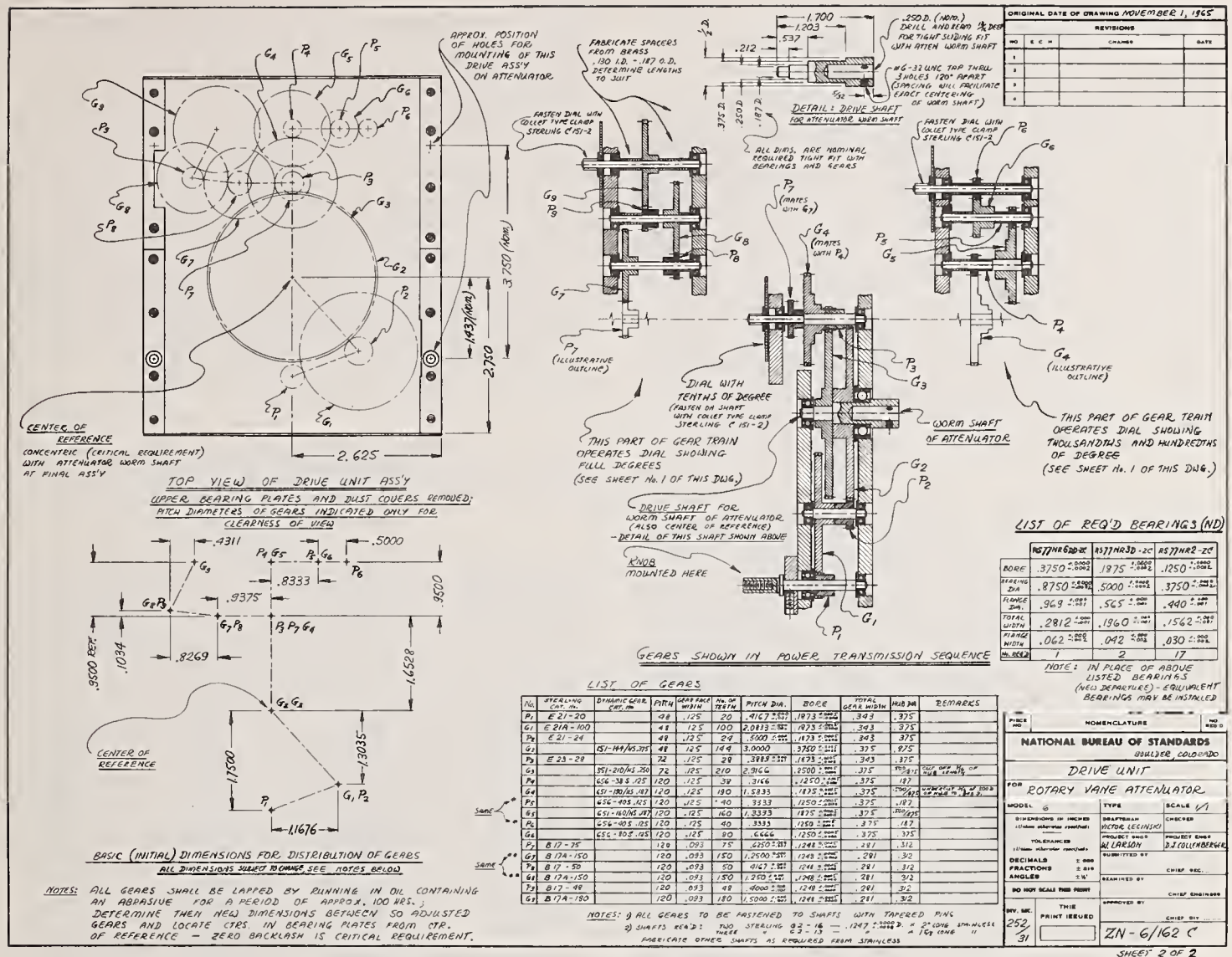


FIGURE 14. Machine drawing of drive unit gearing for rotary-vane attenuator.

range from 1.7 to 65 GHz in the waveguide sizes from WR430 to WR15. The other systems mentioned above were developed predominantly in the X-band region.

During the past 15 years NBS/Boulder has calibrated many rotary-vane attenuators in nine different waveguide sizes. Most of these attenuators have been commercially purchased for use as interlaboratory standards in public, military, and government agencies.

A commercially available X-band rotary-vane attenuator<sup>2</sup> was calibrated by the NBS power ratio method [12]. This work revealed the limitations of commercial rotary-vane attenuators for values greater than 1 dB; it was shown that the resolution and repeatability deteriorate rapidly at the higher values of attenuation. In other words, the power ratio calibration system challenged the pre-

cision and resolution that could be obtained with the present available rotary-vane attenuator.

A short time later another method of measuring microwave attenuation was developed at NBS. This new method known as the modulated sub-carrier technique [13] utilized commercially available components to provide resolution and accuracy comparable to the power ratio method.

In the evaluation of this new method, attenuation measurements were compared with those obtained by the power ratio or (dc-substitution) and the *i-f* substitution (30 MHz standard) techniques. The same commercial rotary-vane attenuator of WR90 waveguide size was calibrated at specific dial settings by each of the above methods at about 9.4 GHz. Although the measurement data was taken some years ago, recent additional evaluations have been made regarding the properties of the rotary-vane attenuator. Also, a recently discovered defect in the fabrication of the interlaboratory standard used in the above measurements sheds new light on this calibration data.

<sup>2</sup> Certain commercial equipment and materials are identified in this paper in order to adequately specify the experimental procedure. In no case does such identification imply recommendation or endorsement by the National Bureau of Standards, nor does it imply that the material or equipment identified is necessarily the best available for the purpose.

## 4.2. Comparison of Modulated Subcarrier and dc Substitution Methods

Table 2 shows a comparison of the modulated subcarrier with those of the dc substitution method (power ratio). The dial setting of the attenuator in decibels is given in column one. In columns two and three the measured values for each dial setting by the modulated subcarrier and dc methods are listed, respectively. Column four gives the discrepancy between the dc and subcarrier methods. This discrepancy between the two methods is shown to be less than 0.0020 dB from 0.01 to 1-dB values, while the discrepancy increases to 0.03 dB at the 30-dB value. A large portion of these discrepancies are due to attenuation resettability and operator performance.

TABLE 2. Comparison of measurements obtained by modulated subcarrier and dc substitution methods

Attenuator dial reading	Measured attenuation (with attenuator vertical)		
	Modulated subcarrier method	dc method	Discrepancy between dc and subcarrier methods
<i>dB</i>	<i>dB</i>	<i>dB</i>	<i>dB</i>
0.01	0.0111	0.0107	+0.0004
.02	.0218	.0214	+ .0004
.03	.0308	.0303	+ .0005
.04	.0413	.0407	+ .0006
.05	.0532	.0521	+ .0011
.06	.0626	.0609	+ .0017
.07	.0718	.0700	+ .0018
.08	.0814	.0802	+ .0012
.09	.0918	.0909	+ .0009
.10	.1037	.1021	+ .0016
.12	.1206	.1191	+ .0015
.14	.1388	.1375	+ .0013
.16	.1590	.1573	+ .0017
.18	.1796	.1783	+ .0013
.20	.2023	.2007	+ .0016
.25	.2482	.2471	+ .0011
.50	.4994	.4979	+ .0015
1	1.004	1.004	.0000
2	1.999	1.996	+ .003
3	3.000	2.998	+ .002
5	4.991	4.990	+ .001
10	9.971	9.965	+ .006
15	15.01	14.99	+ .02
20	19.97	19.95	+ .02
25	25.00	25.01	-.01
30	30.10	30.07	+ .03
40	40.44	40.33	+ .11
50	52.39	52.24	+ .15

## 4.3. Comparison of Modulated Subcarrier and *i-f* Substitution Methods

Table 3 shows the similar comparison between the modulated subcarrier and *i-f* methods with the same rotary-vane attenuator as the interlaboratory standard. A change of position of the attenuator

caused a deviation of about 0.5 dB between the two different subcarrier measurements at the 50 dB dial setting.

The discrepancy between the subcarrier and *i-f* methods was about 0.004 dB at 1-dB dial setting (greater than for the subcarrier and dc methods), while the discrepancy was 0.02 dB at the 30-dB dial setting (less than for the dc and subcarrier methods). In addition, table 2 shows the measured values of attenuation to be less than in table 3 for dial settings of 40 and 50 dB. This change could be caused by the vertical and/or the horizontal positions of the attenuator under calibration [13], as indicated in table 2 and table 3.

TABLE 3. Comparison of measurements obtained by modulated subcarrier and *i-f* substitution methods

Attenuator dial reading	Measured attenuation (with attenuator horizontal)		
	Modulated subcarrier method	<i>i-f</i> method	Discrepancy between <i>i-f</i> and subcarrier methods
<i>dB</i>	<i>dB</i>	<i>dB</i>	<i>dB</i>
0.1	0.1026	0.101	+0.0016
.2	.2010	.199	+ .002
.5	.4978	.498	-.0002
1	1.002	.998	+ .004
2	1.997	1.999	-.002
3	2.998	2.997	+ .001
5	4.989	4.980	+ .009
10	9.958	9.965	-.007
15	14.98	14.99	-.01
20	19.94	19.95	-.01
25	24.95	24.95	.00
30	30.02	30.00	+ .02
40	40.24	40.15	+ .09
50	51.70	51.66	+ .04

The data from each comparison shows that the dial of the attenuator agrees rather closely with the measured values for the range from 0.01 to 30 dB. However, this is not true for the dial settings of 40 and 50 dB. At 50dB the deviation is greater than 2 dB as shown in table 2. An increase in attenuation of this magnitude is not a normal characteristic of a rotary-vane attenuator, especially since it has good agreement to 30 dB. The usual indication is a decrease in attenuation from nominal at the higher values. This older type rotary-vane attenuator has a low maximum attenuation value of about 80 dB. The deviation in attenuation below nominal caused by this low value of maximum attenuation is about 0.3 dB at 50 dB.

### Concentric Rotor Gear Sector

At a later date, the drive mechanism of this attenuator was disassembled. This revealed that the gear concentric to the rotor was a sector of about 120°. This gear sector was welded to the outer case



of the rotor section. A slight tilt of the gear sector during the welding process would cause an angular displacement. It has been shown that an error in the driven gear of  $0.36^\circ$  will produce a deviation in attenuation of more than 2 dB at the 50-dB dial setting [17].

The physical orientation of the attenuator under test can cause deviations in measurements as shown in tables 2 and 3. The measured values at the 50-dB setting deviate by about 0.7 dB between vertical and horizontal positions of the attenuator. End play in the bearings of the rotor section, and backlash in the gearing can cause angular displacement in the cylindrical dial readout. A change of angular displacement equal to  $0.13^\circ$  causes a change of 0.7 dB at 50 dB [17].

#### 4.4. Simultaneous Measurement by Modulated Subcarrier and dc Substitution Methods

In order to more truly compare the subcarrier and dc substitution methods, the rotary-vane attenuator was measured in a special situation. A three channel [13] system was devised so that simultaneous measurements could be made by the dc and subcarrier methods for a given dial setting. The results of these measurements are shown in table 4. The deviations between the two methods are 0.0005 dB up to 0.5-dB measurements, and slightly over 0.001 dB up to 10 dB. While the deviation increased to 0.006 dB at 20 dB, this confirms that the larger deviations shown in tables 2 and 3 are due to mismatch error, resettability, and operator performance.

TABLE 4. Differences between measurements made simultaneously by modulated subcarrier and dc substitution methods

Attenuator dial reading	Difference (with attenuator vertical)
dB	dB
0.01	+0.0002
.02	-.0002
.05	-.0001
.10	+.0005
.50	+.0001
1.0	-.0012
2.0	-.0003
5.0	-.0011
10.0	+.0012
20.0	+.0066

#### 4.5. Measurement of Precision Optical Rotary-Vane Attenuator by dc and *i-f* Substitution Methods

The X-band optical rotary-vane attenuator [3] developed at NBS/Boulder increased the resolution and resettability of the RVA to 2 seconds of arc. In addition, the optical readout feature eliminates angular displacement errors due to gear eccentric-

ity. This precision attenuator was measured over a dial range of 0 to  $87.5^\circ$  in  $2.5^\circ$  increments. The measurements were made using the power ratio method for attenuator dial readings of 0 to  $60^\circ$  and using the *i-f* substitution method for dial settings of  $62.5$  to  $87.5^\circ$ . In table 5, the calibration of the optical attenuator is shown for the frequency of 9.0 GHz. Column one lists the dial setting in degrees ( $\theta$ ). Column two gives the theoretical value of attenuation in decibels corresponding to the angles of column one. Column three shows the calibrated value of attenuation at each dial setting. From this data the average apparent vane angle deviation was determined [18] to correspond to a retardment of the rotor vane of 2 minutes of arc or  $0.033^\circ$ .

The attenuator was recalibrated with a correction of  $2'$  applied to each dial setting. The results are recorded in column four. The application of the correction to the dial reading enabled the measured attenuation values to follow the  $\cos^2$  law more closely. The deviation of these measurements from the corresponding theoretical values of attenuation in decibels are listed in column five. The deviations from the theoretical value are shown to be less than 0.001 dB for measurements up to  $60^\circ$  (12 dB), and vary from 0.001 to 0.012 dB; from  $62.5$  to  $87.5^\circ$  (13 to 54 dB). The values of the discrepancy of the measurements that were made simultaneously between the subcarrier and the dc methods are in close agreement with those made with the high resolution optical attenuator (see tables 4 and 5). This illustrates the excellent agreement of attenuation measurements between systems and that a high resolution attenuator eliminates the need for simultaneous measurement to obtain precise data for intercomparison of systems.

#### 4.6. Power Ratio (dc) Versus Off-Null Measurements

A two-channel off-null technique for measuring small values of attenuation was developed at NBS [14]. The interlaboratory standard chosen for intercomparisons of this measurement system was the X-band rotary-vane attenuator that was calibrated by the power ratio (dc) method eight years previously [12].

The rotary-vane attenuator exhibits very little phase shift and provides high resolution at small values of attenuation; thus these inherent characteristics make the attenuator an excellent device for this intercomparison. The attenuation range for the intercomparison was 0.01 to 0.1 at 0.01-dB intervals. It is estimated that the resettability of this type of rotary-vane attenuator corresponds to an angular displacement of the rotor of about  $0.006^\circ$ . Then the limits of error of resettability for the attenuation from 0.01 to 0.10 dB are about 0.00006 to 0.00020 dB, respectively.



TABLE 5. Calibration data of optical rotary-vane attenuator in power ratio and i-f substitution systems at 9.0 GHz

Dial setting in degrees	Theoretical value of attenuation in decibels	Calibrated value of attenuation in decibels	Calibrated value of attenuation with 2' correction	Deviation from theoretical value in decibels
2.5	0.0165	0.0161	0.0166	+0.0001
5.0	.0662	.0653	.0662	+0.0000
7.5	.1493	.1478	.1491	-.0002
10.0	.2659	.2640	.2658	-.0001
12.5	.4167	.4145	.4166	-.0001
15.0	.6022	.5996	.6022	-.0000
17.5	.8232	.8203	.8233	+0.0001
20.0	1.0805	1.0772	1.0806	+0.0001
22.5	1.3754	1.3715	1.3755	+0.0001
25.0	1.7089	1.7046	1.7091	+0.0002
27.5	2.0828	2.0779	2.0830	+0.0002
30.0	2.4987	2.4931	2.4989	+0.0002
32.5	2.9588	2.9526	2.9587	-.0001
35.0	3.4654	3.4586	3.4657	+0.0003
37.5	4.0213	4.0136	4.0214	+0.0001
40.0	4.6300	4.6218	4.6303	+0.0003
42.5	5.2948	5.2858	5.2957	+0.0009
45.0	6.0206	6.0108	6.0203	-.0003
47.5	6.8127	6.8018	6.8135	+0.0008
50.0	7.6773	7.6653	7.6771	-.0002
52.5	8.6221	8.6094	8.6231	+0.0010
55.0	9.6563	9.6419	9.6569	+0.0006
57.5	10.7913	10.7750	10.7908	-.0005
60.0	12.0412	12.0226	12.0414	+0.0002
62.5	13.424	13.406	13.425	+0.001
65.0	14.962	14.942	14.967	+0.005
67.5	16.686	16.662	16.692	+0.006
70.0	18.638	18.611	18.640	+0.002
72.5	20.874	20.843	20.876	+0.002
75.0	23.480	23.443	23.479	-.001
77.5	26.586	26.543	26.587	+0.001
80.0	30.413	30.357	30.413	.000
82.5	35.372	35.296	35.367	-.005
85.0	42.388	42.266	42.379	-.009
87.5	54.413	54.178	54.401	-.012

TABLE 6. Comparison of calibration data for the same attenuator at 9.39 GHz using two independent methods (power ratio 1960 versus off-null)

Dial setting (dB)	Measured attenuation difference (dB)		Discrepancy between 1960 power ratio and 1968 off-null methods (percent)
	1968 Off-null method [1]	1960 Power ratio method [2]	
0.01	0.0103	0.0107	-3.7
.02	.0208	.0214	-2.9
.03	.0294	.0303	-3.0
.04	.0397	.0407	-2.2
.05	.0513	.0521	-1.5
.06	.0598	.0609	-1.8
.07	.0695	.0700	-.7
.08	.0792	.0802	-1.2
.09	.0896	.0909	-1.4
.10	.1008	.1021	-1.3

Average..... 2.0

TABLE 7. Comparison of calibration for the same attenuator at 9.39 GHz using two independent methods (power ratio 1968 versus off-null)

Dial setting (dB)	Measured attenuation difference (dB)		Discrepancy between 1968 power ratio and off-null methods (percent)
	1968 off-null method [1]	1968 power ratio method	
0.01	0.0103	0.0101	+2.0
.02	.0208	.0205	+1.5
.03	.0294	.0290	+1.3
.04	.0397	.0394	+.8
.05	.0513	.0507	+1.2
.06	.0598	.0595	+.5
.07	.0695	.0687	+1.2
.08	.0792	.0786	+.8
.09	.0896	.0890	+.7
.10	.1008	.1003	+.5

Average..... 1.0

The results of the measurements made by the power ratio methods in 1960 and the off-null method in 1960 are compared in table 6. Column four shows the discrepancy between the two methods in percent of the measured value. The greatest percent discrepancy, 3.7, occurs at the 0.01 dB-dial setting; however the largest deviation in attenuation is 0.0013 dB and occurs at the dial setting of 0.10 dB. But more significant is the negative sign common to all values in column four. Two factors suggest a systematic error, the common minus sign in the discrepancy column, and the 0.0013-dB difference at the 0.10-dB measurement. Table 4 shows that the greatest deviation in measurement for the range of 0.01 to 0.10 dB between the subcarrier and dc substitution method was 0.0005 dB at a dial setting of 0.10 dB. These above factors led us to further measurement and evaluation.

The rotary-vane attenuator was calibrated later in 1968 by the power ratio method. The results of these measurements were compared with those taken with the off-null method, and are shown in table 7. The discrepancy between the 1968 power ratios and off-null methods are listed in column four. The greatest percent discrepancy, 2, occurs at the 0.01 dB-dial setting, as was the case in table 6, but the value of the percent of discrepancy was reduced almost one half. Also, the average value of the percent of discrepancy for all measurements of the latter measurements was decreased by one half.

The measured values of attenuation difference for both the power ratio and the off-null methods were analyzed for apparent angular deviations [18, 19]. The dial setting of the attenuator was assumed to be the true value for this analysis. Figure 15 illustrates the apparent deviation of the rotor from nominal dial setting in degrees, which correspond to attenuation values of 0.01 to 0.10 dB. The average vane angle error representative of each measurement is shown as a straight line with the angular deviation in degrees indicated as follows: the power ratio method of 1960,  $+0.044^\circ$ ; the off-null method of 1968,  $+0.008^\circ$ ; and the power ratio method of 1968,  $-0.012^\circ$ . Note, the average vane angle error line shows a decrease from  $+0.044^\circ$  in 1960 to a  $-0.012^\circ$  in 1968 for the power ratio method. This shift in the average vane angle error line indicates that the rotor-vane changed  $0.056^\circ$  during the eight year period. Angular slippage is very possible when the zero reference of the dial readout is on the shaft of the drive mechanism geared to the rotor section. This is not uncommon if either end stop is struck sharply.

When a correction equal to the slippage for each method is applied, the average vane angle error lies on the zero deviation line, as shown in figure 16. This figure more clearly illustrates the random point to point deviation which indicates the random error in the measurement process. Table 8 shows the deviation in decibels from nominal after the correction was applied to the angular deviation. In addition,

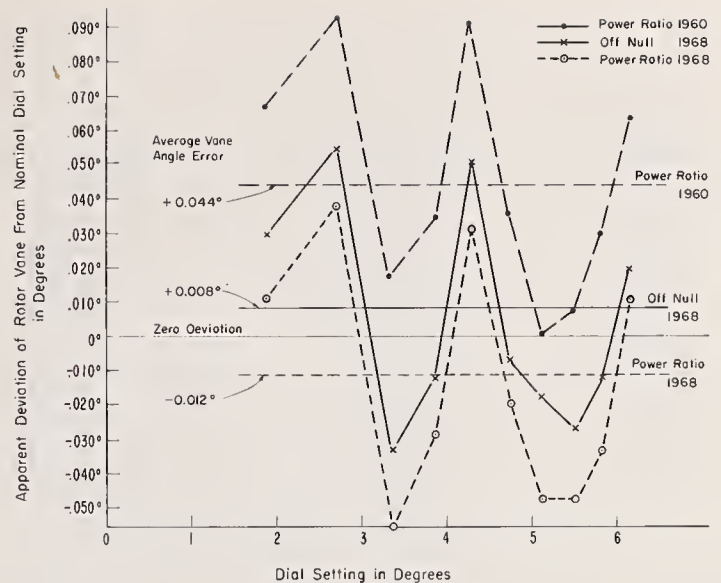


FIGURE 15. Illustrated deviation of the rotor vane of an attenuator calibrated by different methods: power ratio (1960), off-null, and power ratio (1968).

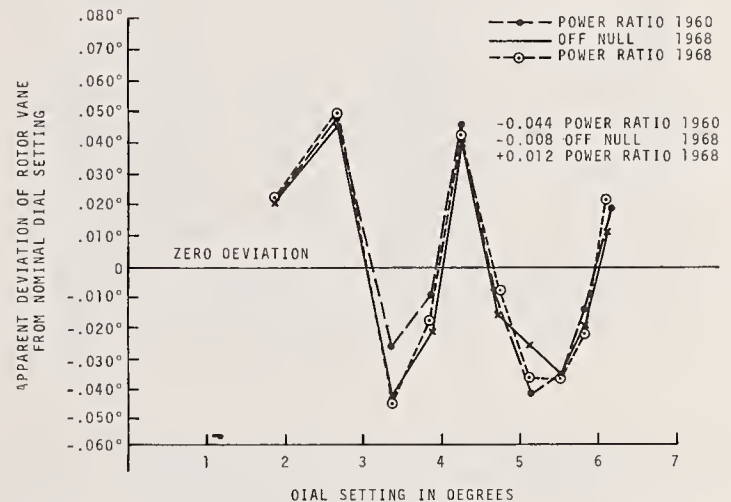


FIGURE 16. Apparent deviation of rotor vane in degrees from nominal at each dial setting in degrees.

The indicated vane angle correction has been applied to each result.

the application of the correction reduced the discrepancy between each comparison. The average discrepancy is improved from 2 to 0.17 percent and from 1 to 0.08 percent, respectively, as shown in table 9, columns five and six.

In figure 16 the large apparent angular deviations are caused by internal reflections and irregularities within the rotary-vane attenuator. The phenomena will be noted in evaluating the low values of attenuation in the optical rotary-vane attenuator. There is a slight indication of a half cycle of eccentricity present, but the 2 degree cycling shown is not caused by eccentricity.



TABLE 8. Comparison of deviation from the average values with vane-angle correction applied

Dial setting (dB)	Average deviation from nominal after correction for rotor slippage	Spread of measured values after correction	Deviation from average value		
			1960 Power ratio	1968 Off-null	1968 Power ratio
0.01	0.00024	0.00003	+0.00001	-0.00002	+0.00001
.02	.00073	.00007	+0.00001	-.00004	+0.00003
.03	.00066	.00021	-.00012	+0.00011	+0.00008
.04	.00020	.00008	-.00001	-.00006	+0.00007
.05	.00011	.00010	.00000	+0.00001	-.00004
0.06	0.00025	0.00020	-0.00001	+0.00015	-0.00010
.07	.00096	.00047	+0.00025	-.00022	-.00004
.08	.00104	.00009	+0.00004	+0.00001	-.00005
.09	.00054	.00021	-.00008	.00011	+0.00005
.10	.00066	.00022	-.00001	-.00010	+0.00012

TABLE 9. Comparison of calibration data with average vane-angle error correction applied

Dial setting (dB)	Deviation (in decibels) from nominal after correction for rotor slippage			Discrepancy between off-null and each power ratio method (in percent) with correction applied	
	1960 Power ratio	1968 Off-null	1968 Power ratio	1960 Power ratio	1968 Power ratio
0.01	-0.00024	-0.00022	-0.00025	-0.2	-0.3
.02	-.00074	-.00069	-.00076	-.25	-.35
.03	+0.00048	+0.00077	+0.00074	+1.0	+1
.04	+0.00019	+0.00014	+0.00027	-.1	-.3
.05	-.00109	-.00114	-.00104	+1	+2
.06	+0.00020	+0.00040	+0.00015	+3	+4
.07	+0.00121	+0.00074	+0.00092	+7	-.3
.08	+0.00108	+0.00105	+0.00099	-.03	+0.7
.09	+0.00046	+0.00065	+0.00059	+2	-.07
.10	-.00065	-.00056	-.00078	-.1	-.2
Average 0.17				0.08	

## 5. Procedures for Evaluating the Rotary-Vane Attenuator

One of the factors affecting the closeness with which the rotary-vane attenuator follows the  $\cos^2$  law is the alignment of the rotor and stator vanes. The ideal properties of this device can be approached when the zero of the dial coincides with the alignment of these vanes. (The limit of idealism is also affected by the maximum attenuation of the rotor section, which will be discussed later.) Several methods are available for the adjustment of the vanes in the rotary-vane attenuator. Optical equipment may be used for a mechanical alignment of the vanes. The electrical method utilizes a waveguide measurement system, where the same energy level is maintained at the detector during the positioning of scale at equal angular marks either side of the  $90^\circ$  position of the rotor vane [5].

Any incorrect alignment of the rotor vane with reference to the scale readout (degrees or decibels) causes a systematic error that is inherent [6] to the rotary-vane attenuator. During the cali-

bration of an attenuator, the operator induces a random error in setting the dial readout on a mark. In making an attenuation difference measurement of a rotary-vane attenuator, the errors at the final setting may be written as

$$\epsilon_{f0} + \epsilon_{ff} = -40 \log_{10} \frac{\cos (\theta_f + \theta_{f0} + \theta_{ff})}{\cos \theta_f} \quad (8)$$

where  $\theta_f$  is the vane angle at the final setting to obtain the calculated attenuation,  $\theta_{f0}$  is the vane-angle error made by the operator at the final setting, and  $\theta_{ff}$  the inherent vane-angle error caused by misalignment.

A table of attenuation error as a function of vane-angle error for rotary-vane attenuators is given in NBS Technical Note 177. The table gives the error,  $\epsilon$ , for a given value of attenuation ( $A = -40 \log_{10} \cos \theta$ ) according to the relationship

$$\epsilon = -40 \log_{10} \frac{\cos (\theta + \theta')}{\cos \theta} \quad (9)$$

where  $\theta$  is the true vane angle and  $\theta'$  is the angle of vane misalignment. Thus, the angle  $\theta'$  is the difference between the indicated vane angle and the correct vane angle. The table is divided into the following intervals of attenuation value increments: 0.01 to 0.1 dB in 0.01-dB increments; 0.1 to 1.0 dB in 0.1-dB increments; 1 to 20 dB in 1-dB increments; and 20 to 70 dB in 5-dB increments. The attenuation errors corresponding to vane-angle error ranging from 0 to  $\pm 0.499^\circ$ , in increments of  $0.001^\circ$ , are presented for each value of attenuation given above.

### 5.1. Determination of Average Vane-Angle Error and Eccentricity from Calibration Data

With the aid of the table of Technical Note 177, the calibration data of the rotary-vane attenuator can be analyzed for numerous characteristics, such as misalignment of the scale readout with reference to the rotor and stator vanes, gear-eccentricity related runout and backlash, realignment techniques, and resettability.

The equal angle technique of rotor vane alignment was assumed to be without error, but NBS has reported that eccentricity in the gear mechanism induces an error of alignment when the above technique is analyzed [6].

#### 5.1.1. Analysis of Calibration Data

Let us evaluate the calibration data at specific dial settings of the rotary-vane attenuator for the presence of an alignment error and eccentricity. A range of attenuation from 10 to 50 dB requires a little more than one cycle of the 3-cycle gear drive

and scale readout. Table 10, columns one and two, show the dial settings and measured values of attenuation in decibels. The dial error or the deviation of the measured values in decibels from nominal are shown in column three. The estimated vane angle for each dial setting is determined by use of NBS Technical Note 177 and is recorded in column four. (An example of the use of Note 177: on page 90, for a nominal setting of 10 decibels, the measured dial error of 0.038 dB is found in row nine, column six, to correspond to a vane-angle error of  $0.085^\circ$ .) Column five shows the attenuation error corresponding to the average vane-angle error of  $0.064^\circ$  for each dial setting. The estimated vane-angle error (column four) minus the average vane-angle error ( $0.064^\circ$ ) yields the values in column six. Column seven shows the error in decibels after correcting for the average vane-angle error. In figure 17a the circles are a plot of column three and the solid curve represents the values from column five. In figure 17b, the circles are a plot of column seven. The deviations around the zero reference line indicate the appropriateness of applying an average vane-angle correction to all the readings.

#### 5.1.2. Cyclic Pattern of Angular Displacement

In order to illustrate the magnitude of the apparent angular displacement in degrees, the values of column four and six (table 10) are plotted in figure 18. The curve  $\theta'_c$  is a plot of column four with the average vane-angle error value,  $0.064^\circ$ , as a reference. The cyclic pattern of the angular displacement indicates the presence of an indexing error [6]. The curve  $\theta'_v$  is a plot of column six, and indicates the reference line shift when the  $0.064^\circ$  correction is applied to the rotor alignment.

TABLE 10. Summary of data for determining average vane-angle error of a rotary-vane attenuator

Dial setting in decibels	Measured value in decibels	Dial error in decibels	Estimated vane-angle error	Attenuation error in decibels for the average of the estimated vane-angle error in degrees	Deviation from average estimated vane-angle errors in degrees	Error in decibels with correction for average estimated vane-angle applied
10	10.038	0.038	+ 0.085	0.028	+ 0.021	+ 0.009
12	12.050	.050	+ .096	.034	+ .032	+ .017
14	14.048	.048	+ .079	.039	+ .015	+ .009
17	17.046	.046	+ .061	.048	- .003	- .002
20	20.026	.026	+ .029	.058	- .035	- .032
25	25.034	.034	+ .027	.080	- .037	- .046
30	30.072	.072	+ .043	.107	- .021	- .035
35	35.160	.160	+ .071	.145	+ .007	+ .016
50	50.475	.475	+ .087	.348	+ .023	+ .127
Average.....			+ 0.064			



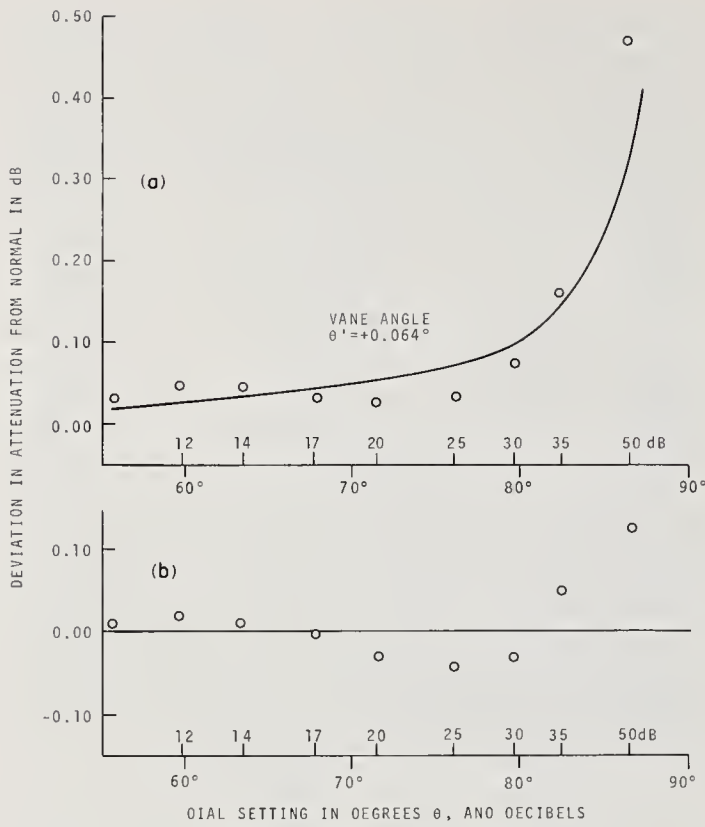


FIGURE 17. Graphs of deviations in attenuation from nominal versus dial setting in decibels and degrees.

- a. Measured deviation (circles) and computed deviation for  $+0.064^\circ$  vane-angle error.  
b. Measured values after applying  $-0.064^\circ$  vane angle correction.

## 5.2. Gearing Errors Related to Rotary-Vane Attenuator

The equations related to the angular errors in gears [20, 21] have been applied to the angular motion of the rotating section of the rotary-vane

attenuator [6]. The angular rotation of the driven gear concentric about the rotor section of the attenuator is represented as the angle  $\theta$ . With a gear ratio of 12 to 1, the angle of the drive gear  $\delta'$  equals  $12\theta$ . Let  $\alpha$  be the angular difference between the zero point of the drive gear eccentricity and the zero point of the scale on the dial in degrees.

The angular displacement of the rotor vane in degrees caused by the indexing error is written as

$$\theta'_{\gamma} = \frac{180 TCE}{\pi D} \sin(12\theta + \alpha) \quad (10)$$

where  $D$  is the pitch diameter and  $TCE$  is the total composite error.

The angular displacement of the rotor vane in degrees caused by backlash error is written as

$$\theta'_{\beta} = \frac{360 TCE}{\pi D} [1 - \cos(12\theta + \alpha)] \tan \phi \quad (11)$$

where  $\phi$  is the pressure angle.

The angular displacement of the rotor vane caused by the total angular error is

$$\theta'_{\tau} = \frac{180 TCE}{\pi D} \cdot [\sin(12\theta + \alpha) + 2\{1 - \cos(12\theta + \alpha)\} \tan \phi]. \quad (12)$$

The total angular displacement,  $\tau$ , is equal to the sum of the backlash error,  $\beta$ , and the indexing error,  $\gamma$ . A relationship of these angular displacements in degrees versus the drive gear rotation is plotted for  $360^\circ$  in figure 19. With a gear ratio of 12, a rotation of the drive gear of  $360^\circ$  ( $12\theta$ , or  $\delta'$ ) is equal to a rotor section rotation of  $30^\circ$  ( $\theta$ ). Thus, the drive gear rotation equals  $1080^\circ$  for a  $90^\circ$  rotation of the rotor section.

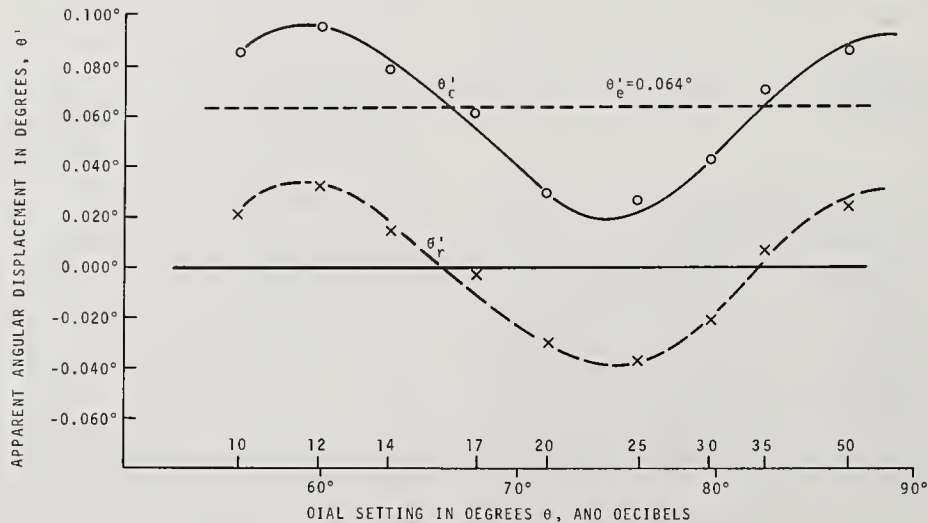


FIGURE 18. Graphs of the cyclic pattern of angular displacement curve,  $\theta'_r$ , with average vane-angle error of  $+0.064^\circ$  and  $\theta'_r$  with  $-0.064^\circ$  correction.



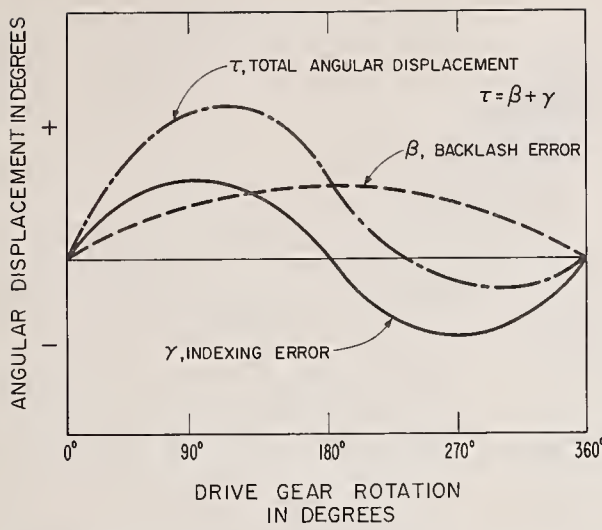


FIGURE 19. Variations in gear eccentricity error.

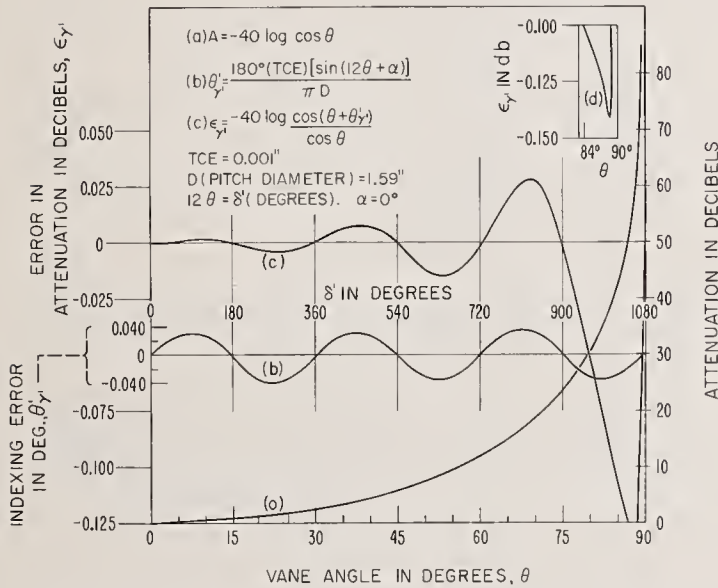


FIGURE 20. Attenuation as a function of vane angle, variation in the indexing error for the three cycles, and the error in attenuation from nominal for the dial settings of 0 to 90°.

The curve of angular displacement for  $\theta'_\gamma$  (fig. 18) shows the maximum value to be  $\pm 0.040^\circ$  between dial setting of 10 to 50 dB ( $55^\circ$  to about  $85^\circ$ ). Let us assume that the pitch diameter of the driven gear (rotor section) is about 1.59" and  $\alpha$  equals zero. Using eq (10) the TCE is calculated to be about 0.001" for this attenuator.

We can best illustrate the effect of the indexing error relative to the error in attenuation by plotting the values obtained in eqs (1), (10), and (9) versus the vane angle rotation,  $\theta$ , in degrees, as shown in figure 20. The curve (a) is a plot of eq (1) showing the increase of attenuation from 0 to greater than 80 dB as  $\theta$  increases from 0 to about  $90^\circ$ . The curve

(b) is a plot of eq (10) displaying the indexing error from maximum to minimum for the 3 cycles of the drive gear ( $\delta'$ ), or as  $\theta$  increases from 0 to  $90^\circ$ . The curve (c) is a plot of eq (9) representing the error in attenuation in decibels for the values of  $\theta$  from 0 to about  $90^\circ$ . The curve of the error in attenuation shows the cyclic pattern similar to the indexing error but the magnitude of the attenuation error increases at the larger values of  $\theta$ . For example, the attenuation error is less than 0.005 dB during the first cycle of the gear drive,  $\theta = 0$  to  $30^\circ$ ; increases to about 0.015 dB in the second cycle,  $\theta = 30$  to  $60^\circ$ ; and reaches a maximum of 0.140 dB in the last cycle,  $\theta = 60$  to  $90^\circ$ . In figure 20 the insert (d) shows that the maximum error occurs at about  $88^\circ$  for the vane angle  $\theta$ , which is about  $5\frac{1}{2}$  degrees from the maximum indexing error during the third cycle.

### 5.2.1. Effects of $\alpha$ on $\epsilon'_{\gamma'}$

The zero point on the scale of the readout does not usually coincide with the zero point of drive gear eccentricity. Nor does the manufacture attempt to control this phenomenon. Therefore the value of the angle  $\alpha$  may vary from 0 to  $\pm 180^\circ$ . Table 11 shows the values of the angle  $\alpha$  where the maximum and minimum deviations in attenuation,  $\epsilon'_{\gamma'}$ , occurs for the dial settings of 10, 20, 30, 40, and 50 dB. It can be seen that the difference between the two values of  $\alpha$  at any setting of  $\theta$  is always  $90^\circ$ .

TABLE 11. Angular values of  $\alpha$  for maximum and minimum  $\epsilon'_{\gamma'}$  at 10, 20, 30, 40, and 50 dB dial settings

Dial setting in decibels	$\theta$	$\alpha$	
		max $\epsilon'_{\gamma'}$	min $\epsilon'_{\gamma'}$
10	55.7821°	-39.3852°	+50.6148°
20	71.5650°	-48.7800°	+41.2200°
30	79.7567°	+32.9196°	-57.0804°
40	84.2608°	-21.1296°	+68.8704°
50	86.7763°	-51.3156°	+38.6844°

The graphs in figures 21, 22, 23, 24, and 25 show the error in attenuation for different pitch diameters of the driven gear for dial settings 10, 20, 30, 40, and 50 dB, respectively. These errors were determined by calculating  $\theta'_\gamma$  for the changes in  $\alpha$ . In figure 21, at a dial setting of 10 dB, the changes in  $\alpha$  vary from -39.3852 to +50.6140°. The dotted line indicates the values of the error in attenuation when  $\alpha$  equals zero, and  $\delta'$  indicates the number of degrees rotation of the drive gear to obtain a dial setting of 10 dB.

In order to change the value of attenuation from 10 to 50 dB, the drive gear has an angular rotation (669.352 to 1041.3156°) of about  $372^\circ$ , or a few degrees beyond one cycle of the possible 3 cycles range of the attenuator. The driven gear has a angular rotation (55.7821 to 86.7763°) of about  $31^\circ$  or

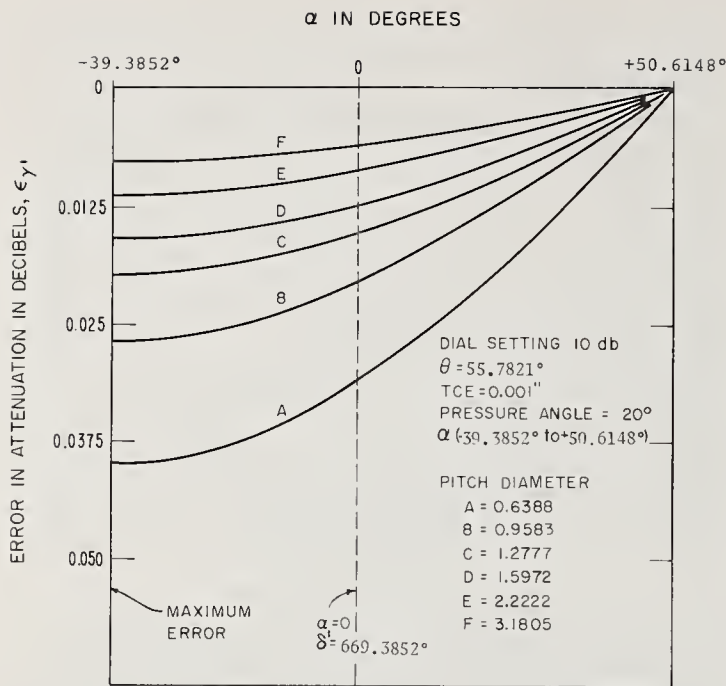


FIGURE 21. Errors in attenuation at the dial setting of 10 dB versus the angle  $\alpha$  for different pitch diameters.

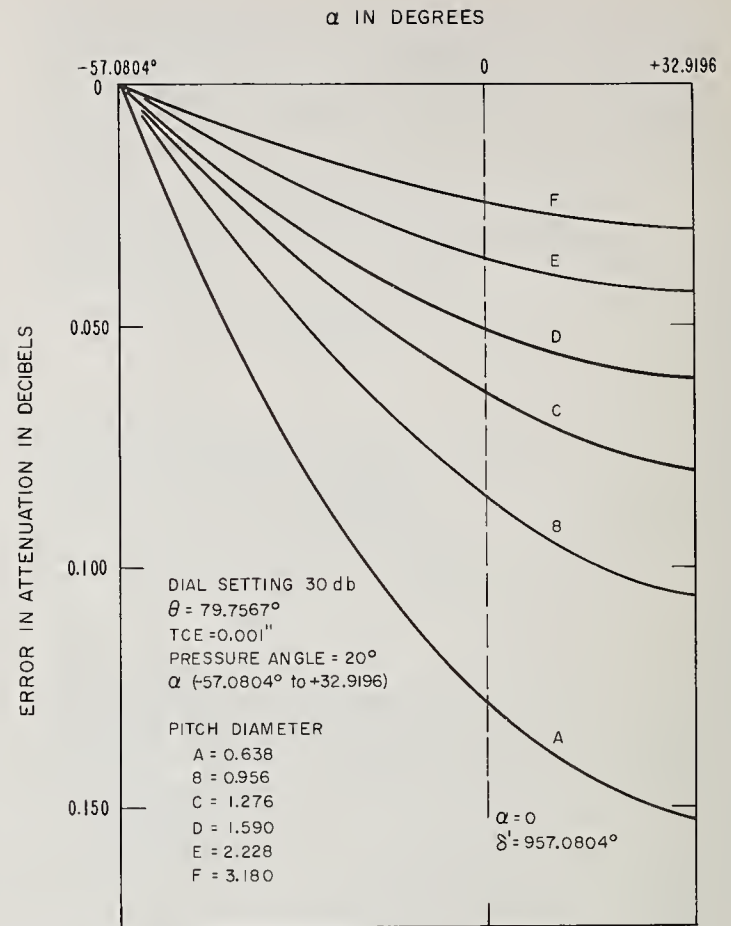


FIGURE 23. Errors in attenuation at the dial setting of 30 dB versus the angle  $\alpha$  for different pitch diameters.

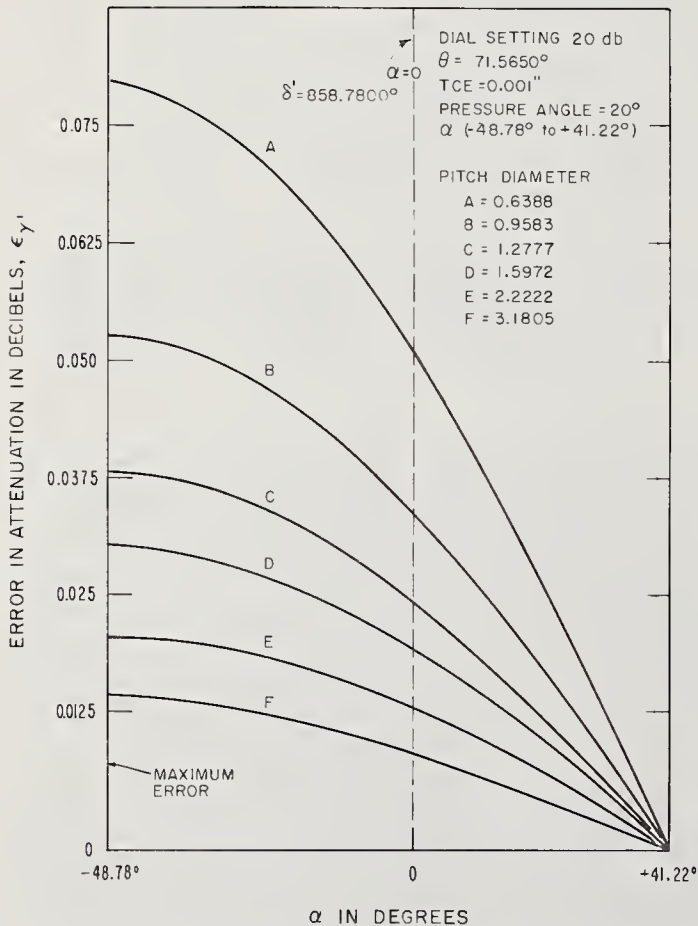


FIGURE 22. Errors in attenuation at the dial setting of 20 dB versus the angle  $\alpha$  for different pitch diameters.

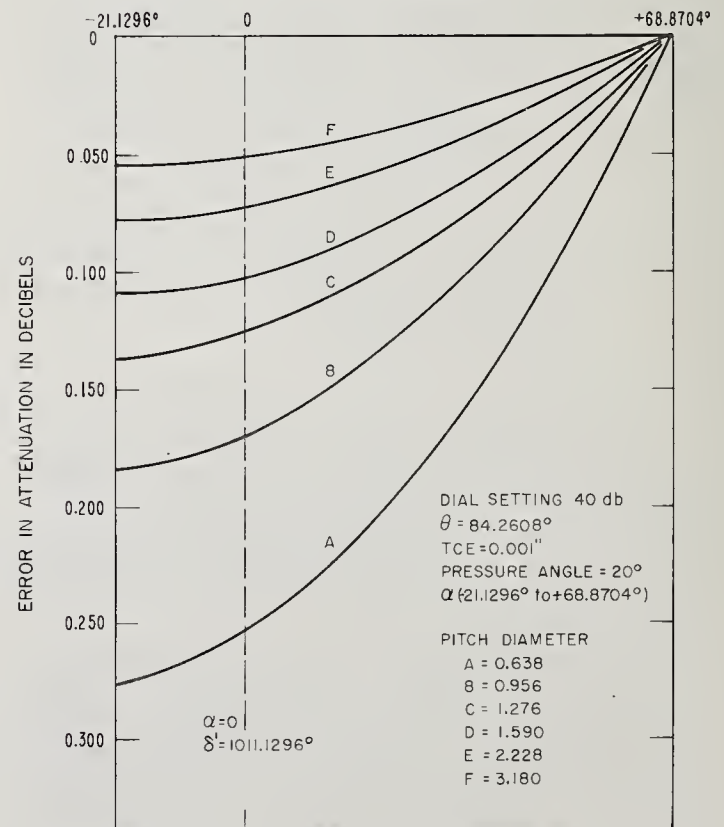


FIGURE 24. Errors in attenuation at the dial setting of 40 dB versus the angle  $\alpha$  for different pitch diameters.

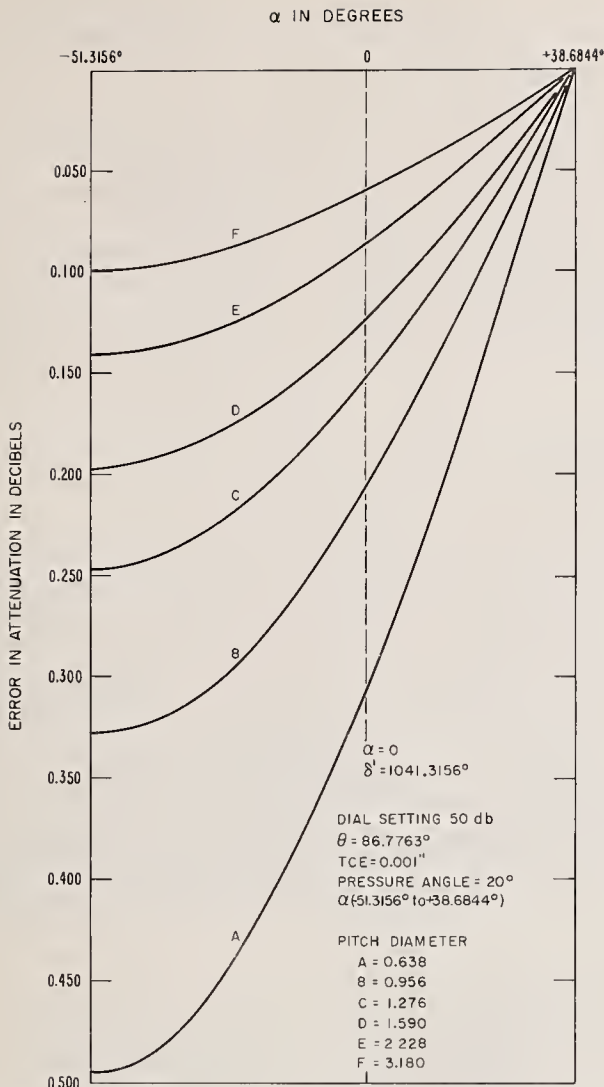


FIGURE 25. Errors in attenuation at the dial setting of 50 dB versus the angle  $\alpha$  for different pitch diameters.

one third of the 0 to 90° possible displacement of the rotor section. As shown in figure 20, the indexing error goes through three positive and three negative maximums from 0 to 1080° rotation,  $\delta'$ , of the drive gear. The maximum positive and negative indexing errors occur at fixed angular displacements of  $\theta$ . Table 12 shows the angular values of  $\theta$  where these maximums occur and their respective theoretical values of attenuation in decibels.

TABLE 12. Angular values of  $\theta$  where maximum (+ or -) deviations of attenuation occur due to indexing error in 3-cycle drive and the corresponding theoretical attenuation values

$\theta$	Max	Decibels
7.5°	+	0.149257
22.5°	-	1.375386
37.5°	+	4.021334
52.5°	-	8.622115
67.5°	+	16.686414
82.5°	-	35.372093

### 5.2.2. Effects of Pitch Diameter on Error of Attenuation

The pitch diameter of the driven gear affects the angular displacement errors as indicated by eqs (10), (11), and (12). The waveguide size usually is the determining factor for the value of the pitch diameter used as the driven gear. The rotary-vane attenuators in the millimeter range require smaller waveguide components and normally a driven gear having a smaller pitch diameter is mounted on the rotor section. The graphs of figures 26, 27, 28, 29, and 30 indicate the maximum error in attenuation for the displacement angles  $\theta'_\gamma$ ,  $\theta'_\beta$  and  $\theta'_\tau$  for changes in pitch diameter at 10, 20, 30, 40, and 50-dB dial settings, respectively. The pressure angle  $\phi$  appears in eqs (11) and (12) and curves are plotted for 20° and 14.5° pressure angles to illustrate the change in attenuation error for  $\theta'_\tau$  and  $\theta'_\beta$ . The indexing error is not changed by the pressure angle of the gears; thus, only one curve is needed to show this error at each dial setting. All graphs show that an increase in pitch diameter of the driven gear decreases the error in attenuation caused by any one of the displacement errors.

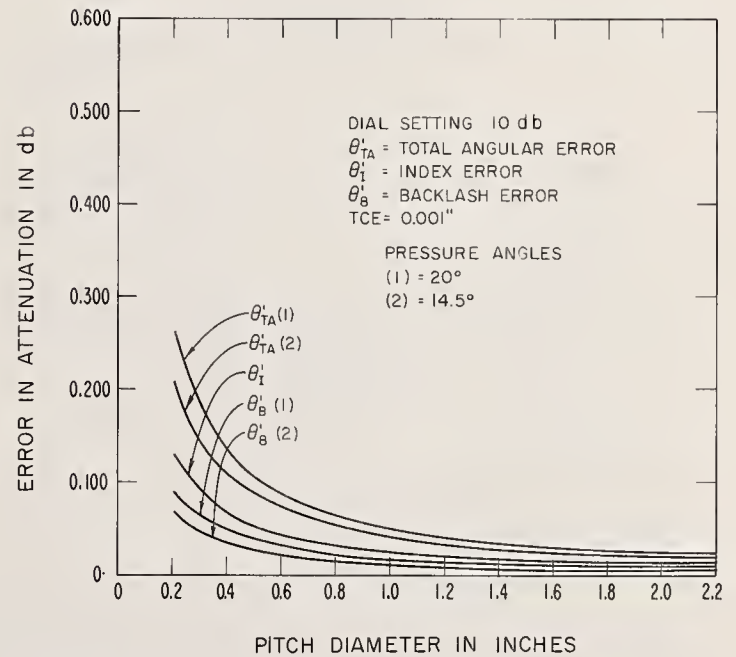


FIGURE 26. Errors in attenuation at the dial setting of 10 dB versus pitch diameter for the angular displacement error.



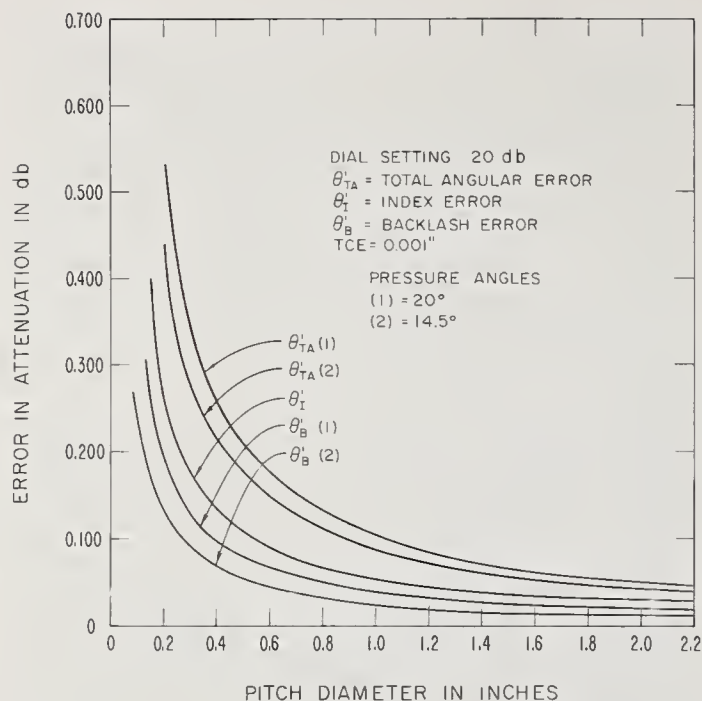


FIGURE 27. Errors in attenuation at the dial setting of 20 dB versus pitch diameter for the angular displacement error.

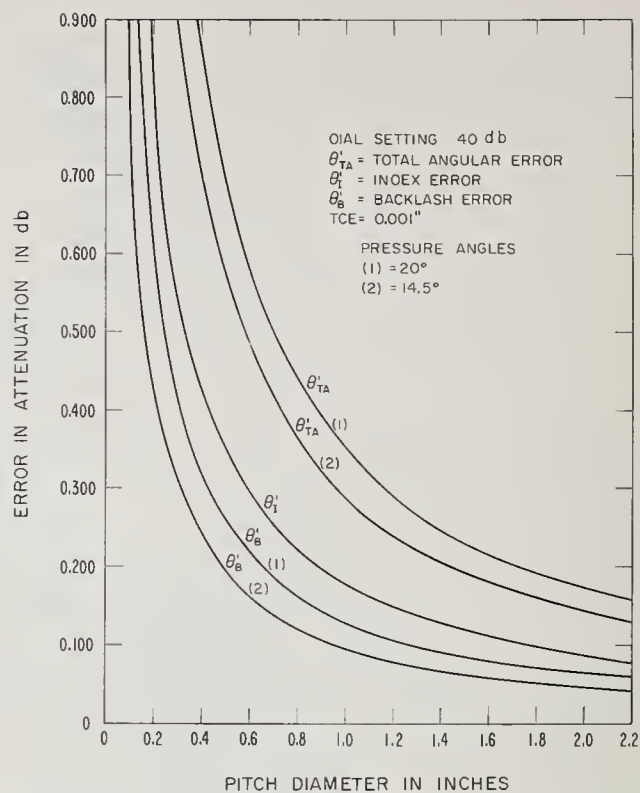


FIGURE 29. Errors in attenuation at the dial setting of 40 dB versus pitch diameter for the angular displacement error.

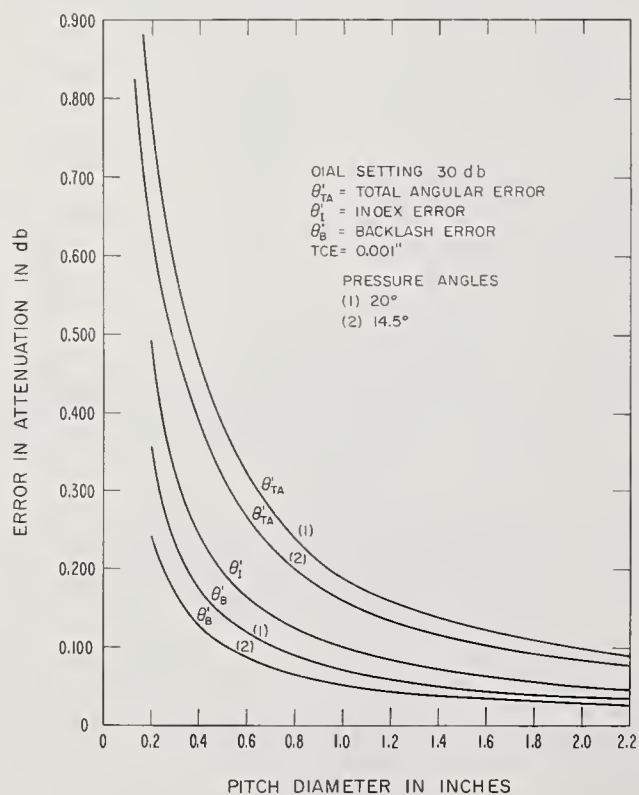


FIGURE 28. Errors in attenuation at the dial setting of 30 dB versus pitch diameter for the angular displacement error.

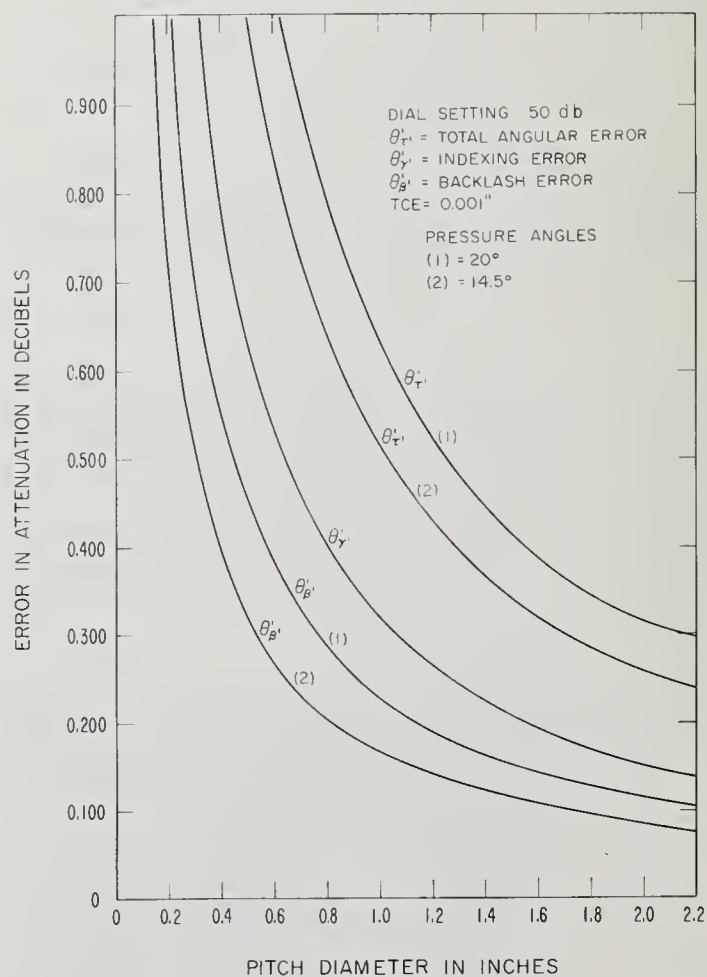


FIGURE 30. Errors in attenuation at the dial setting of 50 dB versus pitch diameter for the angular displacement error.

## 6. Compensation for Transmission Error of Rotary-Vane Attenuator

The transmission error becomes less as the magnitude of the maximum attenuation is increased in the rotor section of the attenuator. Otoshi [9] has presented a modified law that provides a tool for extending the useful dynamic range of the rotary-vane attenuator with low values of maximum attenuation. A mechanical technique of increasing the dynamic range may be achieved by adjusting the input stators of the attenuator.

### 6.1. Transmission Error versus Dial Setting in Decibels

With a known maximum attenuation value at  $\theta$  equals  $90^\circ$ , the transmission error can be determined from eq (5). In order to make quick estimates of the transmission error, eq (5) was used to obtain figure 31. The graphs show that the transmission error is about 0.03 dB at the dial setting of 50 dB for an attenuator with a 100-dB maximum. The error increases to a value of 0.3 dB for a maximum attenuation of 80 dB at the same dial setting. However, the error decreases to about 30 microbels if a 160-dB maximum attenuation can be achieved in the center section of the attenuator.

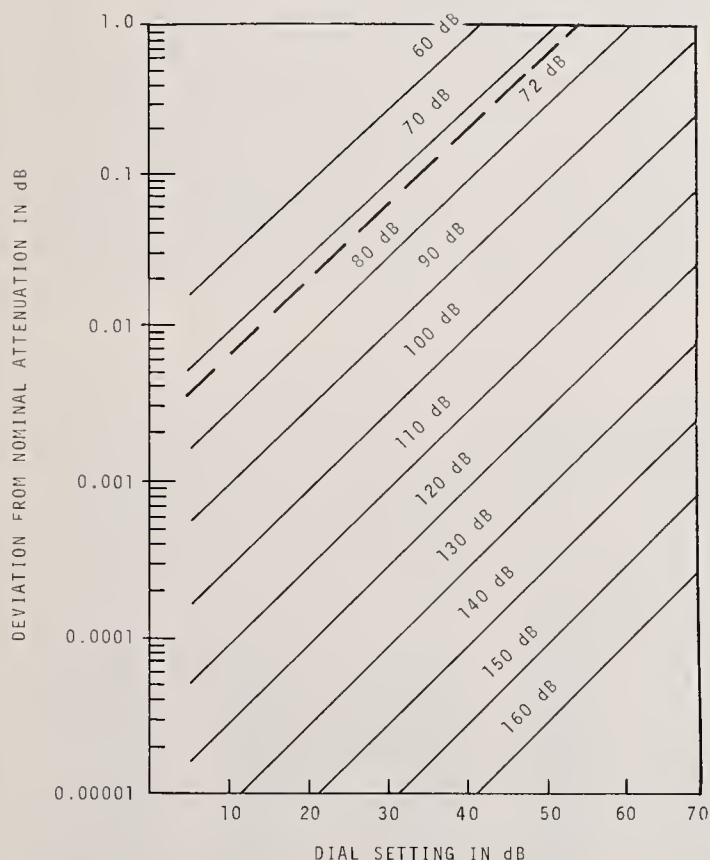


FIGURE 31. Estimate of the transmission error versus dial setting in decibels for maximum attenuation values of 60 to 160 dB.

### 6.2. Stator Realignment

The mounting holes of each stator are enlarged to enable angular rotation around the longitudinal axis of the waveguide sections of the rotary-vane attenuator. The stators may be rotated either direction with reference to the input port of the attenuator, as shown in figure 32. The Type B error in part (A) indicates that stator S1 was rotated  $1/2^\circ$  clockwise and stator S2 was rotated  $1/2^\circ$  counterclockwise; and in part (B) indicates that the stators were rotated conversely. From eq (3) the calculated deviation was determined to be 0.066 dB for the dial setting of 40 dB. The measured attenuation difference deviated from calculated attenuation by 0.009 and 0.015 dB for the conditions A and B, respectively, at the dial setting of 40 dB. However, the  $1/2^\circ$  rotation of the stators induced an increase in the attenuation difference of about 0.08 dB in both cases at the 40-dB setting. In other words the Type B error of misalignment increases the value of attenuation for nominal dial settings. As will be shown later, intentional misalignment of the stators can effectively compensate for insufficient maximum attenuation.

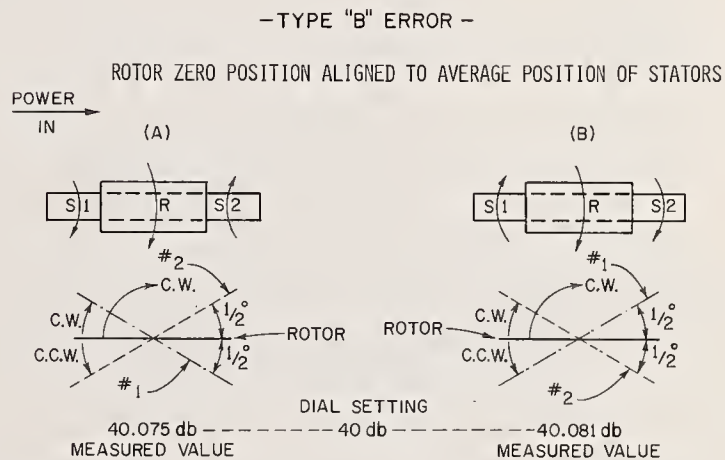


FIGURE 32. Illustration of stator rotation and rotor alignment to induce the Type B error.

#### Angular Displacements versus Maximum Attenuation

In figure 33 the smooth curve provides an estimate of the angular displacement,  $\theta'/2$ , which the stators require to compensate for the values of maximum attenuation. The angular displacement equals about  $1.05^\circ$  for 70 dB and decreases to an angle of  $0.018^\circ$  for 140-dB maximum attenuation. For example, the graph shows that the stators must be rotated about  $0.18^\circ$  to compensate for the transmission error when maximum attenuation equals 100 dB. In order to determine the value of compensation in decibels, refer to NBS Technical Note 177. Page 139 gives the attenuation deviation versus

angular deviation for the nominal value of 50 dB,  $\theta = 86.7763^\circ$ . For example, column 1 and line 2 give values of +0.997123 dB and -0.942820 dB corresponding to the angular deviation of  $0.18^\circ$ . The value of compensation,  $\epsilon'_b$ , equals 0.027515 dB, which is one-half of the algebraic sum of the attenuation deviation in decibels. This result can be computed from eq (3). Figure 31 shows that the deviation from

nominal attenuation in decibels equals about 0.027 dB for a dial setting of 50 dB and the maximum attenuation line of 100 dB.

Realignment of the stators causes the end ports of the rotary-vane attenuator to be out of alignment with the ports at the insertion point of the measurement system. Therefore, a waveguide adapter with an angular twist equal to  $\theta'/2$  should be placed at the ends of each stator. The twists becomes a part of the attenuator after the angular displacement is determined by the maximum attenuation of each attenuator. Table 13 shows the angular correction,  $\theta'/2$ , required for maximum attenuation values of 90 to 160 dB in 10-dB intervals. The distance  $b'$  necessary to produce the angular correction is given for eleven waveguide sizes from WR15 to WR650. The angular displacement has been converted to length in inches or distance  $b'$  from a reference plane, as shown in figure 2.

### 6.3. Illustration of Transmission Error and Compensation for 110-dB Maximum

Figure 34 illustrates the deviations in attenuation from nominal by giving both the increase in attenuation caused by misaligning the stators and the decrease caused by insufficient maximum attenuation, respectively. The deviations are plotted for dial settings from 20 to 70 dB. The solid curve indicates the calculated (eq (5)) deviations in attenuation for an attenuator of 110-dB maximum. (Fig. 31 can be used for rapid estimates.) The dashed curve indicates the calculated (eq (3)) deviation in attenuation for an attenuator with  $0.1^\circ$  ( $\theta'/2$ ) stator misalignment. In other words the misalignment of the stator by  $0.1^\circ$  induces an increase in the attenuation which closely compensates for the decrease in the attenuation caused by an insufficient maximum value of 110 dB.

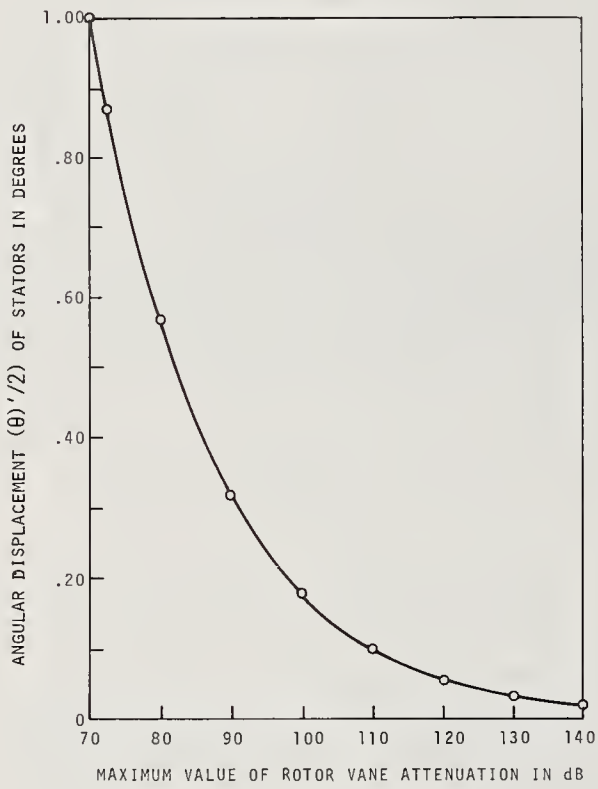


FIGURE 33. Estimated angular displacement of stators in degrees versus the maximum attenuation value of rotor vane in decibels for the compensation required to approach theoretical  $\cos^2 \theta$  law.

TABLE 13. The angular correction required for different values of maximum attenuation and the distance  $b'$  necessary to produce the angular correction for various waveguide sizes

		90 dB	100 dB	110 dB	120 dB	130 dB	140 dB	150 dB	160 dB
$\theta'_2$		0.320°	0.180°	0.100°	0.057°	0.032°	0.018°	0.010°	0.008°
WR	$a$	$b'$							
15	(0.148)	0.00080	0.00046	0.00026	0.00017	0.00008	0.00004	0.00003	0.000020
28	(.280)	0.00150	0.00088	0.00049	0.00031	0.00016	0.00009	0.00005	0.000038
42	(.42)	0.00227	0.00132	0.00073	0.00047	0.00023	0.00013	0.00007	0.000057
62	(.622)	0.00337	0.00195	0.00109	0.00070	0.00035	0.00020	0.00011	0.000084
90	(.900)	0.00488	0.00283	0.00157	0.00101	0.00050	0.00028	0.00016	0.00012
112	(1.122)	0.00608	0.00352	0.00196	0.00126	0.00063	0.00035	0.00019	0.00015
137	(1.372)	0.00745	0.00431	0.00239	0.00154	0.00076	0.00043	0.00024	0.00019
187	(1.872)	0.01015	0.00588	0.00327	0.00211	0.00104	0.00059	0.00033	0.00025
284	(2.840)	0.01541	0.00892	0.00496	0.00319	0.00158	0.00089	0.00050	0.00038
430	(4.300)	0.0233	0.01351	0.00750	0.00484	0.00240	0.00135	0.00075	0.00058
650	(6.500)	0.03527	0.02042	0.01134	0.00731	0.00362	0.00295	0.00113	0.00088

$$b'/2 = a/2 \tan \theta'/2$$

$$b' = a \tan \theta'/2$$



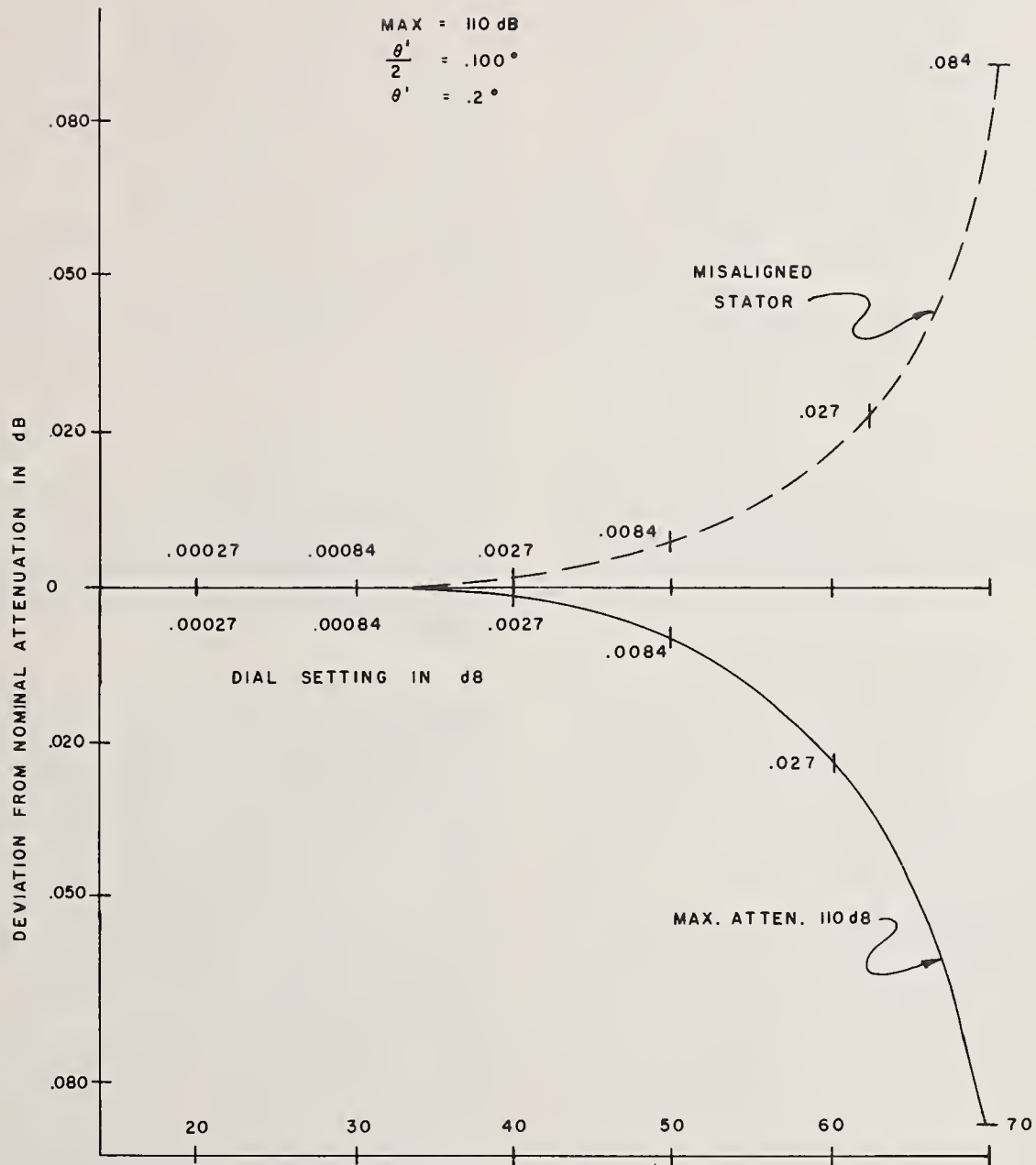


FIGURE 34. Deviation in attenuation caused by misalignment of the stators,  $\theta'$  equals  $0.2^\circ$ , and insufficient maximum attenuation of 110 dB for the dial setting of 20 to 70 dB.

#### 6.4. Mechanical Compensation and Measured Results

In order to experimentally evaluate the compensation technique of stator realignment, a commercially available rotary-vane attenuator was modified. The stator flange bolt holes were enlarged to permit rotation of the stators and the vane in the rotor section was decreased in length. The measured maximum attenuation (at  $\theta$  equals  $90^\circ$ ) dropped from a previous 90 to 72 dB after the rotor section modification. In figure 35, the calibrated values of the modified attenuator are plotted as X points on the solid line curve at dial settings of 20, 30, 40, 50, 60, at 70 dB. The solid line curve indicates the calculated deviation in attenuation for an attenuator with 72-dB maximum attenuation. Referring to figure 33, the angular displacement required for 72-dB maximum is estimated to be about  $0.87^\circ$ . In figure 35, the calculated deviation in attenuation induced by misaligning the stators  $0.87^\circ$  is plotted as the dashed line. The calibration points plotted as  $\otimes$  indicate that the compensation caused the values of 10 to 40 dB to fall in a random manner about the zero deviation line. However, the larger deviation shown at 50 dB is within the limits of the system error and the resettability of the commercial attenuator.

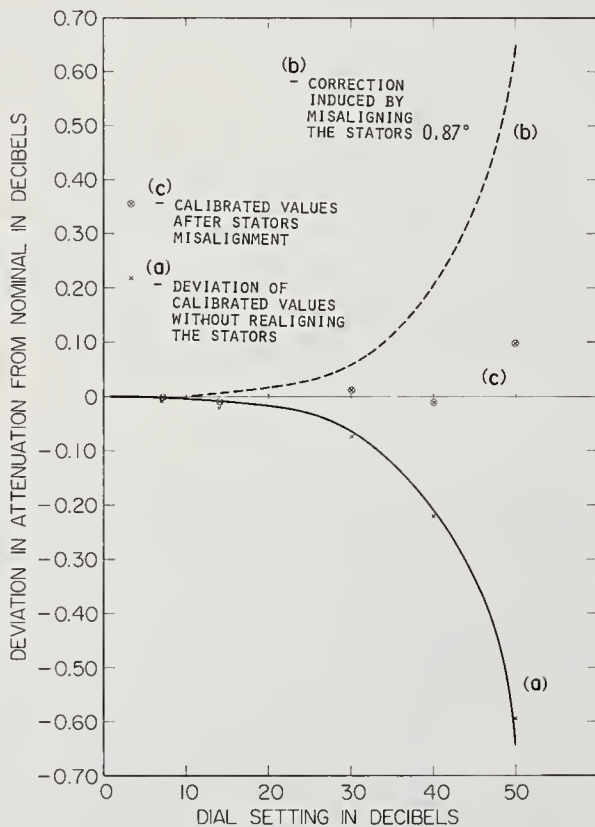


FIGURE 35. Deviation of attenuation from nominal versus dial setting in decibels for rotary-vane attenuator with 72-dB maximum: (a) Curve of calibration points, (b) Curve of correction induced by misaligning the stator  $0.87^\circ$ , and (c) Plot of calibrated values after stator misalignment.

#### 7. Measurements of Precision Rotary-Vane Attenuators With High Resolution Readouts

A calibrated high precision rotary-vane attenuator can be regarded as an ideal working or transfer standard for making precise measurements in a microwave standards laboratory. Regardless of the great care taken in the fabrication of the attenuator, or the high resolution of the dial readout, the device should be evaluated before it is used as a standard. Though several attenuators may be built of identical design and precise fabrication each has distinct inherent characteristics [3, 18].

At present the commercially available rotary-vane attenuators have a dynamic maximum range of 90 to 100 dB. This value of maximum attenuation provides only one-half of the theoretical value attainable at 1 arc second less than  $90^\circ$  rotation of the rotor. The usable scale of these attenuators are marked from 0 to 50 dB. Thus, about one-fourth of the total range of attenuation is at present being used for calibrated interlaboratory standards. Usually this type of rotary-vane attenuator utilizes a spiral scale for the dial readout of attenuation in decibels. The attenuator must be calibrated at nominal values, but even then the resolution and scale readout usually are too coarse for precise interpolation between points of calibration.

At present several angular displacement readouts have been designed for use with precision rotary-vane attenuators. A gear mechanism designed by NBS can be installed onto commercial rotary-vane attenuators to give dial readings of angular displacement of  $0.001^\circ$  from 0 to  $90^\circ$ . The NBS optical rotary-vane attenuator provides an angular displacement with a resolution of  $\pm 1$  second of arc. The Royal Radar Establishment of England has developed a digital angular readout for rotary-vane attenuators. It utilizes a row of numerical indicator tubes and has a resolution of  $0.001^\circ$ .

##### 7.1. Measurement of Rotary-Vane Attenuator With a Gear Driven Readout

The gear mechanism illustrated by the drawings in figures 13 and 14 has been used successfully with commercial rotary-vane attenuators in WR62, WR90, and WR112 waveguide sizes, and adapts to rotary-vane attenuators in waveguide sizes WR137 and WR187 with minor modifications.

The modified attenuator, which now reads in angular displacement of the rotor section, must be calibrated in an attenuation measurement system for use as an attenuation device. The vane-angle error and gear eccentricity can be determined from the calibration data as shown in 5.2. In order to obtain the best possible evaluation of the modified gear driven readout, three measurement systems were used in the calibration of the at-

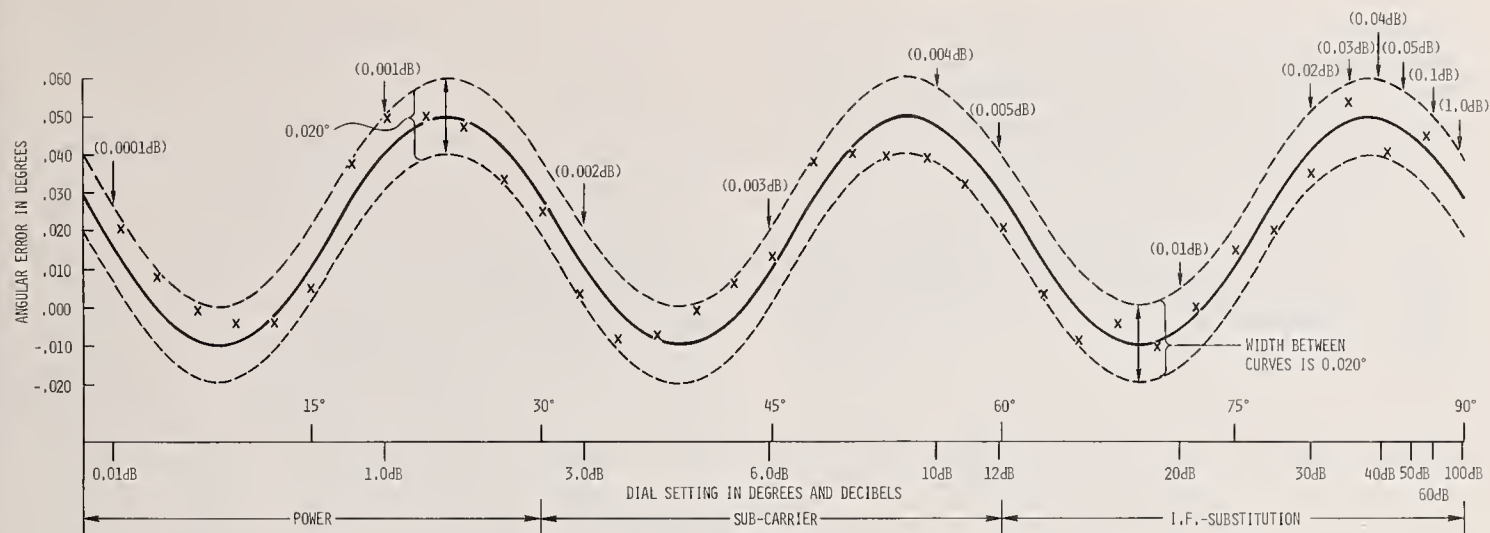


FIGURE 36. Angular error,  $\theta'_r$ , in degrees from nominal (theory) versus the dial setting,  $\theta$ , in degrees, determined from measurements by the power ratio, modulated subcarrier, and i-f substitution methods.

tenuator over a large range. Each measurement system was used to cover a different range of about  $30^\circ$  of angular rotation of the center vane.

#### 7.1.1. Measurements of Precision Gear Driven Rotary-Vane Attenuator

The measured results were obtained as follows: the power ratio method, 0 to  $30^\circ$ ; the modulated subcarrier method, 30 to  $60^\circ$ ; and the i-f substitution method, 60 to  $87.5^\circ$ . The interval of measurement taken was every  $2.5^\circ$  within the  $30^\circ$  section. The measured attenuation at each dial setting was compared with the theoretical value [19] to determine the average vane-angle error in degrees. In figure 36, the curve shows the angular error,  $\theta'_r$ , in degrees from nominal (theory) versus the dial setting,  $\theta$ , in degrees. Each measured value is shown by an X at the  $2.5^\circ$  dial settings of  $\theta$ . The cyclic indexing error is caused by eccentricity (eq (10)) and shows a variation from 0.050 to  $-0.010^\circ$ . The dashed straight line is drawn as the axis of the  $\pm 0.030^\circ$  cyclic indexing error, and represents an average vane-angle error of about  $0.020^\circ$ . In addition to a dial setting scale in degrees, the corresponding values of attenuation in decibels are indicated on the lower part of the horizontal axis of the graph. In other words the range of attenuation difference measurements that were taken by the three different methods were as follows: 0.02 to 2.5 dB, 2.5 to 12 dB, and 12 to 55 dB, by the power ratio, modulated subcarrier, and i-f substitution methods, respectively.

#### 7.1.2. Angular Resettability of Attenuator

The two dashed lines drawn  $\pm 0.010^\circ$  about the cyclic indexing error curve (fig. 36) approximate the

angular resettability of the attenuator. The basic part of the error of resettability is caused by gearing in the commercial attenuator. In addition to the error of resettability the relation of center distances between these gears is the principal cause of the eccentricity or indexing error. The drive gear should be replaced if the runout error is large and the spring loading converted to positive loading of the gear.

The arrows shown on the upper part of the graph give the value of resolution which is indicated within the parenthesis. The resolution in decibels corresponds to the resettability of  $0.020^\circ$  at the various values of  $\theta$ . All values of angular deviation fell within the range of  $0.020^\circ$ , but the deviation in attenuation vary greatly. For example, the deviations in attenuation vary from 10  $\mu$ bels at 0.02-dB dial setting, to about 1 dB at 100-dB dial setting.

When the measured angular deviations were converted to decibels, all the deviations in attenuation were within the systematic and random errors of the corresponding measurement system. This close agreement in following the indexing error of the attenuator shows that any one of the measurement systems could be used to calibrate the attenuator over an assigned part of its range. Therefore extrapolation of the cyclic error over any other part of the range could be used to set limits of error for the entire attenuator.

#### 7.2. Mounting the Gear Drive

We recommend that the drive gear be selected with care and spring loading be removed, before applying a precision gear mechanism to the attenuator. Figure 37 illustrates the angular error of the attenuator when a gear box was mounted on the rotary-vane attenuator without modifying the drive gear. The curve illustrates the angular error over



a range of about  $70^\circ$  rotation of the center vane (about two and one-third revolutions of the drive gear for a 12 to 1 ratio). The large half-cycle error was caused by a binding effect between the drive gear and the driven gear (concentric to the rotor section). When more precise machining techniques were applied to the mounting of the precision readout, the cyclic indexing error became a cyclic pattern as shown in figure 38. Note that the average angular displacement error was reduced from about  $0.450$  to  $0.040^\circ$ .

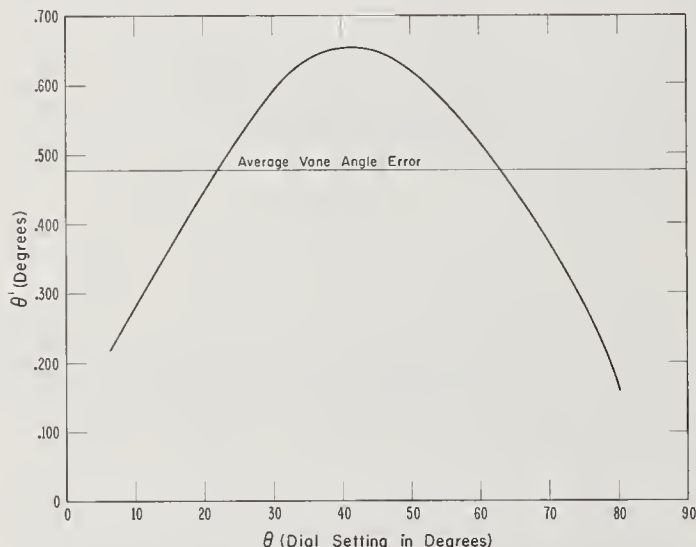


FIGURE 37. Angular error caused by binding effect between the drive gear and the driver gear (concentric to the rotor section).

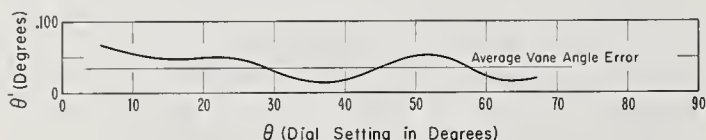


FIGURE 38. Angular error,  $\theta'$ , in degrees versus dial setting in degrees,  $\theta$ , after precise machining was applied.

### 7.3. Optical Rotary-Vane Attenuator

The optical rotary-vane attenuator designed at NBS virtually eliminates gear eccentricity errors. The readout scale of the attenuator gives an optical display of the angular rotation of the rotor section in degrees, minutes, and seconds of arc from 0 to  $360^\circ$ . However, the attenuator is used in its normal function from 0 to  $90^\circ$ . The final version of the optical rotary-vane attenuator followed the cos squared law more closely than any attenuator previously calibrated at NBS. Notwithstanding, earlier fabrications of the attenuator had problems other than gearing to solve.

#### 7.3.1. Measurements on Optical Rotary-Vane Attenuator

In order to evaluate the attenuator over a wide dynamic range, it was calibrated by three different methods in the same manner as was the precision gear driven attenuator. The attenuation deviations in decibels and the angular deviations in degrees are plotted versus dial setting in degrees (refer to fig. 39). The portion of the curves corresponding to the first  $30^\circ$  of dial setting shows the deviations in attenuation and angular displacement as determined by the power ratio measurement system. This portion of the curve shows deviations in attenuation from  $-0.0025$  to  $0.0045$  dB or in angular displacement from  $-0.046$  to  $0.024^\circ$ . Neither the power measurement system nor a precision attenuator cause such large mechanical or electrical deviations. The calibration data for  $30$  to  $60^\circ$  and  $60$  to  $87.5^\circ$  portions of the dial settings were obtained by the modulated subcarrier, and  $i$ - $f$  substitution methods, respectively. Again the electrical deviations were large for each specific method:  $0.004$  dB in the subcarrier system and  $0.026$  dB in the  $i$ - $f$  system. In addition to large electrical and mechanical equivalent angular deviations, the apparent average vane-angle error falls off from a  $+0.010^\circ$  to a  $-0.005^\circ$ . This error falls off more rapidly at the higher values of attenuation. All of these deviations in measurement of attenuation and decrease in the angular errors show that the center vane has insufficient maximum attenuation (below the required amount for a precision rotary-vane attenuator). The evidence of  $0.015^\circ$  decrease in the average vane-angle error indicates that the maximum attenuation is less than  $90$  dB.

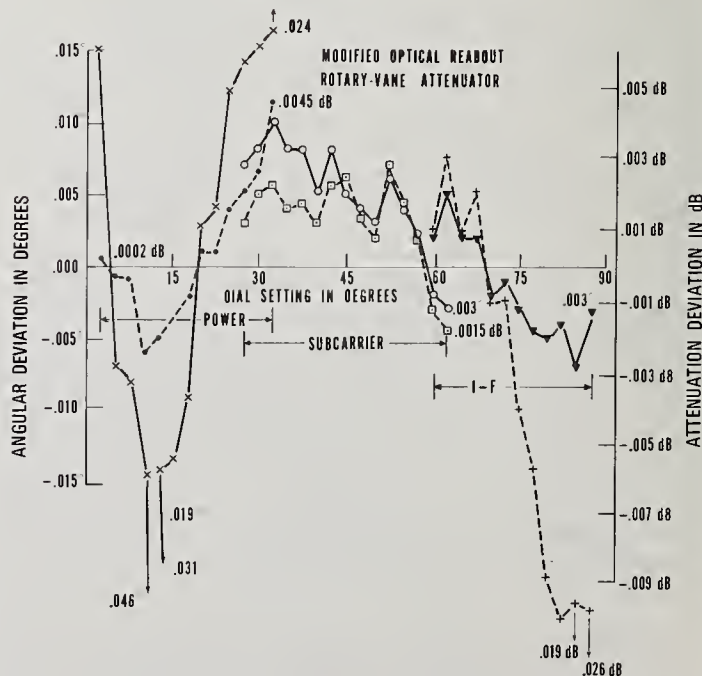


FIGURE 39. Deviation in decibels and degrees versus dial setting in degrees.

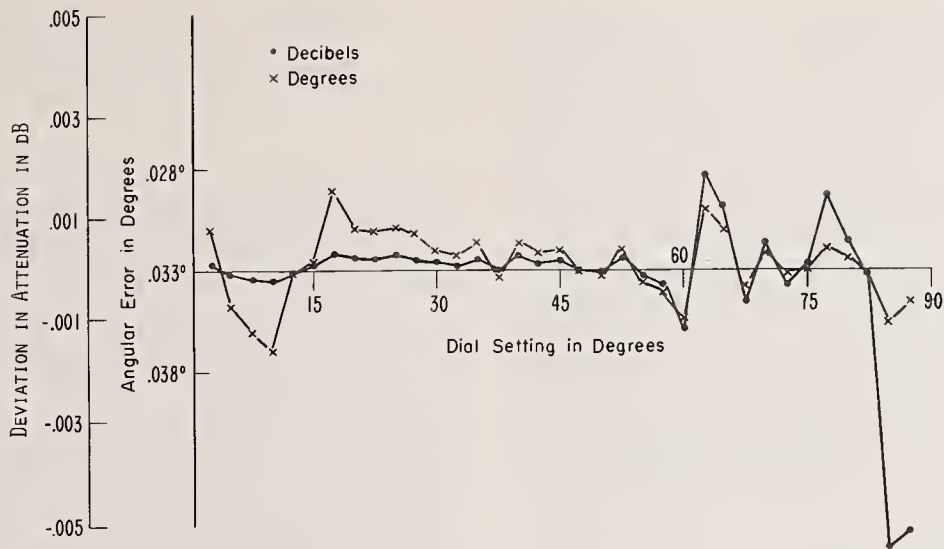


FIGURE 40. Deviation in decibels and degrees versus dial setting in degrees, after repair of the rotor section.

### 7.3.2. Measurements after Rotor Repair

The center vane was replaced and care taken to properly cement it to the rotor section. After repairing the rotor section, the attenuator was recalibrated using the same systems as before. In figure 40 the plot of these measured deviations shows that the average vane-angle error is now  $0.033^\circ$ . The deviation in attenuation difference is about  $\pm 0.001$  dB with reference to the average vane-angle error line from  $0$  to  $60^\circ$  of  $\theta$ , about  $\pm 0.002$  dB from  $60$  to  $80^\circ$ , and  $\pm 0.005$  dB at  $87.5^\circ$  of  $\theta$ . The curve with the mark  $X$  shows the attenuation deviations converted to angular deviations. These deviations have decreased greatly from those shown in figure 39. More important is that the fall off at the higher values of  $\theta$  decreased to about  $0.003^\circ$ ; this corresponds to about 105-dB maximum attenuation in the center vane.

The attenuation deviations from a curve corresponding to a vane-angle misalignment of  $-0.033^\circ$  and to angular deviation from the  $-0.033^\circ$  line were plotted. Figure 41(a) shows the value for a dial setting of  $0$  to  $45^\circ$  while figure 41(b) shows the values for a setting of  $45$  to  $87.5^\circ$ . The deviations of attenuation from the curve corresponding to the  $-0.033^\circ$  vane misalignment were quite small and indicate that such would be a very good compensation for transmission error over the dial range of  $0$  to  $87.5^\circ$ .

## 8. Resolution and Resettability

There are two possible readouts that can be used for rotary-vane attenuators: (1) direct reading of attenuation in decibels; and (2) angular reading of rotor vane rotation in degrees. The use of a readout with angular notation offers the advantage in that the scale is linear, while a direct reading decibel

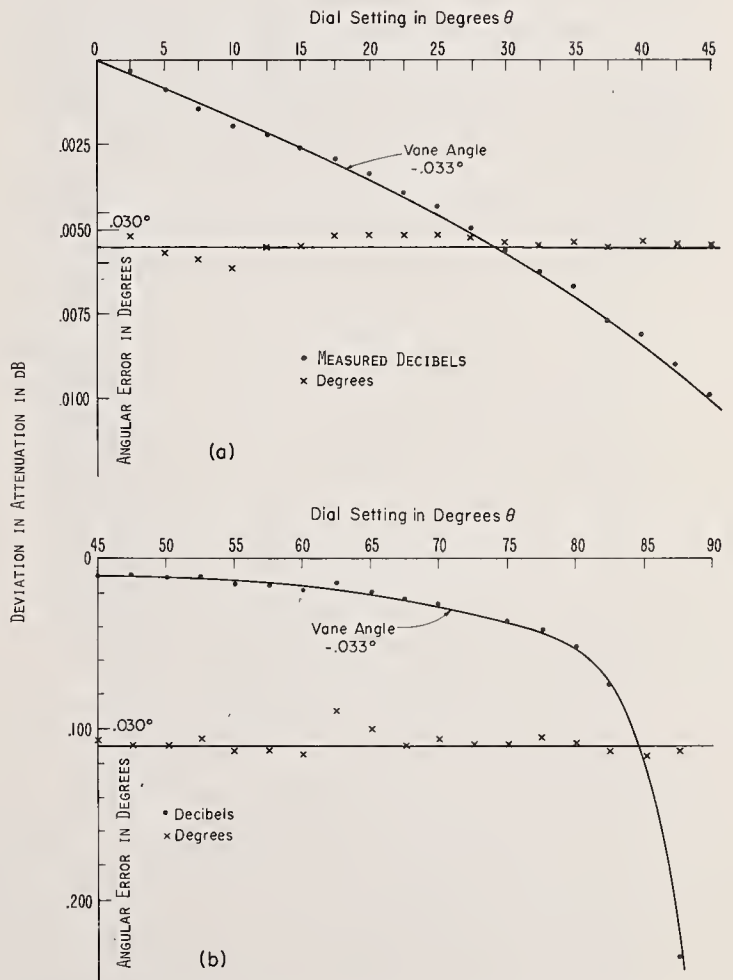


FIGURE 41. (a) Deviation of measured attenuation and equivalent angular deviation from theoretical values for a vane angle correction of  $-0.033^\circ$  versus dial setting of  $0$  to  $45^\circ$ .

(b) Deviation of measured attenuation and equivalent angular deviation from theoretical values for a vane angle correction of  $-0.033^\circ$  versus dial setting of  $45$  to  $87.5^\circ$ .



scale decreases rapidly in resolution at the high values. In addition, interpolation becomes more difficult to estimate as the attenuation rate increases on the decibel scale.

There are occasions when it is important to know to what accuracy a rotary-vane attenuator can be set over its usable range. In order to demonstrate the accuracy of resettability we have elected to use angular notation. Figure 42 shows the resolution error,  $\epsilon_R$ , in attenuation in decibels versus the dial setting,  $A_{dB}$ , in decibels for several values of  $\theta'_R$ , the angular resettability of the rotor vane in degrees. The curves show the magnitude of the resolution error,  $\epsilon_R$ , for values from 0.1  $\mu$ bel to 100 decibels at dial settings of 0.001 to 200 dB for angular resettability of 1 second and 0.001 to 1.0° of arc.

The curves (A to H) provide a quick and convenient means of determining the accuracy in decibels one can expect for a known angular resolution. Also, if the deviation in attenuation from nominal is known, the required angular correction can be determined from the graph. For example, for a rotary-vane attenuator with a deviation of about 0.013 dB at a 10-dB dial setting, curve (E) shows that a correction of 0.03° would be required to give the nominal value of attenuation.

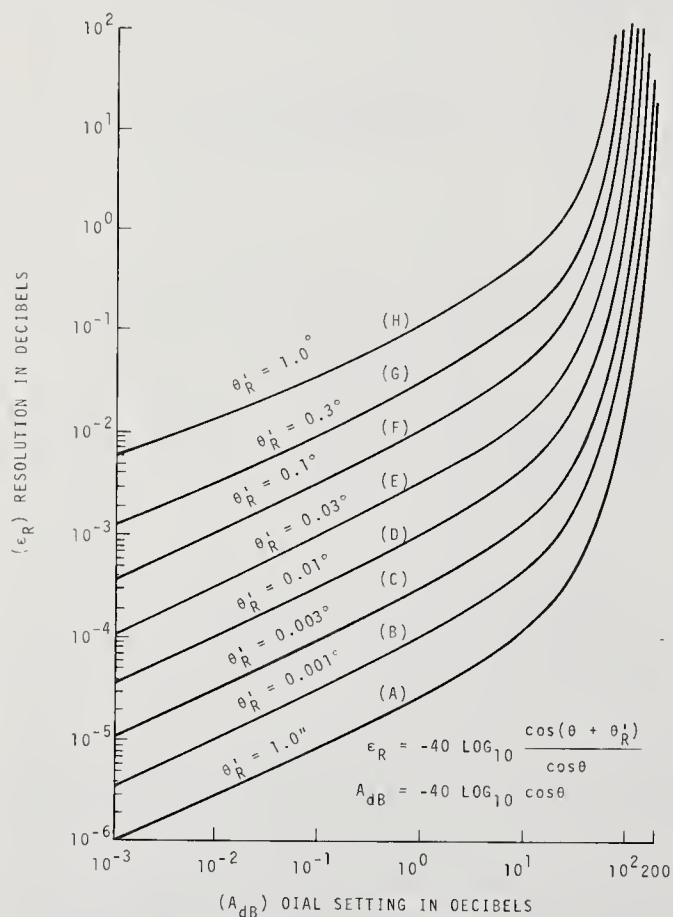


FIGURE 42. Resolution error in decibels versus dial setting in decibels.

## 9. Resolution of Rotary-Vane Attenuator in Percent of Dial Setting

The question may arise as to the optimum value of attenuation to measure for intercomparison of laboratory standards, or to determine the characteristics of a variable attenuator standard. In figure 43, the resolution of the dial in percent of dial setting is plotted versus dial setting in decibels for a rotary-vane attenuator with an angular resolution of 0.01°. At each end of the curve the resolution of dial in percent of attenuation value rises very rapidly. For example, at the dial settings of 0.01 and 100 dB, the resolution of dial is about 1 percent and appears to have the lower percent values from 6 to 20-dB dial settings, with the lowest occurring at about 12 dB. If an attenuator has finer resolution, such as 0.001° or 1 second of arc, then the resolution of dial in percent of attenuation will be correspondingly lower. From figure 42 it can be determined that for attenuation values of 1, 12, and 40 dB, the resolution of dial in percent are 0.011, 0.0045, and 0.0075 percent, respectively, for 0.001° dial resolution, and the corresponding values are about 0.003, 0.0013, and 0.002 percent for one second dial resolution. Again in both cases, the 12-dB dial setting has the lower resolution of dial in percent of attenuation.

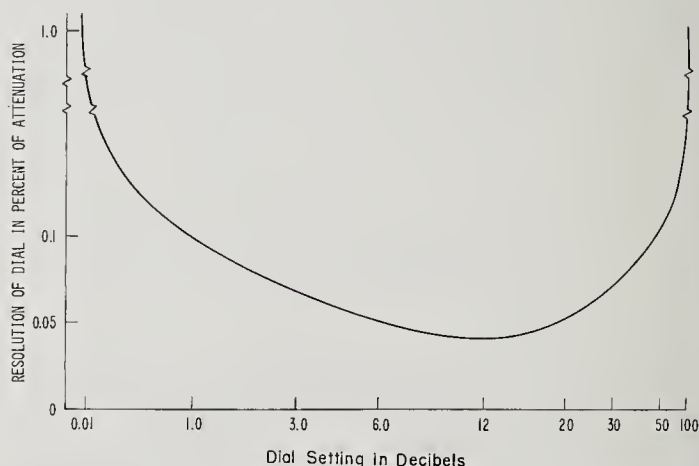


FIGURE 43. Resolution of the dial in percent of attenuation versus dial setting in decibels for an attenuator with angular resolution of 0.01°.

## 10. Frequency Sensitivity of the Rotary-Vane Attenuator

Although the rotary-vane attenuator has some excellent properties, such as stability, resolution and low reflection at the input and output ports, all of which are necessary criteria for good transfer standards, it also exhibits an undesirable characteristic, frequency sensitivity. The frequency sensitivity



becomes more pronounced at high values of attenuation; thus calibration of the attenuator at the operating frequency is essential for precise measurement with this device over large ranges of attenuation.

### 10.1. Spectrum of Microwave Attenuation Calibration Systems 2.6 to 40 GHz

For a period of more than 15 years, the microwave attenuation calibration system [16] has been used at NBS to calibrate rotary-vane attenuators over the microwave spectrum of 2.6 to 40 GHz. This included the following waveguide sizes: WR284, WR187, WR137, WR112, WR90, WR62, WR42, and WR28. Three frequencies for microwave calibrations were suggested for each waveguide size. These three frequencies were approximately as follows: the lower frequency limit increased 10 percent, the middle of the waveguide band, and the upper frequency limit decreased 10 percent. For example, the frequency band for WR90 waveguide is 8.2 to 12.4 GHz, and the suggested frequencies for calibration were 9, 9.8, and 11.2 GHz.

#### 3 Selected Frequencies Each in WR284, WR90, and WR28 Waveguide Sizes

It is helpful to use the data of calibrated rotary-vane attenuators in several waveguide sizes to evaluate their frequency sensitivity. For example, the waveguide sizes WR284, WR90, and WR28 cover the lower, middle, and upper portion of the

microwave frequency range used in this sample of rotary-vane attenuators. The deviations of attenuation from nominal in decibels versus dial settings of 10 to 50 dB at three NBS selected frequencies in each of the above waveguide sizes are shown in figures 44 to 50. In each figure the points plotted for each dial setting are coded as follows: the square,  $\square$ , at the lower frequency; the triangle,  $\triangle$ , at the middle frequency; and the circle,  $\circ$ , at the higher frequency. The smooth curves indicate the average deviation in attenuation and the corresponding vane-angle error is shown in degrees [17]. The spread between the curves indicates the magnitude of the error caused by frequency sensitivity. Corrections can be applied to minimize the frequency sensitivity.

Figures 44 and 45 show the deviations of attenuation for two attenuators in WR90 waveguide. In figure 44 the average vane-angle error is positive and yields values of attenuation greater than nominal, while in figure 45 the average vane-angle error is negative and gives values of attenuation less than nominal. The random variation of the calibrated points at each dial setting are due to gearing runout, resettability, mismatch, and system drift.

An example will now be given to show how the deviation in frequency sensitivity across a given waveguide size can be minimized. If a vane angle correction of  $-0.067^\circ$  is applied to the data plotted in figure 44, then the average vane-angle error at 9.0, 9.8, and 11.2 GHz will be  $+0.031$ ,  $+0.013$ , and  $-0.031^\circ$  respectively.

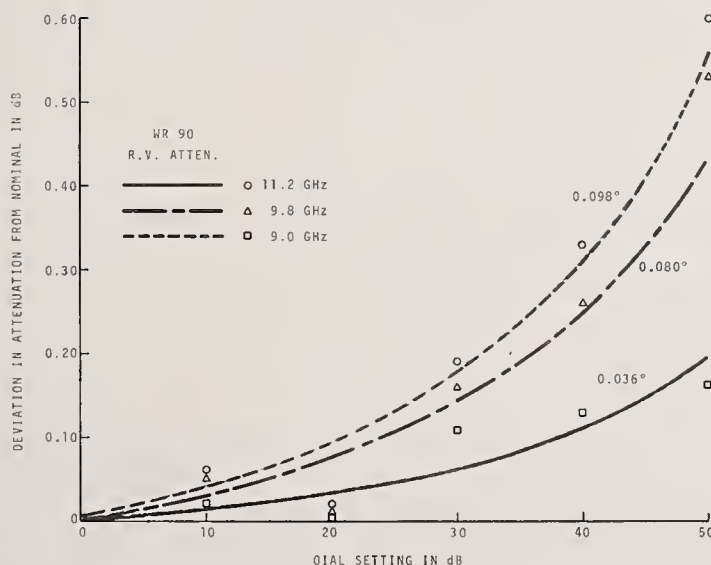


FIGURE 44. Deviation of attenuation for average vane-angle errors of  $0.098$ ,  $0.080$ , and  $0.036^\circ$  versus dial setting in decibels at 9.0, 9.8 and 11.2 GHz.

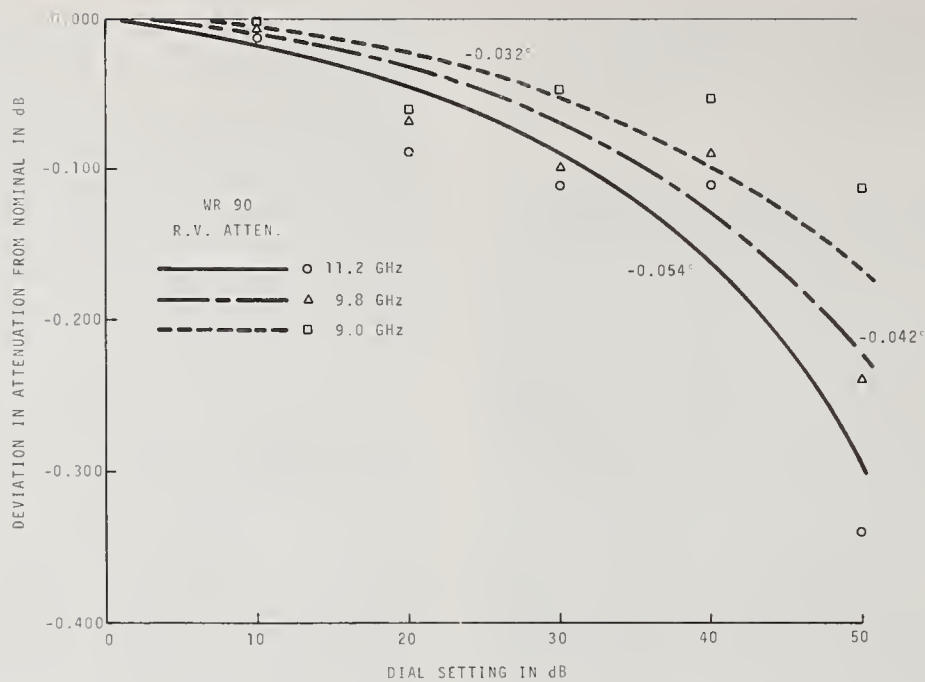


FIGURE 45. Deviation of attenuation for average vane-angle errors of  $-0.032^\circ$ ,  $-0.042^\circ$ , and  $-0.054^\circ$  versus dial setting in decibels at 9.0, 9.8, and 11.2 GHz.

Figures 46 and 47 show the deviations in attenuation for two rotary-vane attenuators in WR28. The random scatter of the point-by-point values are larger in the smaller waveguide size because gearing runout can produce greater angular displacement error [6], which correspondingly induces larger deviations in attenuation. The deviations in attenuation from nominal are illustrated for three WR284 rotary-vane attenuators in figures 48, 49, and 50. These curves show that two attenuators have a negative average vane-angle error while the

third has a positive angular error. In addition, in figures 48 and 49, the curve showing the higher frequency error falls between the middle and lower frequency errors. This could be caused by the warping or curling of the tapered vanes in the end sections, which is characteristic of this model of rotary-vane attenuator. However, the curve for the higher frequency did not fall between the other two and the spread of the deviation in attenuation appears to be less for the data obtained with another model of WR 284 attenuator, shown in figure 48.

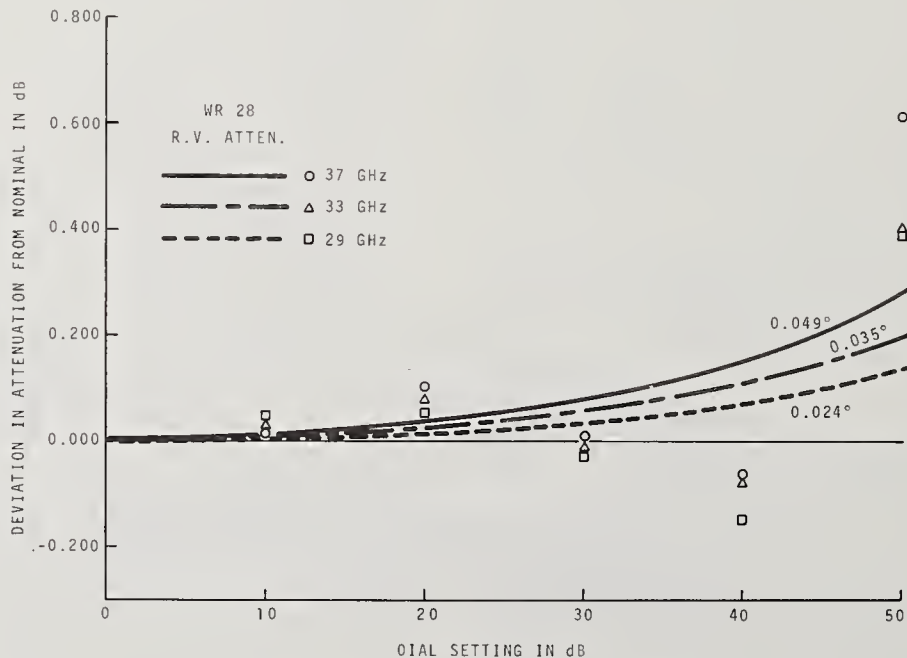


FIGURE 46. Deviation of attenuation for average vane-angle errors of  $0.024^\circ$ ,  $0.035^\circ$ , and  $0.049^\circ$  versus dial setting in decibels at 29, 33, and 37 GHz.

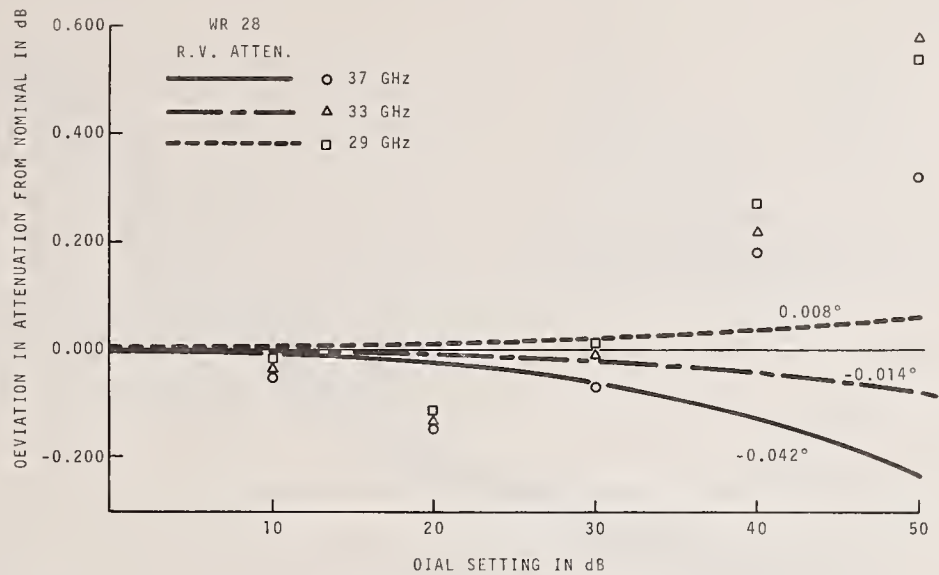


FIGURE 47. Deviation of attenuation for average vane-angle errors of  $0.008^\circ$ ,  $-0.014^\circ$ , and  $-0.042^\circ$  versus dial setting in decibels at 29, 33, and 37 GHz.

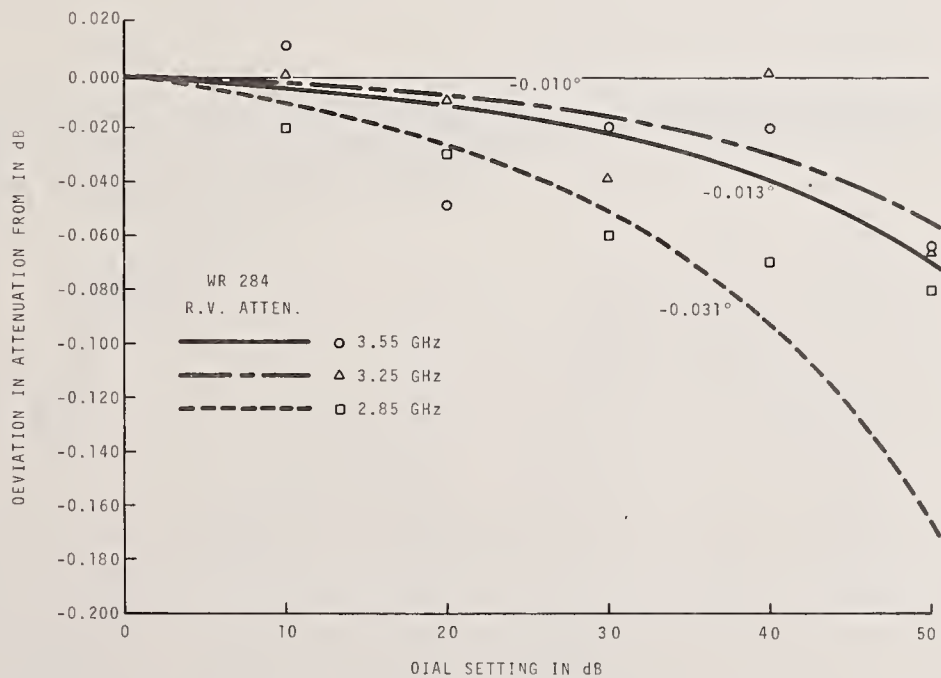


FIGURE 48. Deviation of attenuation for average vane-angle errors of  $-0.031^\circ$ ,  $-0.010^\circ$ , and  $0.013^\circ$  versus dial setting in decibels at 2.85, 3.25 and 3.55 GHz.



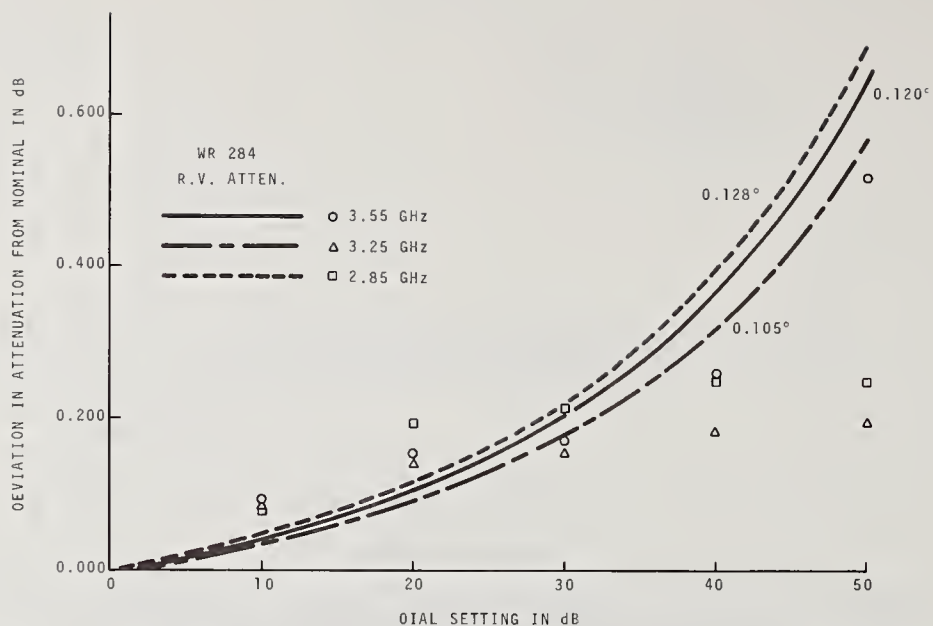


FIGURE 49. Deviation of attenuation for average vane-angle errors of  $0.128^\circ$ ,  $0.105^\circ$ , and  $0.120^\circ$  versus dial setting in decibels at 2.85, 3.25, and 3.55 GHz.

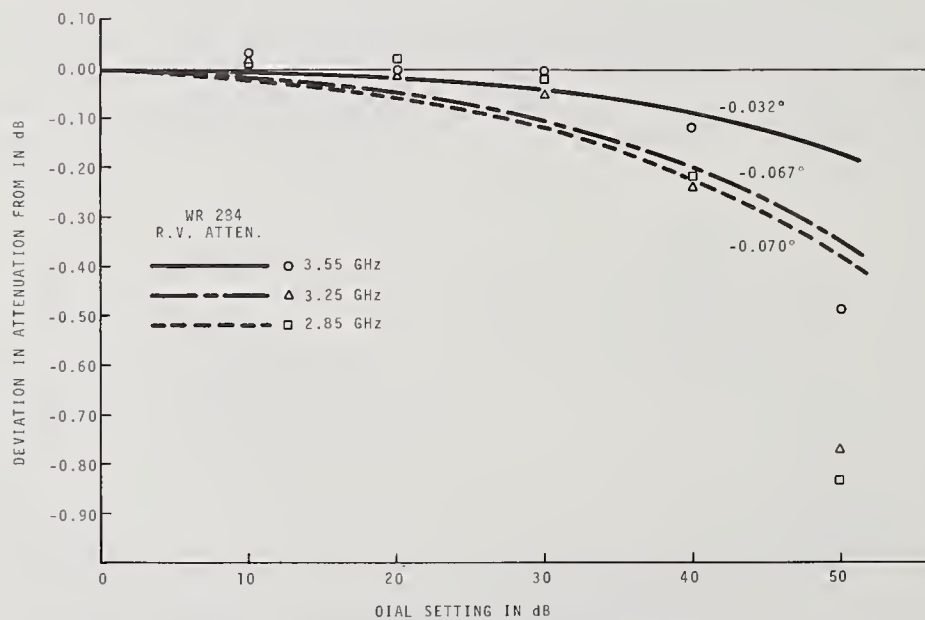


FIGURE 50. Deviation of attenuation for average vane-angle errors of  $-0.070^\circ$ ,  $-0.067^\circ$ , and  $-0.032^\circ$  versus dial setting in decibels at 2.85, 3.25, and 3.55 GHz.

## 10.2. Statistical Analysis of the Frequency Sensitivity from Calibration Data at 30, 40, and 50 dB

In order to obtain a statistical analysis of the frequency sensitivity, data were selected from calibrations performed on 154 attenuators at the established frequency limits. The analysis utilized the calibration data of the higher dial settings of 30, 40, and 50 dB of each rotary-vane attenuator. Since these dial settings were common to all calibrations, these values were used in computing the standard deviation for each waveguide size. In figures 51 to 58 each graph shows the limits of one-sigma error in attenuation in decibels versus frequency in GHz for the rotary-vane attenuator in

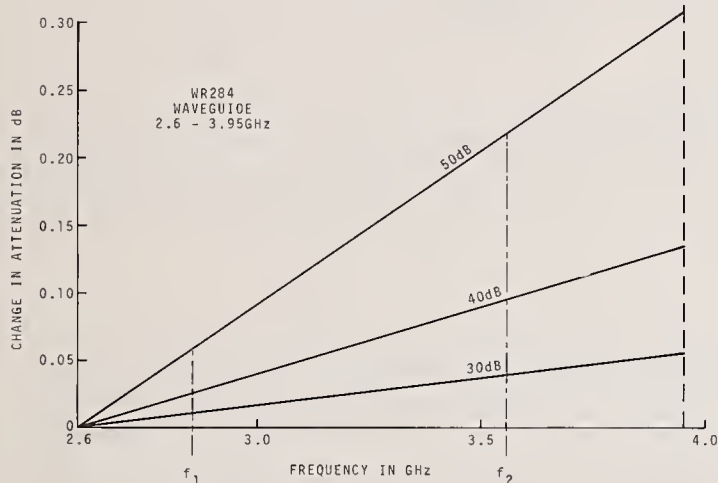


FIGURE 51. Limits of magnitude of one-sigma error in attenuation versus frequency in GHz for twenty WR284 rotary-vane attenuators at 30, 40, and 50-dB dial settings.

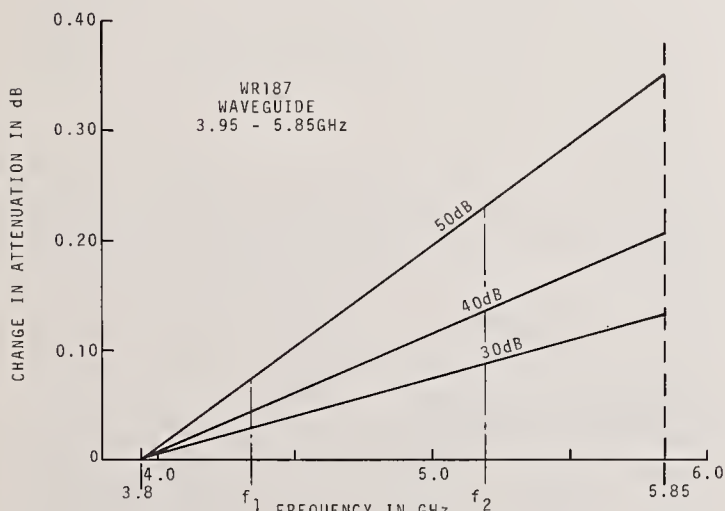


FIGURE 52. Limits of magnitude of one-sigma error in attenuation versus frequency in GHz for twenty-one WR187 rotary-vane attenuators at 30, 40, and 50-dB dial settings.

each specific waveguide size at 30, 40, and 50-dB dial settings. In each figure the vertical lines  $f_1$  and  $f_2$  are the limits of the selected frequencies. However, the frequency of each graph was extended to include the total frequency range of that specific waveguide size. The greatest change in attenuation in decibels occurs at the dial setting of 50 dB in WR62 waveguide and is about 0.75 dB for a frequency range of 12.4 to 18.0 GHz, as shown in figure 56. The least change in attenuation for the 50-dB dial setting was about 0.3 dB in WR284 and WR42 waveguide sizes (figs. 51 and 57).

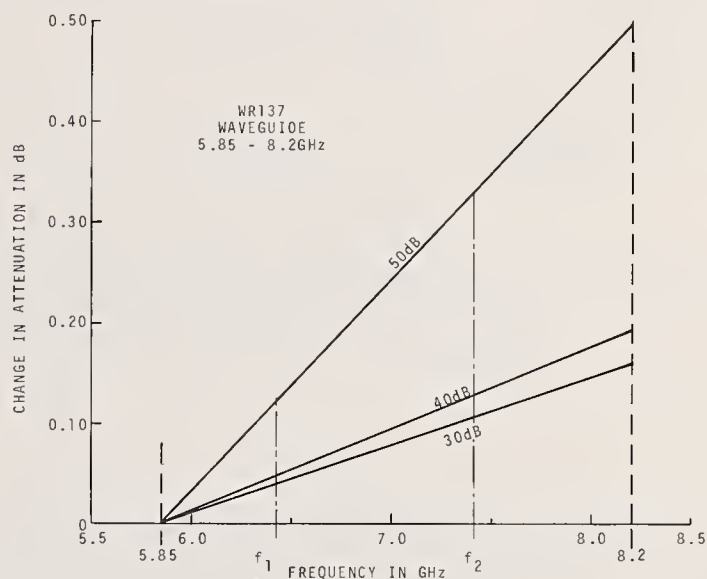


FIGURE 53. Limits of magnitude of one-sigma error in attenuation versus frequency in GHz for eighteen WR137 rotary-vane attenuators at 30, 40, and 50-dB dial settings.

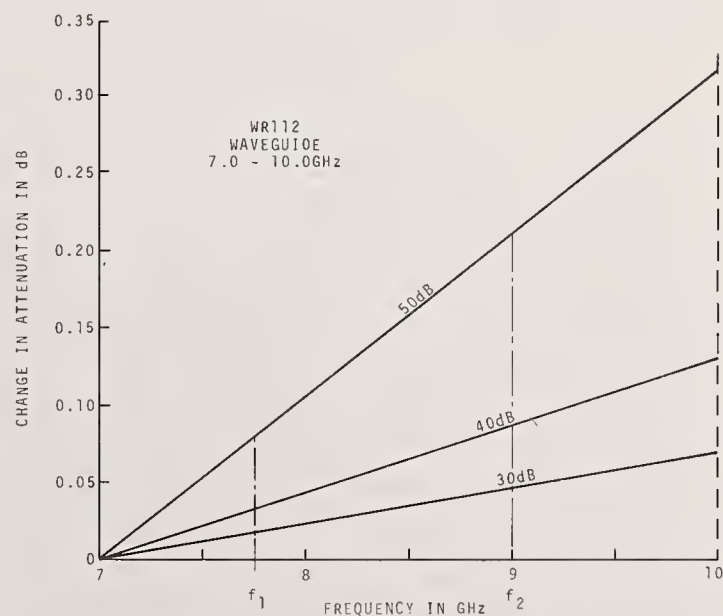


FIGURE 54. Limits of magnitude of one-sigma error in attenuation versus frequency in GHz for twenty-three WR112 rotary-vane attenuators at 30, 40, and 50-dB dial settings.

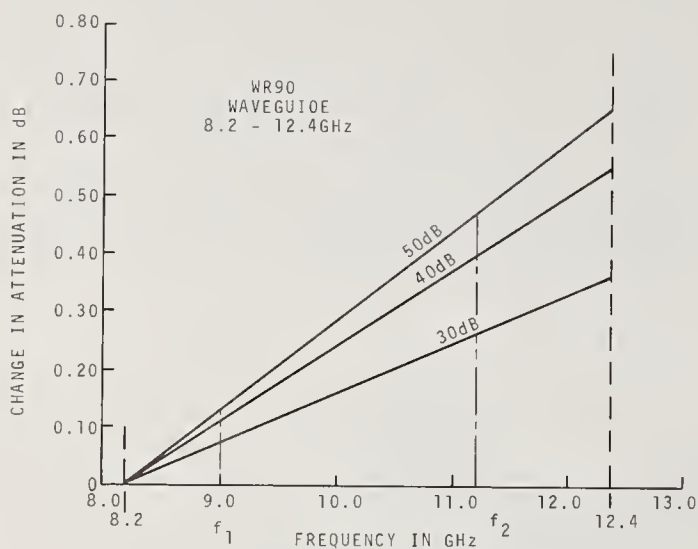


FIGURE 55. Limits of magnitude of one-sigma error in attenuation versus frequency in GHz for fifty-one WR90 rotary-vane attenuators at 30, 40, and 50-dB dial settings.

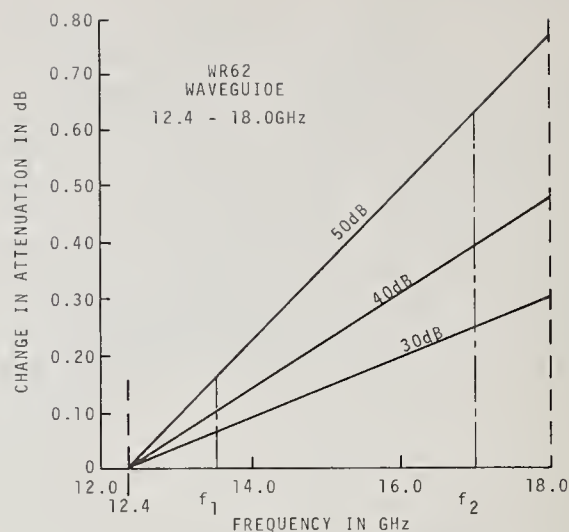


FIGURE 56. Limits of magnitude of one-sigma error in attenuation versus frequency in GHz for seven WR62 rotary-vane attenuators at 30, 40, and 50-dB dial settings.

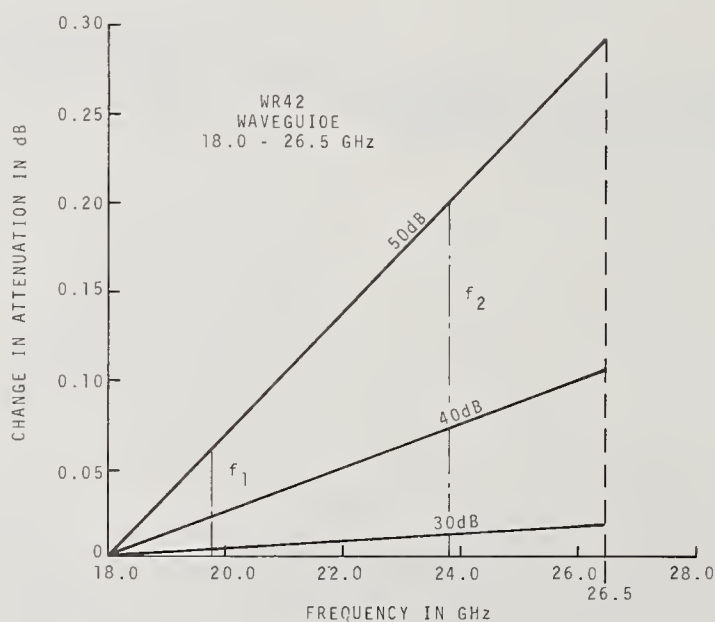


FIGURE 57. Limits of magnitude of one-sigma error in attenuation versus frequency in GHz for seven WR42 rotary-vane attenuators at 30, 40, and 50-dB dial settings.



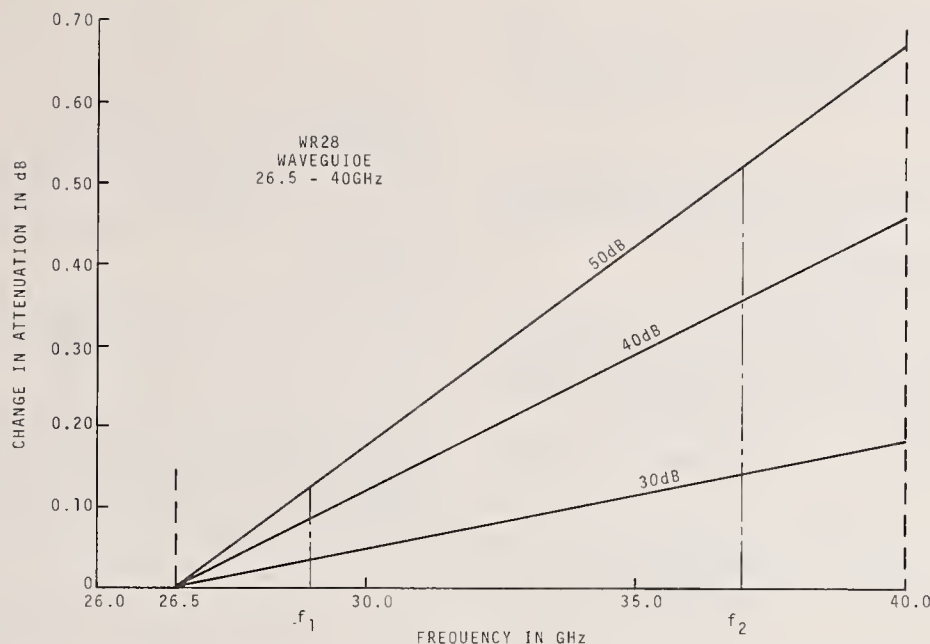


FIGURE 58. Limits of magnitude of one-sigma error in attenuation versus frequency in GHz for seven WR28 rotary-vane attenuators at 30, 40, and 50-dB dial settings.

### 10.3. Frequency Sensitivity of Rotary-Vane Attenuators for Eight Waveguide Frequency Ranges

Table 14 summarizes the frequency sensitivity of the rotary-vane attenuators for eight waveguide designations. The term dB/GHz indicates the deviation from nominal attenuation adjusted so that the deviation is zero at the bottom frequencies of the waveguide range. The values of dB/GHz were determined from  $\sigma_{f_2}$  minus  $\sigma_{f_1}$  divided by  $f_2$  minus  $f_1$  (upper and lower selected frequencies, respectively) where  $\sigma_{f_2}$  and  $\sigma_{f_1}$  are the standard deviations of the respective frequencies. These values of dB/GHz are listed in columns four, five, and six for the dial settings of 30, 40, and 50 dB, respectively.

TABLE 14. Limits of magnitude of one-sigma error in attenuation in dB per GHz for rotary-vane attenuators in WR28, WR42, WR62, WR90, WR112, WR137, WR187, and WR284 waveguide at 30, 40, and 50-dB dial settings

WR	Frequency range in GHz	Band width in GHz	dB/GHz		
			30 dB	40 dB	50 dB
28	26.5 - 40.0	13.5	.014	.034	.050
42	18.0 - 26.5	8.5	.002	.013	.035
62	12.4 - 18.0	5.6	.054	.086	.137
90	8.2 - 12.4	4.2	.089	.132	.158
112	7.0 - 10.0	3.0	.023	.044	.106
137	5.85 - 8.20	2.35	.068	.081	.212
187	3.95 - 5.85	1.9	.072	.129	.176
284	2.6 - 3.95	1.35	.043	.099	.227

tively. Note that the frequency sensitivity in dB/GHz shows the smallest limits of magnitude of one-sigma in attenuation at each dial setting for the WR42 waveguide rotary-vane attenuator, and yields the largest limits of magnitude of one-sigma in attenuation at 30 and 40, and 50-dB dial settings for WR90, and WR284 waveguide rotary-vane attenuators, respectively.

## 11. Evaluation of the Rotary-Vane Attenuator by "Bootstrapping" and Check Standards

Bootstrapping (often erroneously referred to as self-calibrating) as used here is a technique of calibrating or evaluating a device by utilizing its own characteristics instead of absolute standards. Only dimensionless quantities, of which attenuation is one, can be determined. For example, a stable repeatable attenuation step whose absolute value in decibels is unknown can be measured by the rotary-vane attenuator at several different values of dial settings. In this case the increment of attenuation difference is the same for each measurement, but the location of the increment will be at different positions on the dial. To best utilize this technique, certain characteristics of the attenuator, such as rotor misalignment and resettability must be known or determined. In any case rotary-vane attenuators having optical [2] or digital [4] readouts are the most desirable to use, as gear-driven readouts are subject to runout and backlash errors [6].

### 11.1. Errors in Attenuation for the Initial and the Final Setting of the Rotary-Vane Attenuator for an Attenuation Difference Measurement

The initial setting of an attenuation difference measurement of a rotary-vane attenuator can be written as

$$A'_i = A_i \pm \epsilon_{i0} + \epsilon_{iI},$$

where  $A_i$  is the theoretical value of attenuation at the initial setting;  $\epsilon_{i0}$  and  $\epsilon_{iI}$  are the errors due to the operator and inherent error, respectively, at the initial setting.

The error in attenuation at the initial setting may be expressed as

$$\epsilon_{i0} + \epsilon_{iI} = -40 \log_{10} \frac{\cos(\theta_i \pm \theta_{i0} + \theta_{iI})}{\cos \theta_i}$$

where the angular values at the initial setting are:  $\theta_i$ , the vane angle to obtain the theoretical attenuation;  $\theta_{i0}$ , the vane-angle error due to the operator; and  $\theta_{iI}$ , the inherent vane-angle error.

In a like manner, the final setting of an attenuation difference measurement may be expressed as

$$A'_f = A_f \pm \epsilon_{f0} + \epsilon_{fI}$$

where  $A_f$  is the theoretical value of attenuation at the final setting,  $\epsilon_{f0}$  and  $\epsilon_{fI}$  are the errors due to the operator and the inherent error, respectively, at the final setting.

The error in attenuation at the final setting may be expressed as

$$\epsilon_{f0} + \epsilon_{fI} = -40 \log_{10} \frac{\cos(\theta_f \pm \theta_{f0} + \theta_{fI})}{\cos \theta_f}$$

where the angular values at the final setting are:  $\theta_f$ , the vane angle to obtain the theoretical attenuation;  $\theta_{f0}$ , the vane-angle error due to the operator; and  $\theta_{fI}$ , the inherent vane-angle error [18].

Any deviation from ideal alignment of the rotor vane with reference to the scale readout causes a systematic error in the attenuation rate of the entire range of the rotary-vane attenuator. Though this mechanical error can be constant angular displacement, it produces an increasingly greater error in attenuation as the value of  $\theta$  increases. Also, the error in attenuation caused by angular limits of resettability becomes greater with increases of  $\theta$ . Since bootstrapping action usually results in higher value of attenuation, the smallest errors of alignment and resettability are essential to keep the limits of uncertainty minimal.

### 11.2. Graphical Presentation

In order to illustrate the deviation in attenuation due to rotor-vane alignment error, graphs are used to display these deviations from nominal attenuations. This deviation from nominal in a determination of attenuation difference occurs at both the initial and final dial settings of the rotary-vane attenuator.

#### 11.2.1. Deviations in Attenuation Due to Rotor-Vane Alignment Error

Figure 59(a) is a graph of error,  $\epsilon'$ , in decibels for attenuation in 10-dB increments with assumed rotor-vane alignment error,  $\theta'_I$ , equal to 0.100, 0.200, and 0.300°. The value of  $\epsilon'$ , the error from nominal, is determined from  $\epsilon'_b$  minus  $\epsilon'_a$ , when

$$\epsilon'_a = -40 \log_{10} \frac{\cos(\theta_a + \theta'_I)}{\cos \theta_a}$$

and

$$\epsilon'_b = -40 \log_{10} \frac{\cos(\theta_b + \theta'_I)}{\cos \theta_b};$$

$\theta_a$  is the initial rotor vane angle,  $\theta_b$  is the final rotor vane angle, and  $\theta'_I$  is defined above.

The magnitude variations of  $\epsilon'$  are illustrated by three different straight lines: the solid line for  $\theta'_I = 0.300^\circ$ , the dot line for  $\theta'_I = 0.200^\circ$ , and the dash-dot-dash line for  $\theta'_I = 0.100^\circ$ . (This legend also applies to the figs. 61, 63, 65, and 67.) Five different increments of 10 dB each were measured as follows: 0 to 10 dB, 3 to 13 dB, 6 to 16 dB, 10 to 20 dB, 15 to 25 dB. The values of  $\epsilon'$  at the same 10-dB increments are smaller when  $\theta'_I$  is equal to 0.200 and 0.100° as indicated by the dot, and the dash-dot lines. For a given  $\theta'_I$ , the value of  $\epsilon'$  is the least at the dial settings of 3 to 13 dB.

#### 11.2.2. Attenuation Versus $\theta$ in Degrees

Figure 59(b) is the curve of attenuation versus  $\theta$  in degrees of rotor angular displacement. The segments of the curve, numbered (1), (2), (3), (4), and (5), are equal to 10-dB increments of attenuation. The chart shows three positions of the rotor vane in degrees; the initial,  $\theta'_i$ ; the final,  $\theta_f$ ; and their difference,  $\Delta\theta$ .

Although the increments of attenuation are equal, the angular increments,  $\Delta\theta$ , become less at higher values of  $\theta$ . For example, the angular displacement for the 15 to 25-dB increment is approximately one-fifth of the value for the 0 to 10-dB increment.

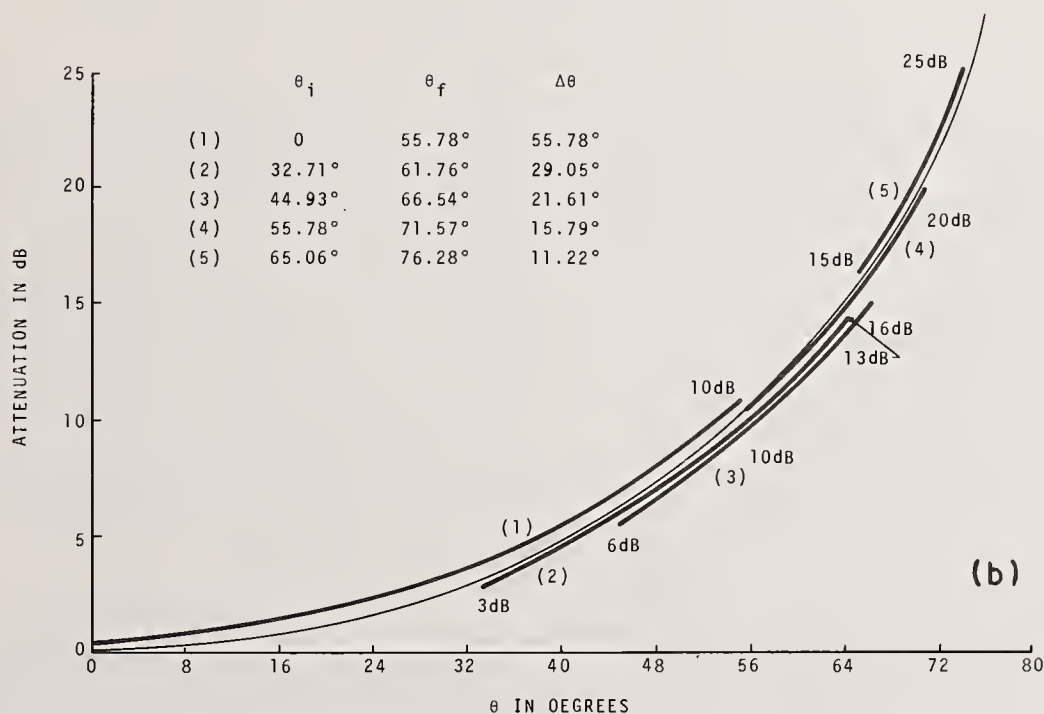
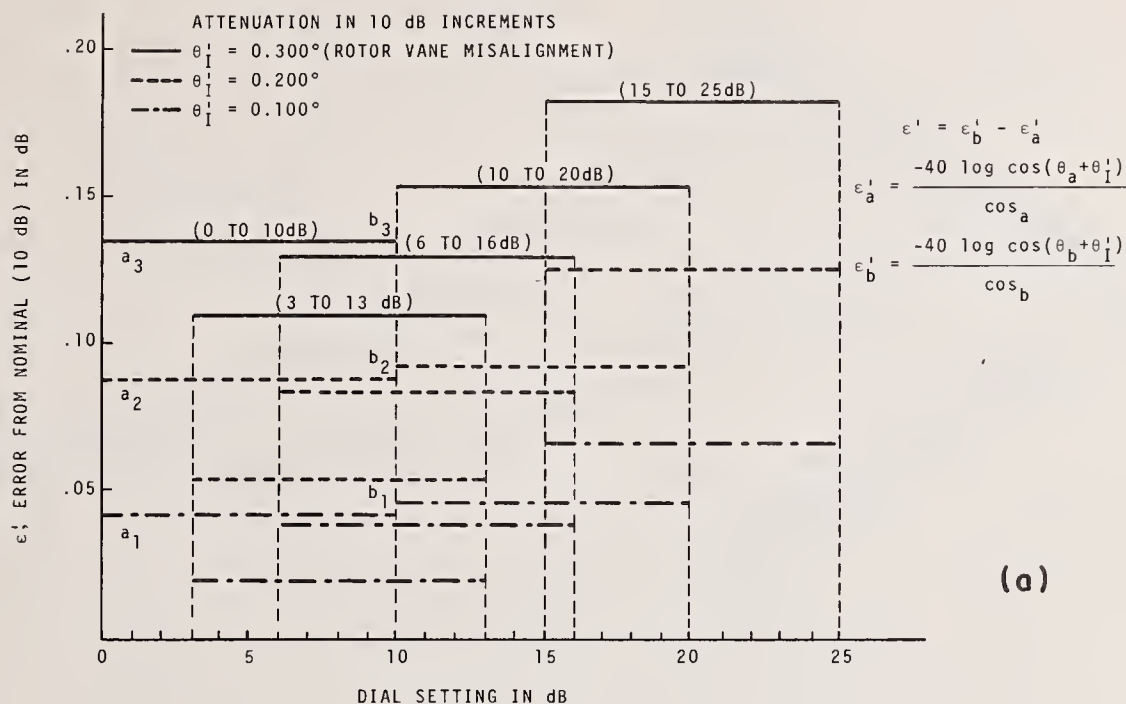


FIGURE 59. (a)  $\epsilon'_I$  error from nominal (10 dB) increments versus dial setting in decibels for rotor misalignment,  $\theta'_I$  equal to 0.100, 0.200, and 0.300°.

(b) Attenuation in decibel versus  $\theta$  in degrees, and angular limits in degrees for attenuation difference of 10 dB.



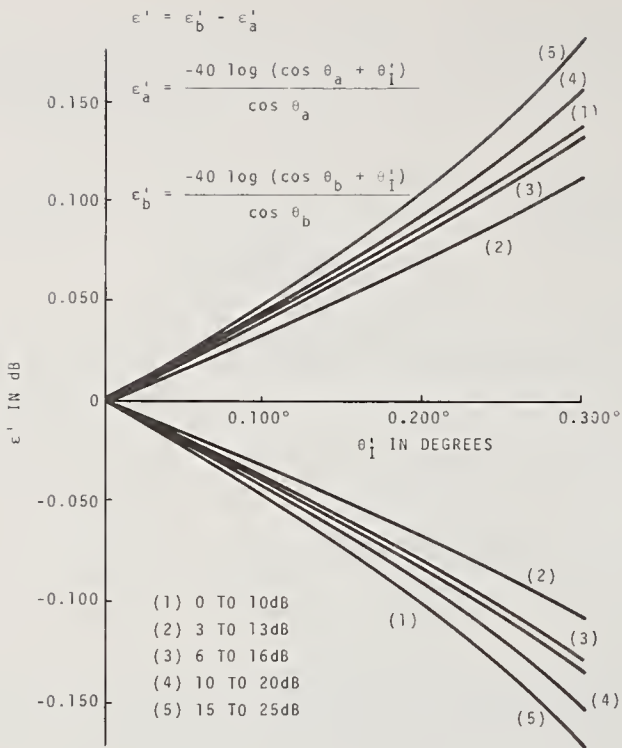


FIGURE 60.  $\epsilon'$  error in decibels versus  $\theta'_I$  from 0 to  $\pm 0.300^\circ$  for 10-dB increments as follows: 0 to 10 dB, 3 to 13 dB, 6 to 16 dB, 10 to 20 dB, and 15 to 25 dB.

The change in the  $\epsilon'$  error in decibels versus  $\theta'_I$  is plotted for both the positive and negative values of vane misalignment in figure 60. The lower portion of the graph shows the limits of the 10-dB increments which are numbered to correspond with the specific curve. The error  $\epsilon'$  in this sample of 10-dB increments is a minimum for 3 to 13 dB and a maximum for 15 to 25-dB dial settings.

In figures 61(a, b), 63(a, b), 65(a, b), and 67(a, b) are plots of the error,  $\epsilon'$ , in decibels for 6, 3, 1, and 0.1-dB increments with assumed rotor vane misalignment,  $\theta'_I$ , of 0.100, 0.200 and 0.300°. The plots of each of the different decibel increments illustrate that the minimum value of the error,  $\epsilon'$ , occurs when the angular displacement limits of the rotor vane are centered near 45°.

The change in the  $\epsilon'$  error versus  $\theta'_I$  is plotted for the positive values  $\theta'_I$  only in figures 62, 64, 66, and 68. The negative values of  $\theta'_I$  would plot as a near mirror image with a slight decrease in error (see fig. 60).

The difference in the error,  $\epsilon'$ , does increase at higher values of attenuation. For example, the difference between the positive and negative value of  $\epsilon'$  for  $\theta'_I$  equals 0.300° is about 0.0015 dB at the 10-dB dial setting, and about 0.152 dB at the 50-dB dial setting.

### 11.2.3. $\epsilon'_0$ and $\epsilon'$ Versus Dial Setting (in Degrees and decibels)

In order to illustrate the relationship of the

inherent misalignment error,  $\epsilon'_I$ , to the resettability error,  $\epsilon'_0$ , we have plotted their deviations in attenuation from nominal in figure 69. The values of  $\theta'_{I1}$ ,  $\theta'_{I2}$ , and  $\theta'_{I3}$  are shown as 0.100, 0.200, and 0.300°, respectively, and  $\theta'_0$  equal to  $\pm 0.010^\circ$ . The three curves are a plot of the deviations in attenuation from nominal versus dial setting (degrees and decibels) from 1 to 10 dB. The center lines are the deviations in attenuation caused by  $\theta'_I$ , and the lines on each side of the center lines are the limits of deviation caused by  $\theta'_0$ . The curves show that each subsequent 1-dB increment requires less angular rotation of the rotor as  $\theta$  increases. However, the errors in attenuation caused by  $\theta'_I$  and  $\theta'_0$  are greater as  $\theta$  increases.

### 11.2.4. Minimal Value of $\epsilon'$

Since the error,  $\epsilon'$ , is minimal at the mid-region of the angular displacement of the rotor, the attenuation increment of 1 dB between the 5 and 6-dB dial settings of the rotary-vane attenuator was selected for further investigation. Let us examine in detail this 1-dB nominal value of attenuation with limits of  $\theta'_0$  equal  $\pm 0.010^\circ$ , and  $\theta'_I$  equal  $\pm 0.100$ ,  $\pm 0.200$ , and  $\pm 0.300^\circ$ . Figure 70 shows the deviations in attenuation versus dial setting (degrees and decibels) for the above conditions, where  $\theta$  are the rotor angles corresponding to 5 and 6-dB dial settings. The nominal values of 5 and 6 dB are given at the end segment of each curve, and the vertical segments indicate the limits of resettability.

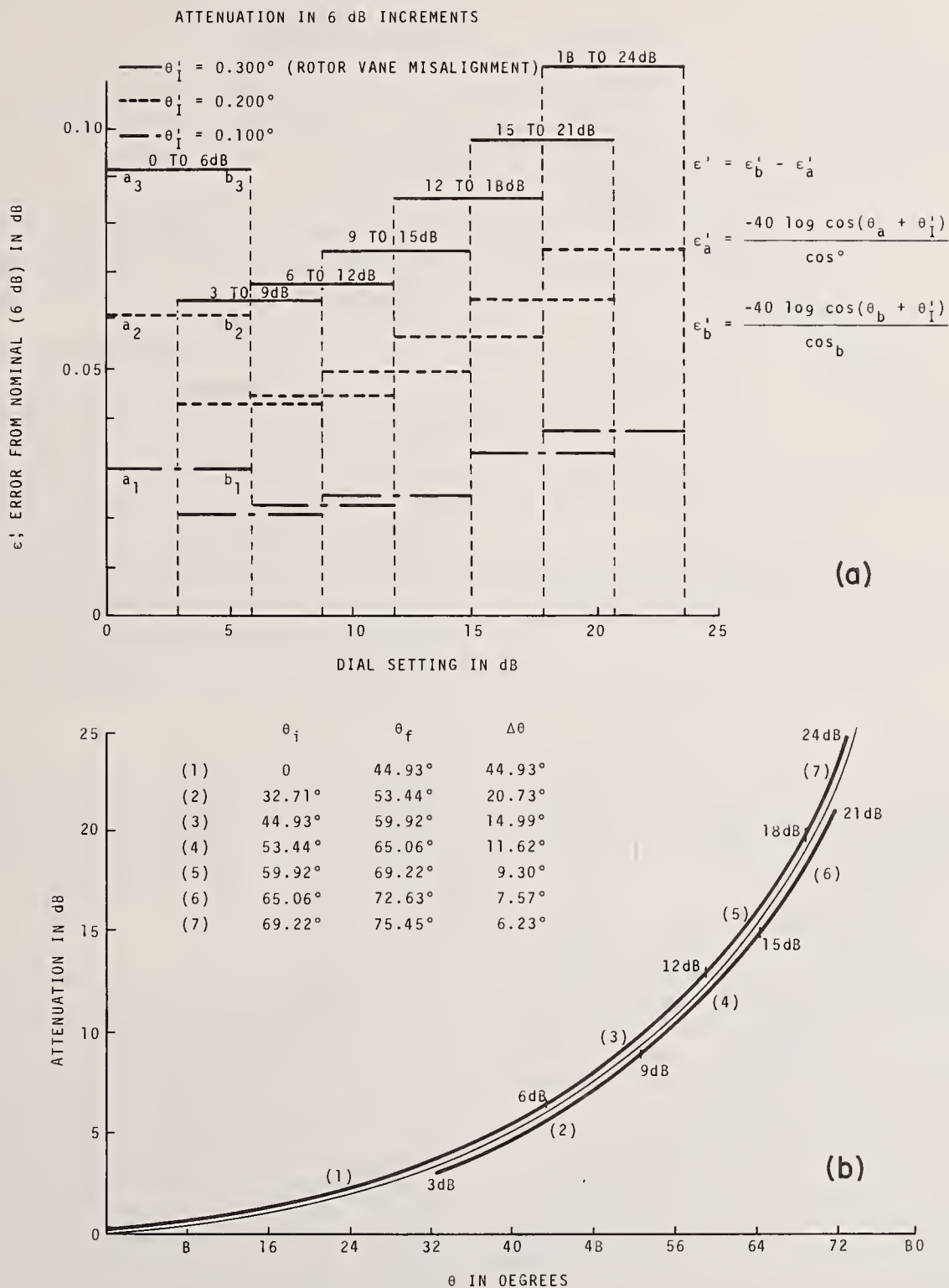


FIGURE 61. (a)  $\epsilon'$  error from nominal (6 dB) increments versus dial setting in decibels for rotor misalignment,  $\theta_i'$ , equal to 0.100, 0.200, and 0.300°.

(b) Attenuation in decibels versus  $\theta$  in degrees, and angular limits in degrees for attenuation difference of 6 dB.

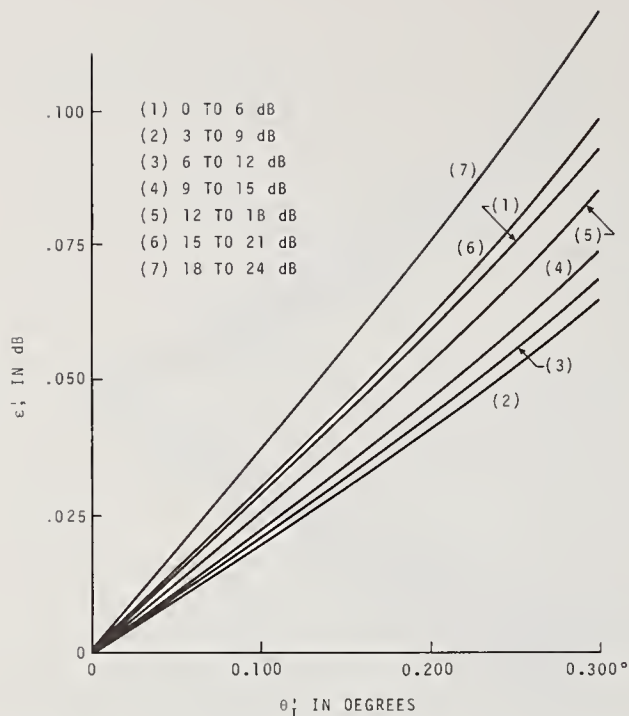


FIGURE 62.  $\epsilon'$  error in decibels versus  $\theta'_i$  from 0 to  $+0.300^\circ$  for 6-dB increments as follows: 0 to 6 dB, 3 to 9 dB, 6 to 12 dB, 9 to 15 dB, 12 to 18 dB, 15 to 21 dB, and 18 to 24 dB.

## 12. Evaluation of Precision Rotary-Vane Attenuator With Waveguide Fixed-Step Attenuator

Evaluation of a precision rotary-vane attenuator by using a repeatable step attenuator requires a stable high-resolution measurement system. A nominal 7-dB waveguide step attenuator and the microwave attenuation measurement system (series substitution) were used with the optical rotary-vane attenuator as the standard to obtain determinations of attenuation difference.

A summary of these measurements is shown in table 16. The attenuation difference of the step attenuator was measured by using several different initial dial settings from 0 to 60 dB on the rotary-vane attenuator. Column one lists the initial dial settings of the standard rotary-vane attenuator for each determination. The measured values of the waveguide-step attenuator are recorded in column two, with the average value of 7.6544 dB listed at the bottom of the column. These results were obtained by applying a negative rotor vane angle correction,  $\theta'_i$ , of  $1'18''$  or  $0.0217^\circ$  (previously determined) to all readings. In column three is given the deviation from the average attenuation difference. The random deviation from the average is about  $\pm 0.005$  dB for initial dial settings of 0 to 45 dB, and increases to about 0.02 dB for settings

of 50 to 60 dB. Column four gives the deviations from average before applying the rotor vane angle correction to the readings. It will be noted that these are all positive and increase as the initial dial setting increases.

Note that the deviations were minimal at the mid-angular regions of the rotary-vane attenuator. This was true regardless of the correction of  $\theta'_i$ ; however, for the most accurate results, the correction must be applied.

## 13. Attenuation Measurement With the Rotary-Vane Attenuator as the Standard

### 13.1. Introduction

In order to fully utilize the attenuation properties of the precision optical-rotary-vane attenuator as the standard, a dual detection microwave bridge system was incorporated in a series substitution system, providing an ingenious technique for microwave attenuation measurements [22]. The stability and resolution of this microwave attenuation measurement system is consistent with the rotary-vane attenuator standard's resolution of 0.00005 dB at 1-dB dial setting. The system maintains this stability and resolution up to a 30-dB measurement of attenuation difference or insertion loss.

The frequency band covered with this WR90 waveguide system is 8.2 to 12.4 GHz, and the attenuation measurement of fixed and/or variable devices ranges from 0 to 70 dB. The following discussion of the measurement system is adapted from NBS Tech. Note 647.

### 13.2. The Measurement System

A simplified block diagram of the microwave attenuation calibration system is shown in figure 71. The attenuator under test is located in the same waveguide section as the standard attenuator, between the standard and the waveguide detector. A change in the attenuator under test is equal to the change required in the standard attenuator to rebalance the bridge. An attenuation measurement is made in the following manner: (1) at the start set standard and attenuator under test to their respective initial setting and balance the bridge for a null using the level-set attenuator, (2) make the desired change in the attenuator under test, and (3) rebalance the bridge with the final setting of the standard attenuator.

Figure 72 shows a more detailed block diagram of the system and illustrates the interconnection of the waveguide components, standard attenuator, and associated electronic equipment. The basic waveguide components and instrumentation equipment of the system were developed with commer-



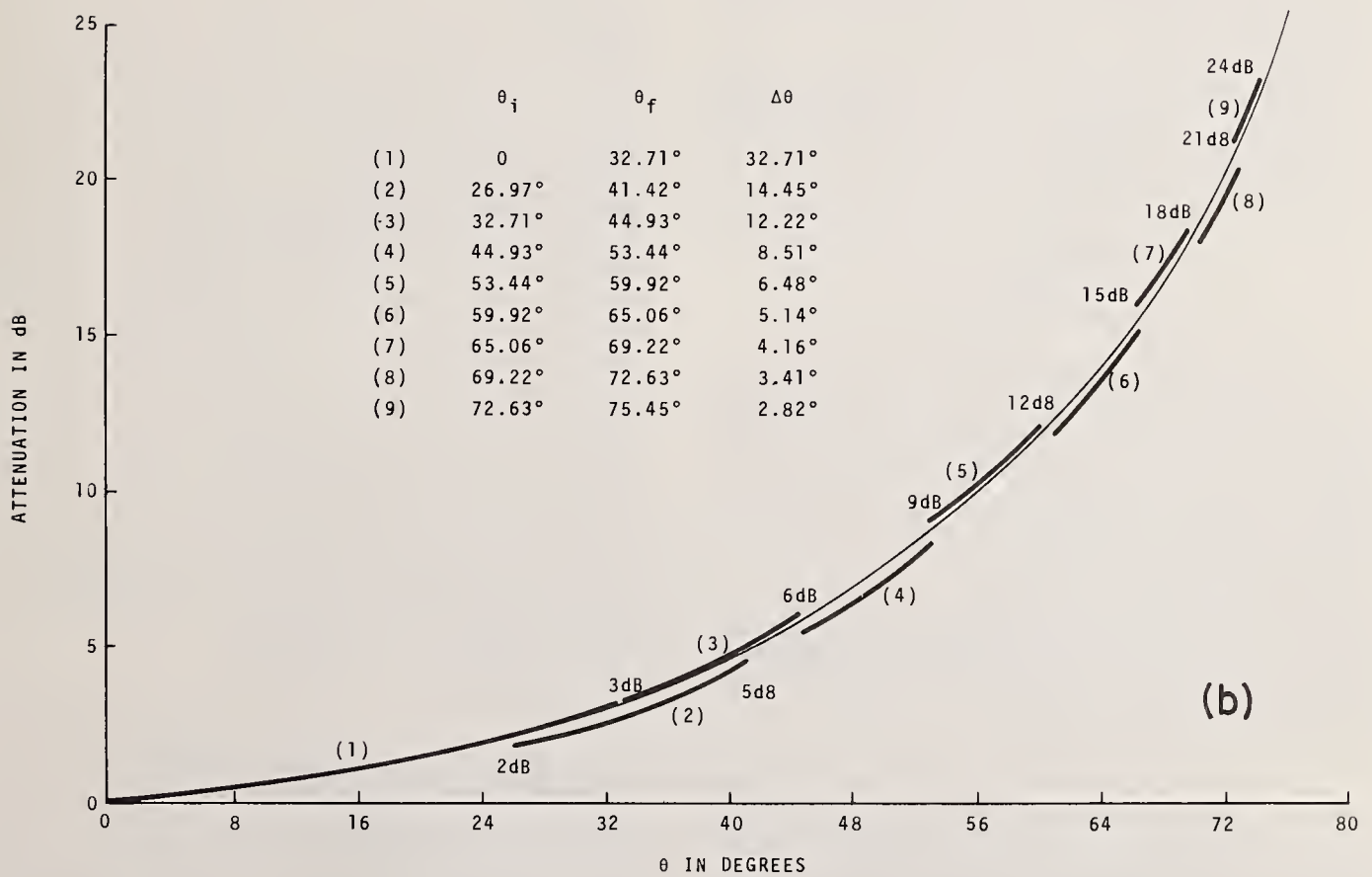
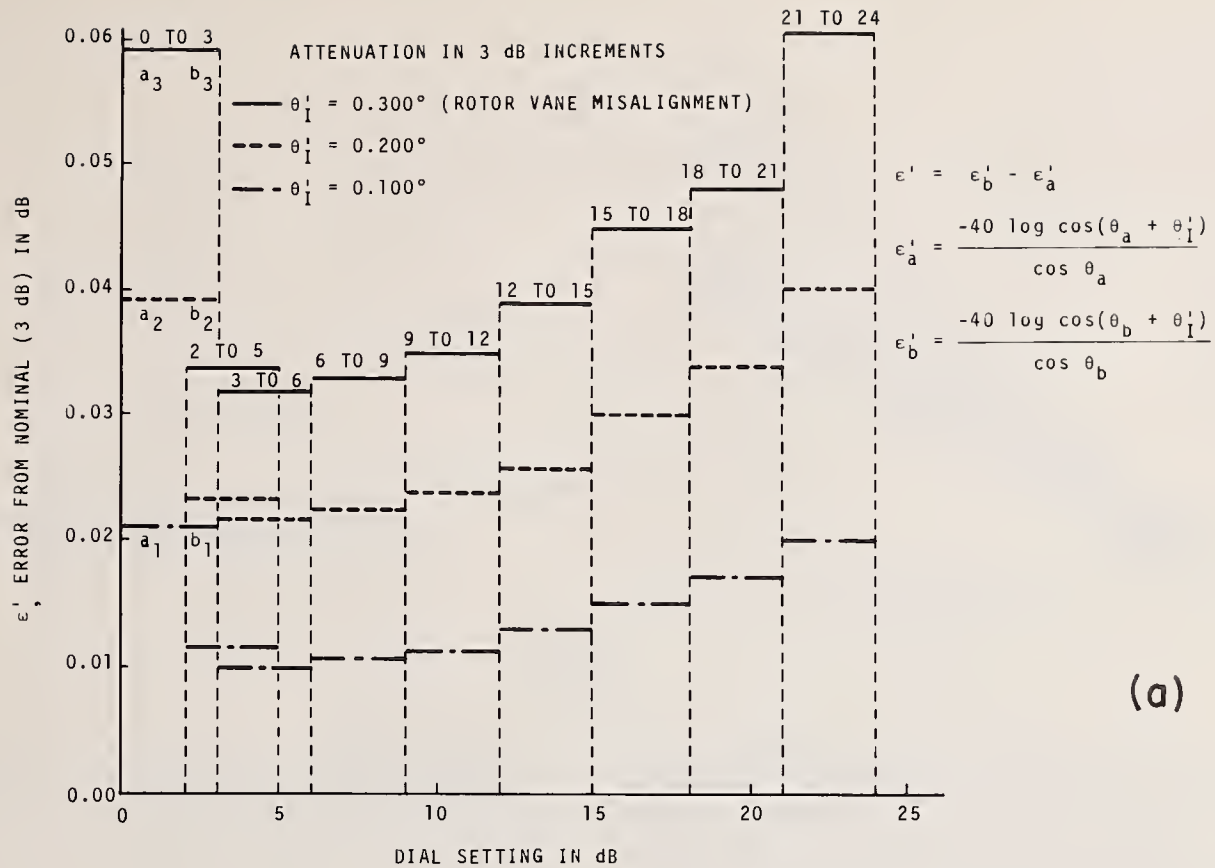


FIGURE 63. (a)  $\epsilon'$  error from nominal (3 dB) increments versus dial setting in decibels for rotor misalignment,  $\theta'_I$ , equal to 0.100, 0.200, and 0.300°.

(b) Attenuation in decibels versus  $\theta$  in degrees, and angular limits in degrees for attenuation difference of 3 dB.

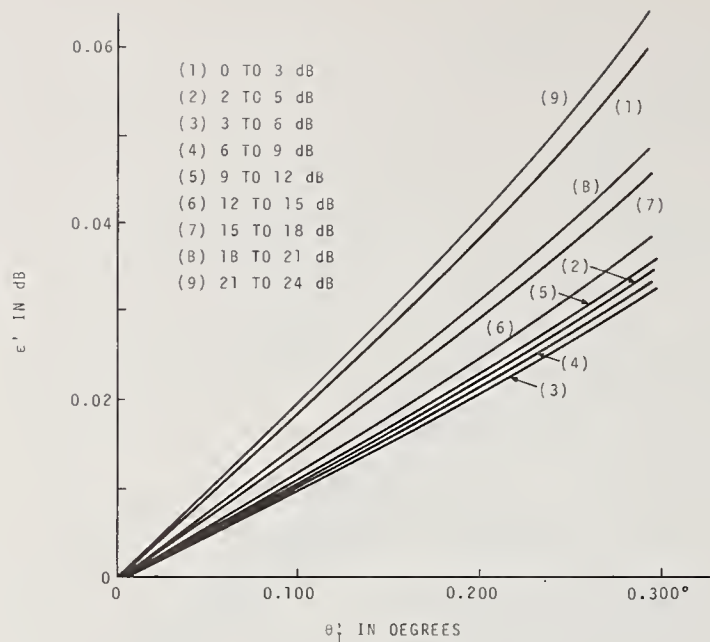


FIGURE 64.  $\epsilon'$  error in decibels versus  $\theta_1$  from 0 to  $+0.300^\circ$  for 3-dB increments as follows: 0 to 3 dB, 2 to 5 dB, 3 to 6 dB, 6 to 9 dB, 9 to 12 dB, 15 to 18 dB, 18 to 21 dB, and 21 to 24 dB.

cially available components. In addition, this measurement system has the favorable feature that attenuation measurements are obtained to a high degree of precision without power stabilization of the RF signal source, and employs a single RF source. The null amplifier was designed at NBS and a detailed schematic diagram is given in NBS Tech Note 647.

In figure 73, a recording chart of the stability of measurement indicates that for a 30-dB value of attenuation maximum variations are in the order of  $\pm 10 \mu\beta$  at the output detection system.

### 13.3. Errors of the Microwave Measurement System

#### 13.3.1. Systematic and Random Errors

With the application of the correction required for rotor-vane misalignment of the rotary-vane attenuator standard, and precise matching technique, the estimated systematic error, at the two insertion points of the waveguide system, is reduced to about  $\pm 0.002$  dB for values of attenuation measurement from 0 to 30 dB.

The measurement of attenuation difference and insertion loss of five precision interlaboratory transfer standards gave a preliminary estimate of the standard deviation, sigma ( $\sigma$ ), equal to 0.0010 dB for over one hundred determinations.

#### 13.3.2. Insertion Point of the Device Under Test

Two tuned insertion points are required in the microwave attenuation measurement system (series substitution), one for the working standard (precision rotary-vane attenuator), the other for the device under test. Refer to the block diagram in figure 72.

Only the insertion point for the device under test is opened during an insertion loss measurement. Also, this point is located in the system in such a way that the least possible movement of waveguide components is required. An opened insertion point of rectangular waveguide and an inserted fixed rectangular waveguide attenuator under test are shown in figures 74 and 75, respectively. This insertion point can be adapted very easily for use as a coaxial insertion point. In figure 76 the photo shows the insertion point converted to admit coaxial devices by using waveguide *E*-plane bends, coax to waveguide adapters, and a double (male) coaxial adapter as added components to the waveguide line. The addition of these components does not increase greatly the length of the movable section or hinder the ease of inserting coaxial devices into the line of the system (fig. 77).

The waveguide multistub tuners adjacent to each side of the insertion point are used to match the line to either rectangular waveguide or coaxial insertion point. The waveguide insertion point can be tuned by using a portable reflectometer [23], or the built-in reflectometer that is located in the waveguide section of the system. Tuning the coaxial insertion point requires the use of a coaxial slotted section.

#### 13.3.3. Mismatch Error in Attenuation Measurement

Mismatch is a significant source of error that should be considered in the calibration of microwave fixed or variable attenuators. In the measurement process of any attenuation device, a large amount of degrading of the accuracy will depend upon the matching of the insertion point of the calibration system. The match of the insertion point becomes more critical for low values of attenuation [24, 25, 26].

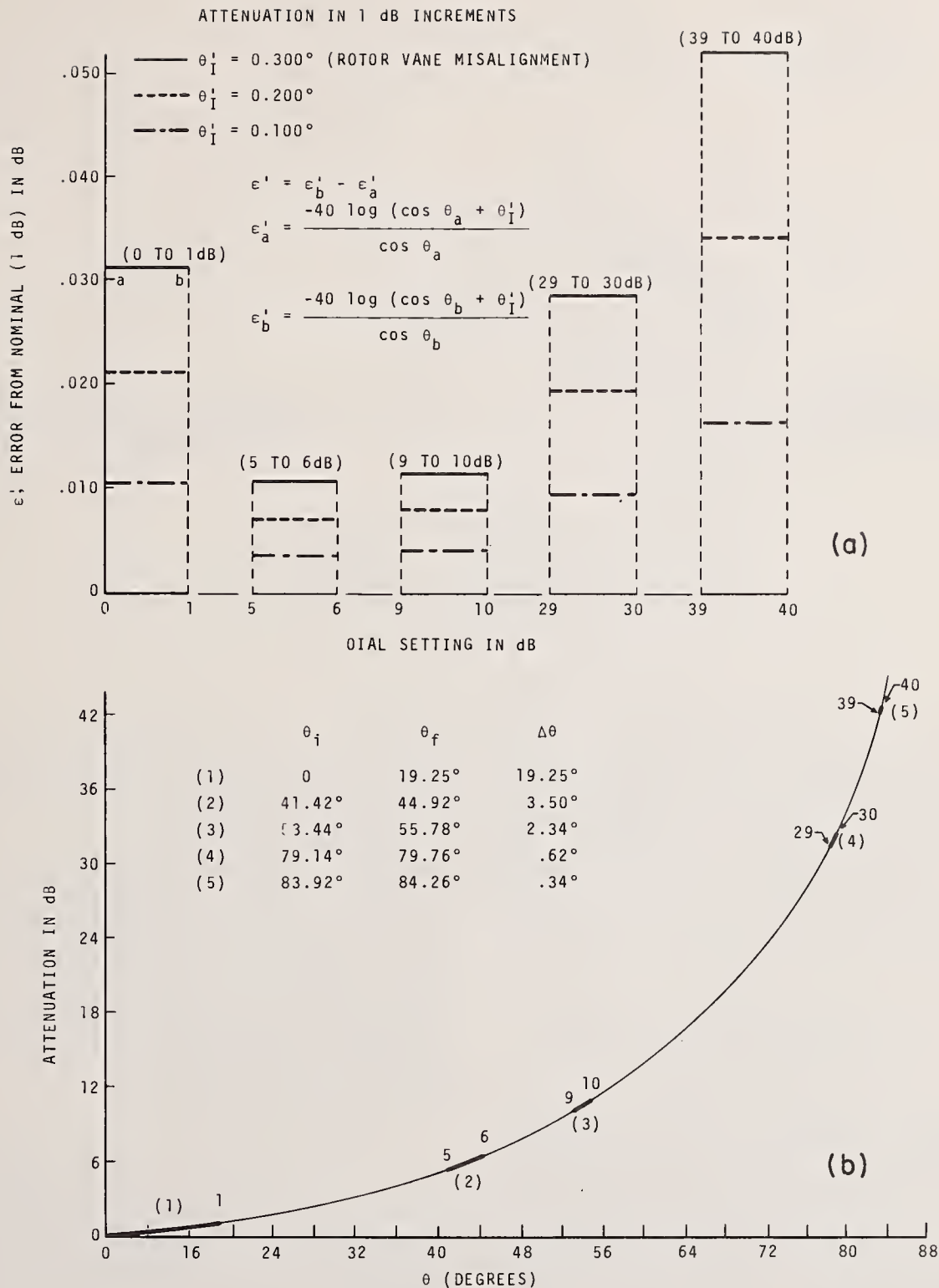


FIGURE 65. (a)  $\epsilon'$  error from nominal (1 dB) increments versus dial setting in decibels for rotor misalignment,  $\theta_I'$ , equal to 0.100, 0.200, and 0.300°.

(b) Attenuation in decibels versus  $\theta$  in degrees, and angular limits in degrees for attenuation difference of 1 dB.



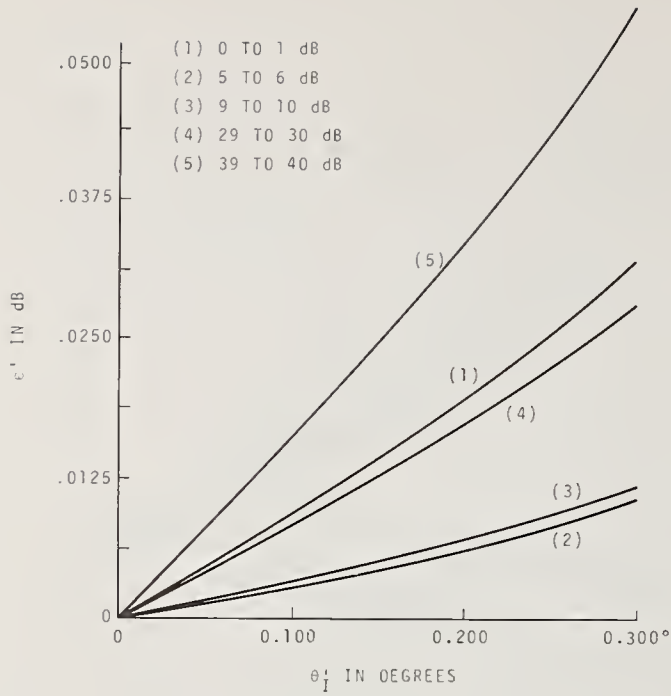


FIGURE 66.  $\epsilon'$  error in decibels versus  $\theta'$  from 0 to  $+0.300^\circ$  for 1-dB increments as follows: 0 to 1 dB, 5 to 6 dB, 9 to 10 dB, 29 to 30 dB, and 39 to 40 dB.

In a microwave measurement system, attenuation difference of a variable or rotary-vane attenuator can be measured by using the zero setting as a reference angular position, then moving to the attenuation or the vane angle desired to establish the value of attenuation difference to be measured.

For an attenuation difference measurement of a variable attenuator the mismatch error can be expressed as

$$\epsilon_r(\text{dB}) = 20 \log_{10} \frac{|(1 - (f)\Gamma_i\Gamma_g)(1 - (f)S_{22}\Gamma_L)|}{|(-i)\Gamma_i\Gamma_g(1 - (f)S_{22}\Gamma_L)|}$$

where the frontscripts (i) and (f) pertain to the initial and final values, respectively, and  $\Gamma_i$  is the input voltage reflection coefficient of the variable attenuator that is terminated with a load of reflection coefficient,  $\Gamma_L$ . The reflection coefficient of the generator is  $\Gamma_g$ , and  $S_{22}$  is the reflection coefficient at the output port when the input port is terminated with a nonreflecting load. Engen and Beatty show that the mismatch error becomes very low when small incremental attenuation measurements are made on a rotary-vane attenuator [12].

The mismatch error for insertion loss measurement of a fixed attenuator can be expressed as

$$\epsilon_f(\text{dB}) = 20 \log_{10}$$

$$\frac{|(1 - S_{11}\Gamma_g)(1 - S_{22}\Gamma_L) - S_{12}S_{21}\Gamma_L\Gamma_g|}{|1 - \Gamma_g\Gamma_L|}$$

where  $S_{11}$  is the attenuator input reflection coefficient when the output is terminated in a non-reflecting load, and  $S_{12}$  and  $S_{21}$  are the attenuator transmission coefficients.

In addition to the mismatch error caused by the reflections at the input and output ports of the attenuator, internal reflections can occur between the stator and rotor which must be added to the total reflection error. Mariner [5] indicates that there are eight main places where reflections can occur, namely, each end of the three vanes, and the two waveguide transitions. Mariner concludes that usually these internal reflections will not contribute significantly to the total error.

### 13.4. External Leakage

The effects of RF leakage from microwave components upon the performance of a microwave measurement system are often subtle and difficult to identify. Thus leakage from a good standard must be kept to an absolute minimum. In the NBS optical X-band rotary-vane attenuator [3], the leakage was reduced more than 120 dB below the incident power. This was achieved by the use of chokes and liberal amounts of microwave absorbing material around the rotary-joints of the attenuator, as shown in figure 78 and figure 86.

Figure 88 shows how microwave absorbing material was used to reduce external leakage from the modified WR15 rotary-vane attenuator.

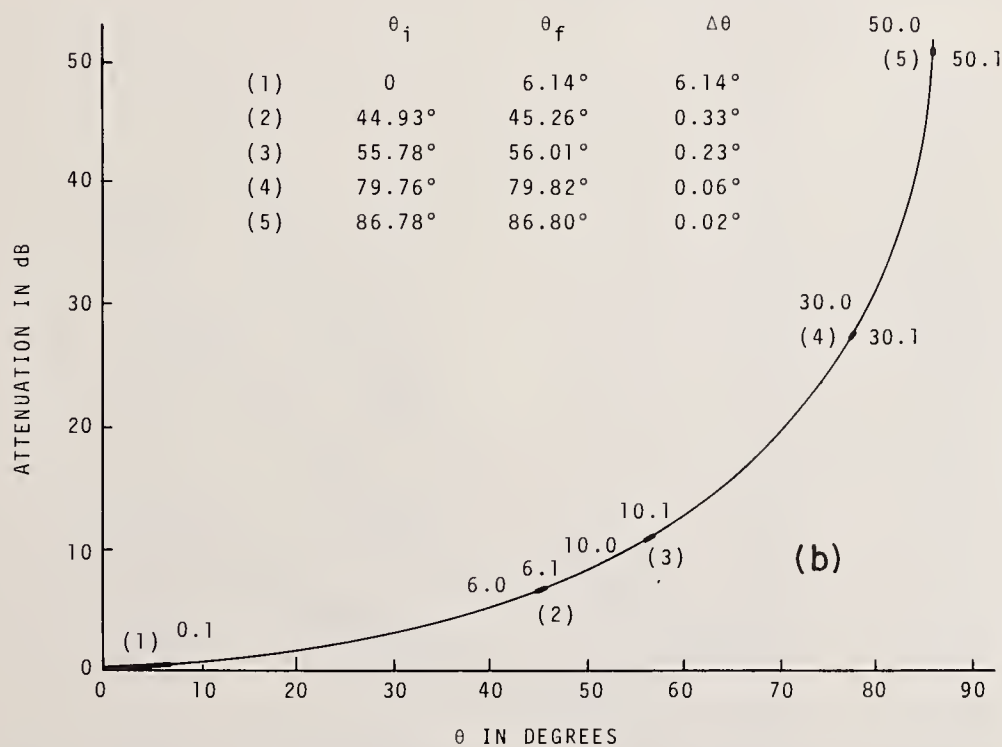
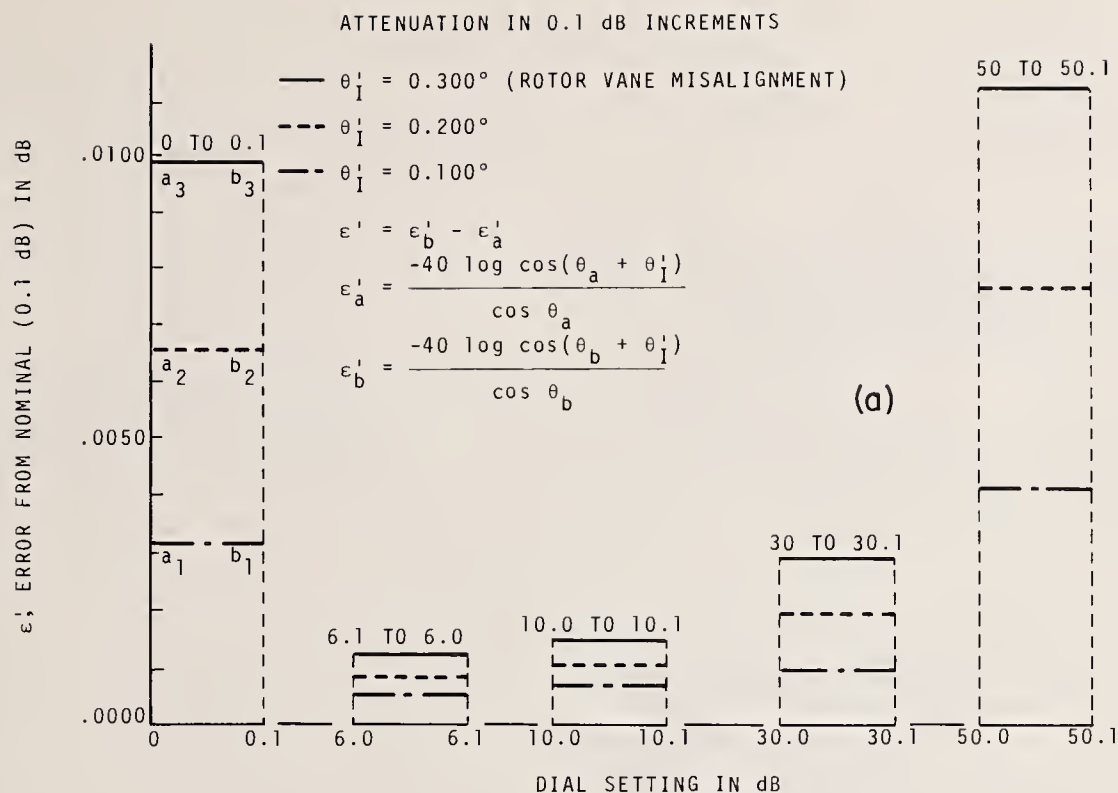


FIGURE 67. (a)  $\epsilon'$  error from nominal (0.1 dB) increments versus dial setting in decibels for rotor misalignment,  $\theta_I'$ , equal to 0.100, 0.200, and 0.300°.

(b) Attenuation in decibels versus  $\theta$  in degrees, and angular limits in degrees for attenuation difference of 0.1 dB.

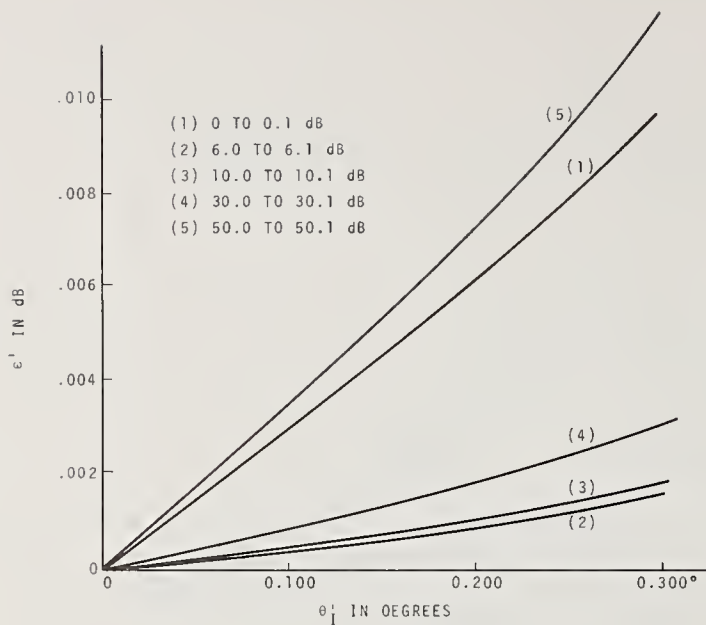


FIGURE 68.  $\epsilon'$  error in decibels versus  $\theta'_1$  from 0 to  $+0.300^\circ$  for 0.1-dB increments as follows: 0 to 0.1 dB, 6.0 to 6.1 dB, 10 to 10.1 dB, 30 to 30.1 dB, and 50 to 50.1 dB.

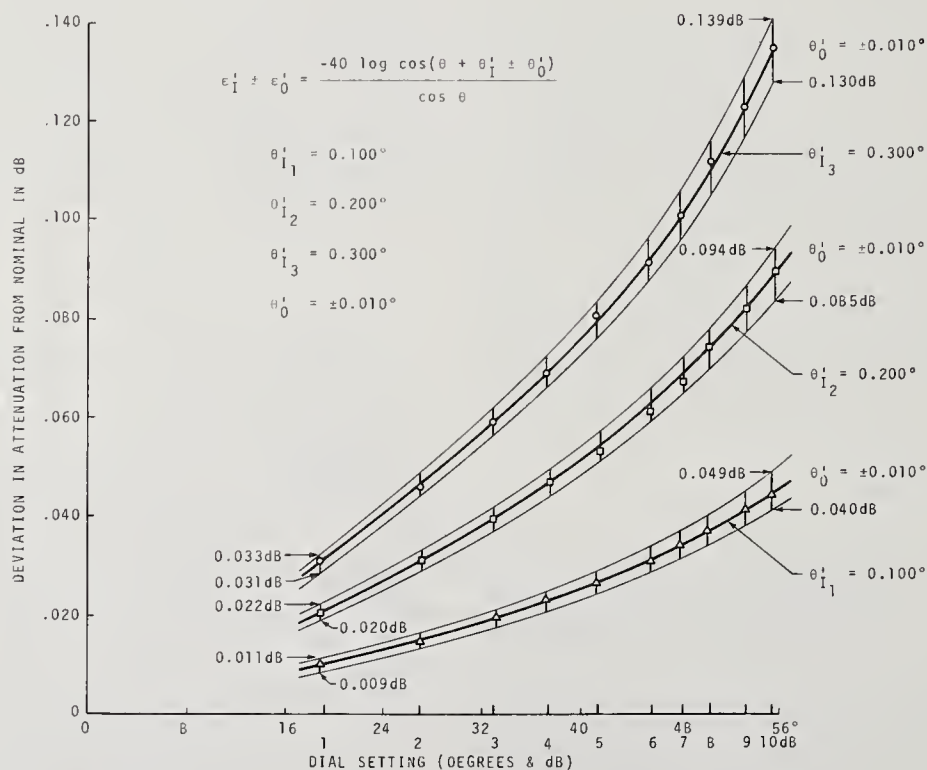


FIGURE 69. Deviations in attenuation from nominal in decibels versus dial setting in degrees and decibels for  $\theta'_1$  equal 0.100, 0.200, and 0.300°, and  $\theta'_0$  equal  $\pm 0.010^\circ$ .



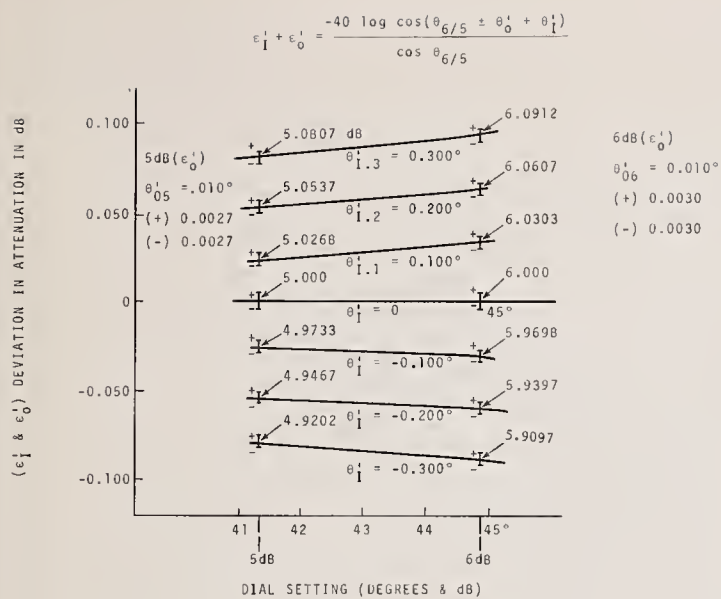


FIGURE 70. Deviations in attenuation from nominal in decibels versus dial setting in degrees and decibels (for 5 to 6 dB) when  $\theta_1'$  equal  $\pm 0.100$ ,  $\pm 0.200$ , and  $\pm 0.300^\circ$ , and  $\theta_0'$  equal  $\pm 0.010^\circ$ .

TABLE 15. Deviations from nominal 1-dB increment of attenuation (dial setting changed from 5 to 6 dB) for  $\theta_0' = \pm 0.010^\circ$  and  $\theta_1' = 0, \pm 0.100, \pm 0.200$ , and  $\pm 0.300^\circ$ .

$\theta_0' = \pm 0.010^\circ$		$\theta_1'$	Actual attenuation increment
6 dB	5 dB	6/5	
+	+	$+ 0.300^\circ$	1.0108
+	-	$+ .300^\circ$	1.0162
-	+	$+ .300^\circ$	1.0048
-	-	$+ .300^\circ$	1.0102
+	+	$+ .200^\circ$	1.0073
+	-	$+ .200^\circ$	1.0127
-	+	$+ .200^\circ$	1.0013
-	-	$+ .200^\circ$	1.0067
+	+	$+ .100^\circ$	1.0039
+	-	$+ .100^\circ$	1.0093
-	+	$+ .100^\circ$	0.9979
-	-	$+ .100^\circ$	1.0033
+	+	.000	1.0003
+	-	.000	1.0057
-	+	.000	0.9943
-	-	.000	.9997
+	+	-.100	.9968
+	-	-.100	1.0022
-	+	-.100	0.9908
-	-	-.100	.9962
+	+	-.200	.9933
+	-	-.200	.9987
-	+	-.200	.9873
-	-	-.200	.9927
+	+	-.300	.9898
+	-	-.300	.9952
-	+	-.300	.9838
-	-	-.300	.9892

TABLE 16. Attenuation difference measurements of a waveguide step attenuator at 10 GHz with initial dial settings of the standard RVA from 0 to 60 dB.

Initial setting of standard in decibels	Measured attenuation difference in decibels with $\theta_1'$ correction	Deviation from average	Deviation from average without $\theta_1'$ correction (all positive)
0	7.6590	+0.0046	0.0139
1	7.6548	+ .0004	.0075
2	7.6536	- .0008	.0052
3	7.6533	- .0011	.0050
4	7.6549	+ .0005	.0065
5	7.6549	+ .0005	.0066
6	7.6558	+ .0014	.0076
7	7.6553	+ .0009	.0073
8	7.6559	+ .0015	.0083
9	7.6562	+ .0018	.0087
10	7.6522	- .0022	.0051
11	7.6530	- .0014	.0062
12	7.6550	+ .0006	.0085
13	7.6552	+ .0008	.0092
14	7.6538	- .0006	.0082
15	7.6540	- .0004	.0087
16	7.6533	- .0011	.0085
17	7.6536	- .0008	.0079
18	7.6548	+ .0004	.0102
19	7.6539	- .0005	.0108
20	7.6545	+ .0001	.0120
22	7.6522	- .0022	.0110
24	7.6540	- .0004	.0144
26	7.6545	+ .0001	.0176
28	7.6549	+ .0005	.0190
30	7.6515	- .0029	.0173
32	7.6546	+ .0002	.0236
34	7.6490	- .0054	.0211
36	7.6586	+ .0042	.0342
38	7.6500	+ .0044	.0356
40	7.6590	+ .0046	.0396
45	7.6539	- .0005	.0412
50	7.6374	- .0170	.0426
55	7.6360	- .0180	.0650
60	7.6352	- .0192	.0854
	7.6544		
	Average	$\theta_1' = -1'18'' = -0.0217^\circ$	

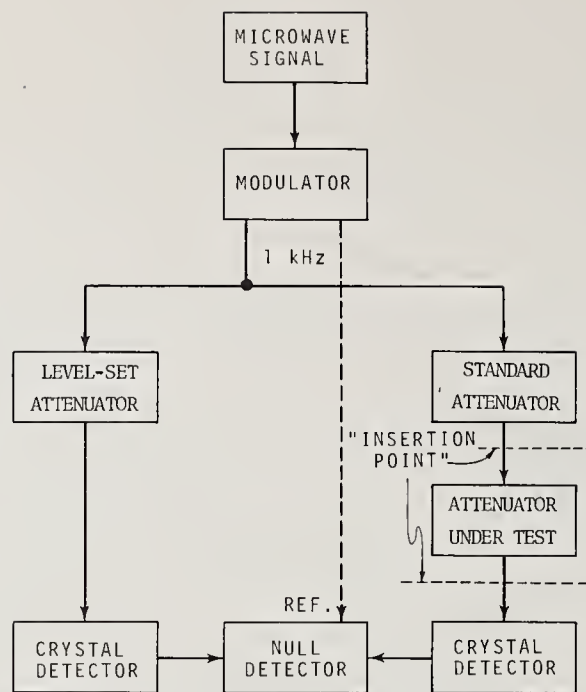


FIGURE 71. Block diagram of microwave attenuation measurement system.

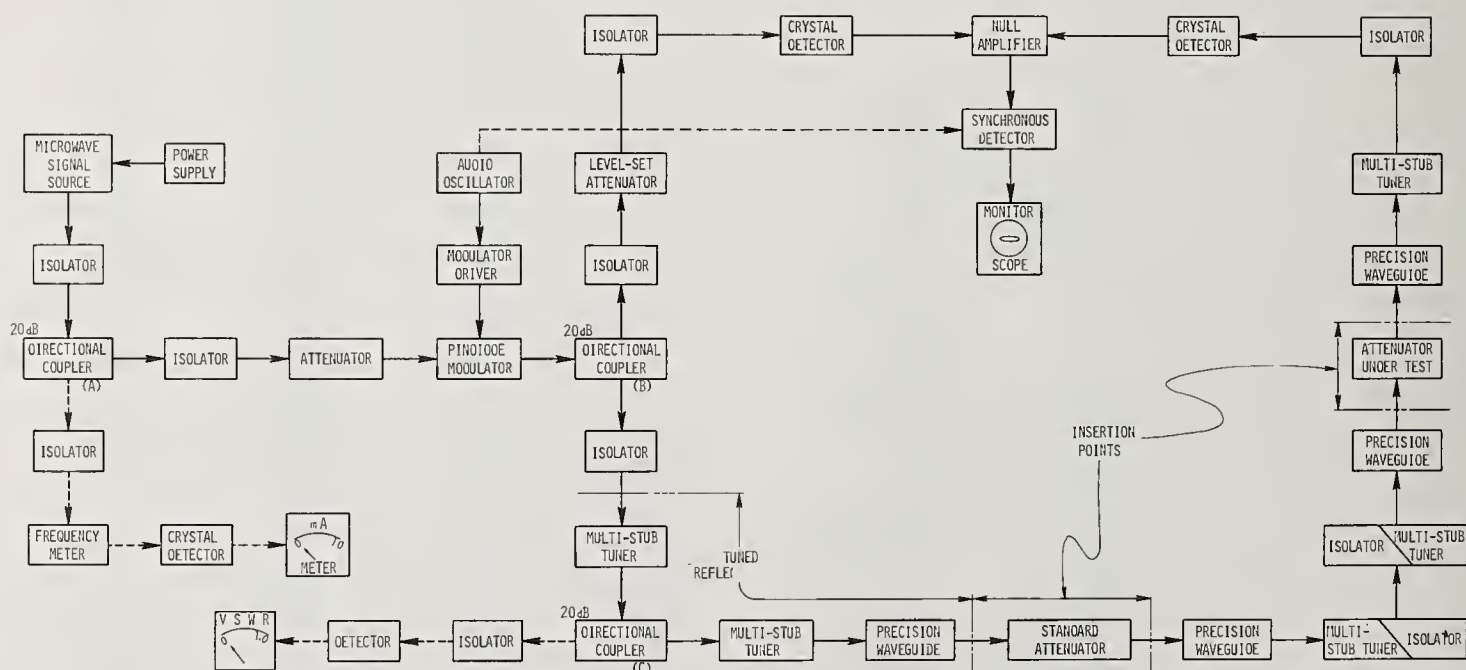


FIGURE 72. Detailed block diagram of microwave attenuation measurement system.

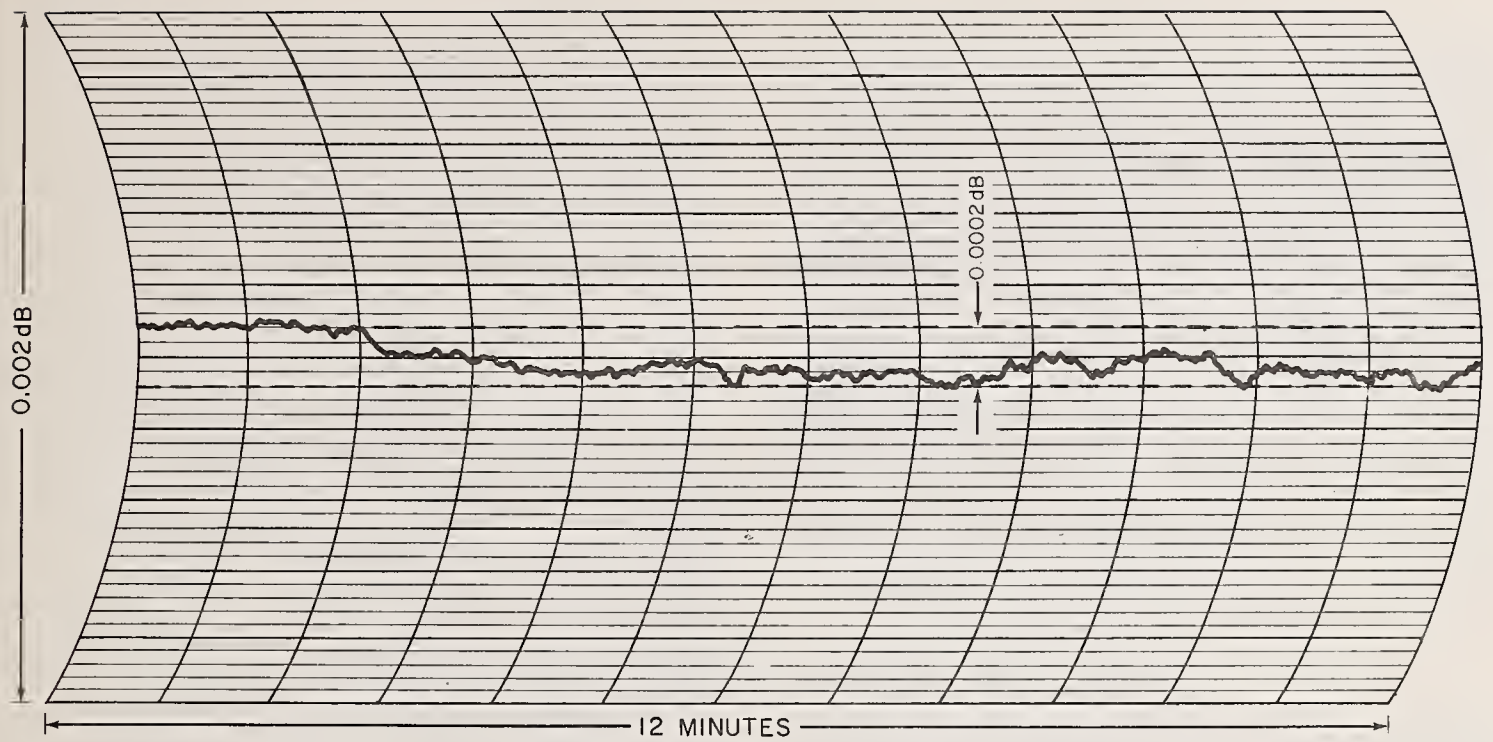


FIGURE 73. A recording showing the system stability at a 30-dB measurement level.

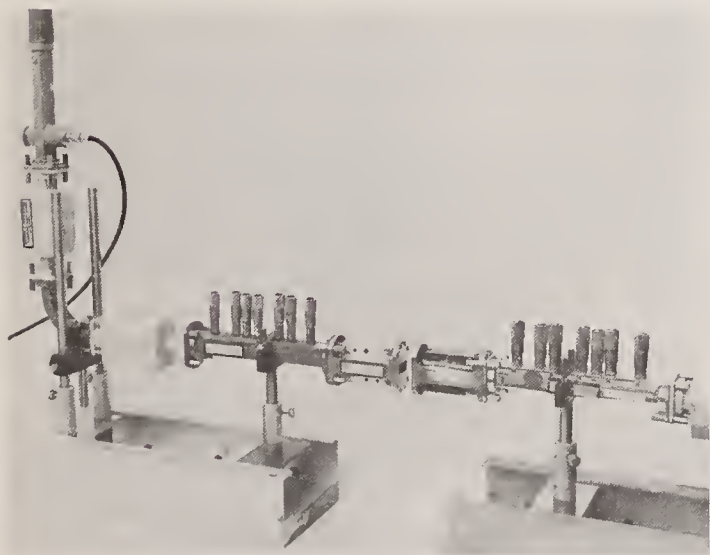


FIGURE 74. Photo of the open rectangular waveguide at the insertion point for devices under test.

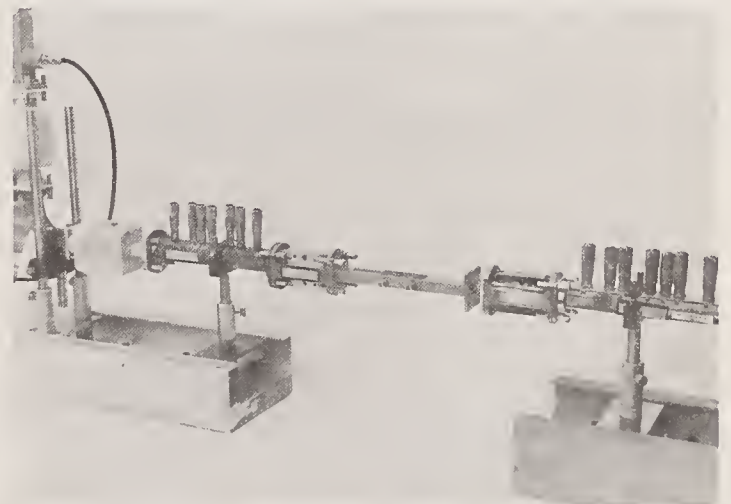


FIGURE 75. Photo of a fixed waveguide attenuator under test being inserted into the rectangular waveguide at the insertion point.



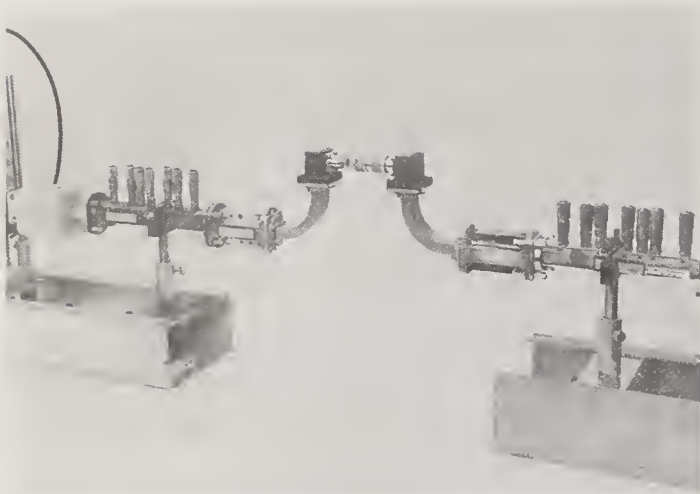


FIGURE 76. *Photo of the rectangular waveguide with adapters to admit coaxial devices at the insertion point.*



FIGURE 77. *Photo of a fixed coaxial attenuator under test being inserted into the line at the coaxial insertion point.*

## 14. Conclusion

The departure of a rotary-vane attenuator from the ideal behavior is caused by the following: insufficient attenuation in the center vane; angular displacement errors when eccentricity is present in the gear drive; the inherent error related to rotor vane alignment; and the Type *A* and Type *B* errors caused by rotationally misaligned stators. Each of the above causes the attenuation to deviate from the nominal (theoretical) value and the deviations will become larger as the rotor angle,  $\theta$ , increases.

A precision rotary-vane attenuator with an optical angular readout attached to its rotor has excellent properties as a primary standard, and provides a readout that eliminates the eccentricity error of angular displacement common to the gear driven readout. The error misalignment of the rotary-vane

attenuator can be improved an order of magnitude by applying correction of vane alignment equal to the average vane-angle error. The Type *A* error is the larger error caused by misaligned stators. To reduce the Type *A* error, the zero or index can be corrected by one-half the angle between the misaligned stators. The deviations from nominal setting then become the Type *B* error provided gear eccentricity is not present. However, if the zero or index is not exactly coincident with the average position of the stators, the Type *A* error can be the predominant factor in the deviations from nominal.

The compact rotary-vane attenuator is a useful device where large dynamic attenuation range is not required or where length of the device is at a premium. The modified law for rotary-vane attenuators gives an accurate result of the attenuation difference that is obtainable with the device.

The precision optical rotary-vane attenuator is a very excellent working standard for attenuation difference employed with the microwave attenuation measurement system (series substitution). The use of the precision optical attenuator with the above RF system yielded the resolution and stability that provided a very accurate international intercomparison of attenuation difference; the spread between the mean values of five different interlaboratory standards was about 0.001 dB.

The work of this paper is not the work of one person but the coordinated effort of many coworkers in the Electromagnetics Division. The author is indebted especially to Eugene Campbell and Ron Hunter for their contributions over a period of several years in fabrication of waveguide components, and instrumentation design used in the measurement systems; Edward Holland for suggestions in design and precise fabrication of the optical rotary-vane attenuator standard; C. C. Cook and F. L. Warner for the thorough review of the paper, helpful suggestions and corrections; and Janet R. Jasa for the excellent job of typing.

## 15. References

- [1] Southworth, G. C., *Principles and Applications of Waveguide Transmission* (Van Nostrand, New York, 1950), p. 374.
- [2] Hand, B. P., Broadband rotary waveguide attenuator, *Electronics* **27**, 184-185 (Jan. 1954).
- [3] Little, W. E., Larson, W., and Kinder, B. J. A rotary-vane attenuator with an optical readout, *J. Res. Nat. Bur. Stand. (U.S.)*, **75C** (Eng. and Instr.), No. 1, 1-67 (Jan.-Mar. 1971).
- [4] Warner, F. L., Watton, D. O., and Herman, P., A very accurate X-band rotary attenuator with an absolute digital angular measuring system, *IEEE, Trans. on Instr. and Meas.* **IM-21**, No. 4 (Nov. 1972).
- [5] Mariner, P. F., An absolute microwave attenuator, *Proc. IEEE (London)*, 415-419 (Sept. 1962).
- [6] Larson, Wilbur, Gearing errors as related to alignment techniques of the rotary-vane attenuator, *IEEE Trans. Instr. and Meas.* **IM-14**, No. 3 (Sept. 1965).

- [7] Larson, Wilbur, Analysis of rotationally misaligned stators in the rotary-vane attenuator, IEEE Trans. Instr. and Meas. **IM-16**, No. 3 (Sept. 1967).
- [8] James, Allan V., A high-accuracy microwave attenuation standard for use in primary calibration laboratories, IRE Trans. on Instrumentation **I-11**, 285–290 (Dec. 1962).
- [9] Otschi, Tom Y., and Stelzried, Charles T., A precision compact rotary-vane attenuator, IEEE Trans. on Microwave Theory and Tech. **MTT-19**, No. 11, 843–854 (Nov. 1971).
- [10] Foote, W. J., and Hunter, R. D., Improved gearing for rotary-vane attenuators, Rev. Sci. Instr. **43**, 1042–1043 (July 1972).
- [11] Beatty, R. W., Microwave attenuation measurements and standards, Nat. Bur. Stand. (U.S.), Monogr. 97, 49 pages (Apr. 1967).
- [12] Engen, G. F., and Beatty, R. W., Microwave attenuation measurements with accuracies from 0.0001 to 0.06 decibel over a range of 0.01 to 50 decibels, J. Res. Nat. Bur. Stand. (U.S.), **64C** (Eng. and Instr.), No. 3, 139–145 (Apr.–June 1960).
- [13] Schafer, G. E., and Bowman, R. R., A modulated subcarrier technique of measuring microwave attenuation, Proc. IEE (London) **109**, Pt. B, Suppl. No. 23, 783–786 (May 1962).
- [14] Nemoto, T., Beatty, R. W., and Fentress, G. H., A two channel off-null technique for measuring small changes in attenuation, IEEE Trans. Microwave Theory and Tech. (correspondence), **MTT-17**, 396–397 (July 1969).
- [15] Grantham, R. E., and Freeman, J. J., A standard of attenuation for microwave measurements, Trans. AIEE **67**, 329–335 (June 1948).
- [16] Larson, R. E., Microwave measurements in the NBS electronic calibration center, Proc. IEE (London), **109**, Pt. B, Suppl. 23, 644–650 (May 1962).
- [17] Larson, W., Table of attenuation error as a function of vane-angle error for rotary-vane attenuators, Nat. Bur. Stand. (U.S.), Tech. Note 177, 154 pages (May 1963).
- [18] Larson, W., Analysis of rotation errors of a waveguide rotary-vane attenuator, IRE International Convention Record, Pt. 3, pp. 213–219 (1962).
- [19] Larson, W., Table of attenuation as a function of vane angle for rotary-vane attenuators ( $A = -40 \log_{10} \cos \theta$ ), Nat. Bur. Stand. (U.S.), Tech. Note 229, 186 pages (Jan. 1965).
- [20] Nielsen, T. C., Angular errors in gears, Product Engineering, pp. 56–61 (Aug. 15, 1960).
- [21] Michales, G. W., Gear position error control (American Society of Mechanical Engineers, New York, N.Y.), Paper No. 59A-21 (Dec. 1959).
- [22] Larson, W., and Campbell, Eugene, Microwave attenuation measurement system (series substitution), Nat. Bur. Stand. (U.S.), Tech. Note. 647, 24 pages (Feb. 1974).
- [23] Anson, W. J., A guide to the use of the modified reflectometer technique of VSWR measurement, J. Res. NBS, **65C**, No. 4, 217–223 (Oct.–Dec. 1961).
- [24] Beatty, R. W., Mismatch errors in the measurement of ultrahigh-frequency and microwave variable attenuators, J. Res. Nat. Bur. Stand. (U.S.), **52**, No. 1, 7–9 (Jan. 1954) RP 2465.
- [25] Rahman, M. H., and Gunn, M. W., Waveguide reflections from rotary-vane attenuator (correspondence), IEEE Trans. on Microwave Theory and Tech., pp. 402–403 (July 1969).
- [26] Holm, J. D., Johnson, D. L., and Champlin, K. S., Reflections from rotary-vane precision attenuator, (correspondence) IEEE Trans. on Microwave Theory and Tech., pp. 123–124 (Feb. 1967).

## 16. Appendix A. Definitions and Terms

$TCE$  = Total composite error.

$\tau'$  = Total angular displacement ( $\beta' + \gamma'$ ) in degrees.

$\delta$  = Angle of drive gear rotation in radians.

$\delta'$  = Angle of drive gear rotation in degrees.

$\theta$  = Angular rotation of center section vane (rotor) relative to the stationary end section vane stator in degrees.

$\theta'$  = Misalignment angle of center vane (difference between the indicated vane angle and the true vane angle) in degrees.

$\epsilon$  = Error in attenuation caused by incorrect vane rotation in decibels.

$\theta'_e$  = Estimated average vane-angle error in degrees.

$\theta'_{\beta'}$  = Angular displacement of the vane caused by backlash error in degrees.

$\theta'_{\gamma'}$  = Angular displacement of the vane caused by indexing error in degrees.

$\theta'_{\tau'}$  = Angular displacement of the vane caused by total angular error in degrees.

$R$  = Pitch radius in inches.

$D$  = Pitch diameter in inches.

$\phi$  = Basic pressure angle in degrees.

$\alpha$  = Angular difference between the zero point of the drive gear eccentricity and the zero point of the scale on the dial in degrees.

$\epsilon'_{\gamma'}$  = Error in attenuation caused by the indexing error in decibels.

$\epsilon_a$  = The error, in decibels, for Type A misalignment.

$\epsilon_b$  = The error, in decibels, for Type B misalignment.

$\epsilon'$  = The error from nominal in decibels,  $\epsilon'_b$  minus  $\epsilon'_a$

$\epsilon_t$  = Transmission error due to insufficient attenuation in the rotor.

$\phi_t$  = The phase shift of the transmitted signal as a function of  $\theta$ .

$A'_i$  = Initial setting of an attenuation difference measurement of a rotary-vane attenuator.

$A'_f$  = Final setting of an attenuation difference measurement of a rotary-vane attenuator.

$A_i$  = Theoretical value of attenuation at the initial setting.

$A_f$  = Theoretical value of attenuation at the final setting.

$\epsilon'_{i0}$  = Error due to operator at initial setting.

$\epsilon_{i0}$  = Inherent error at the initial setting.

$\epsilon_{f0}$  = Error due to operator at final setting.

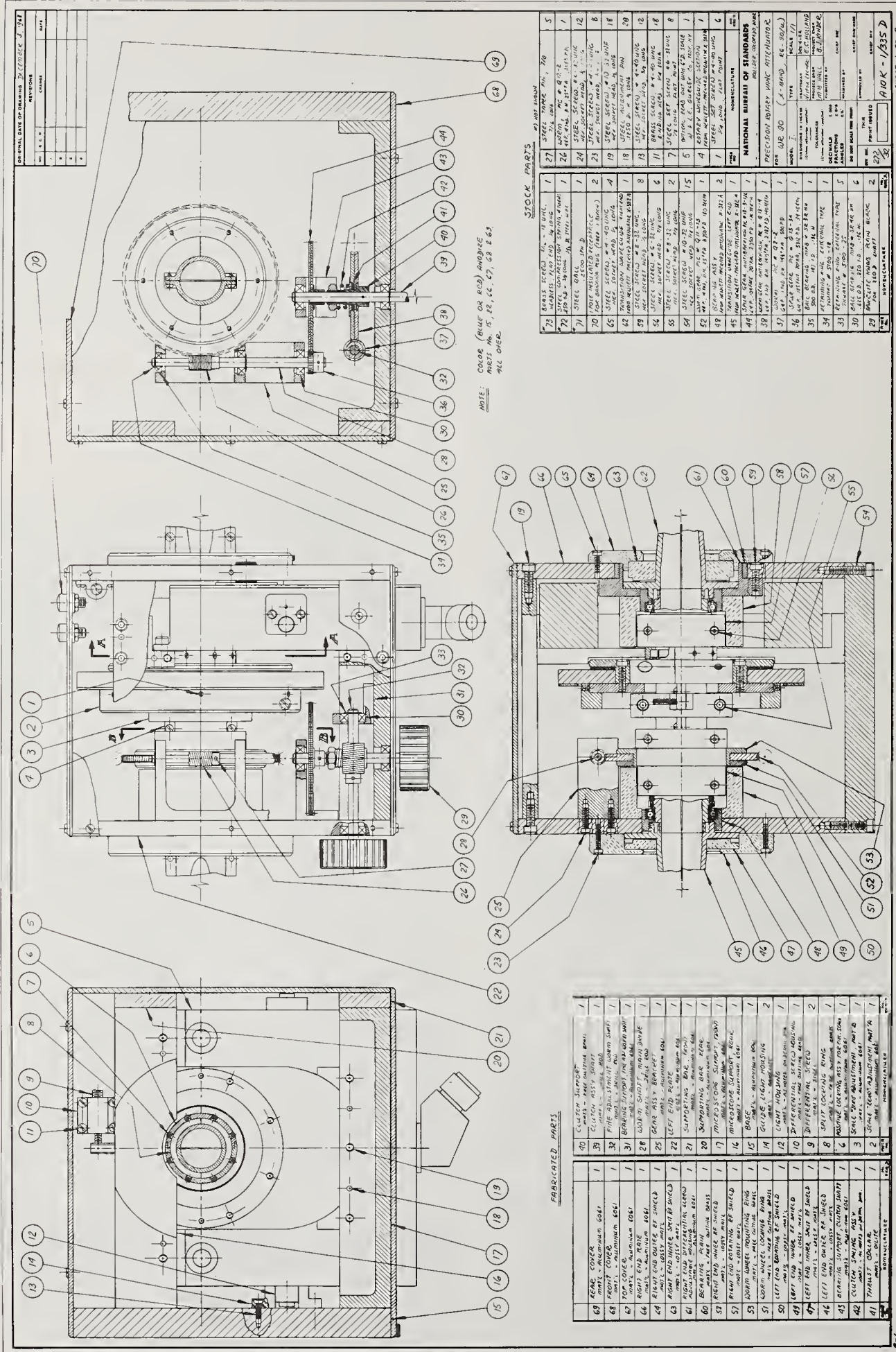
$\epsilon_{f1}$  = Inherent error at the final setting.

$\epsilon_v$  = Mismatch error in decibels for a variable attenuator.

$\epsilon_f$  = Mismatch error in decibels for a fixed attenuator.

## Appendix B. Machine Drawings for Optical Rotary-Vane Attenuators

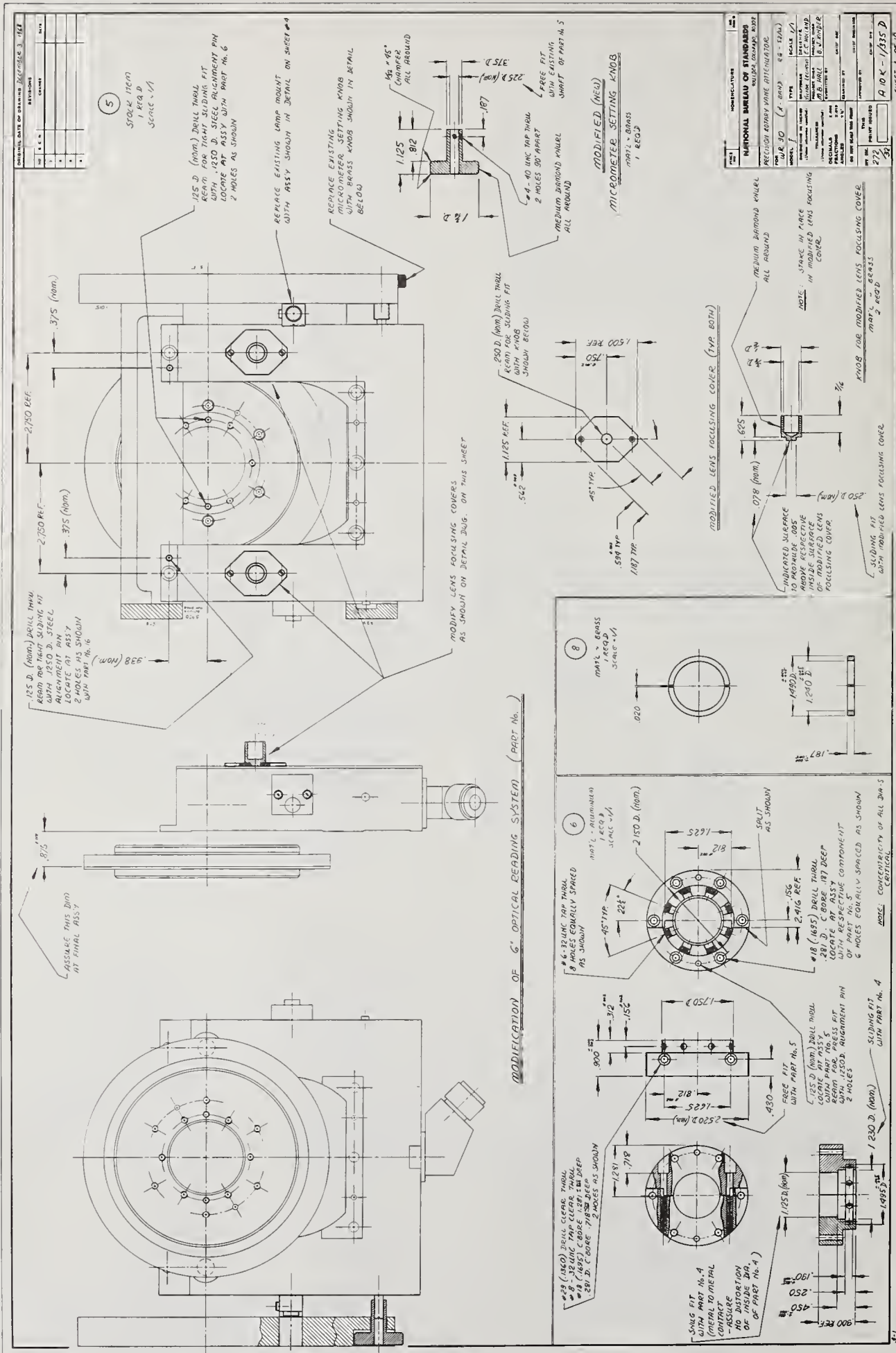




FIGURES 78-87. Machine drawings for optical rotary-vane attenuator.





















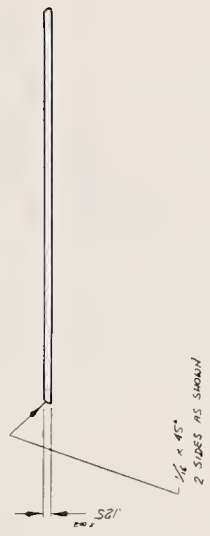
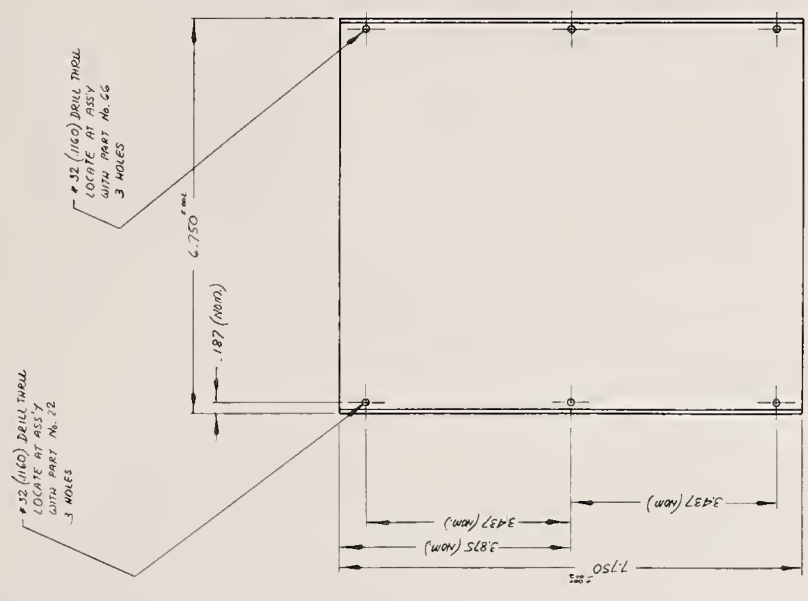






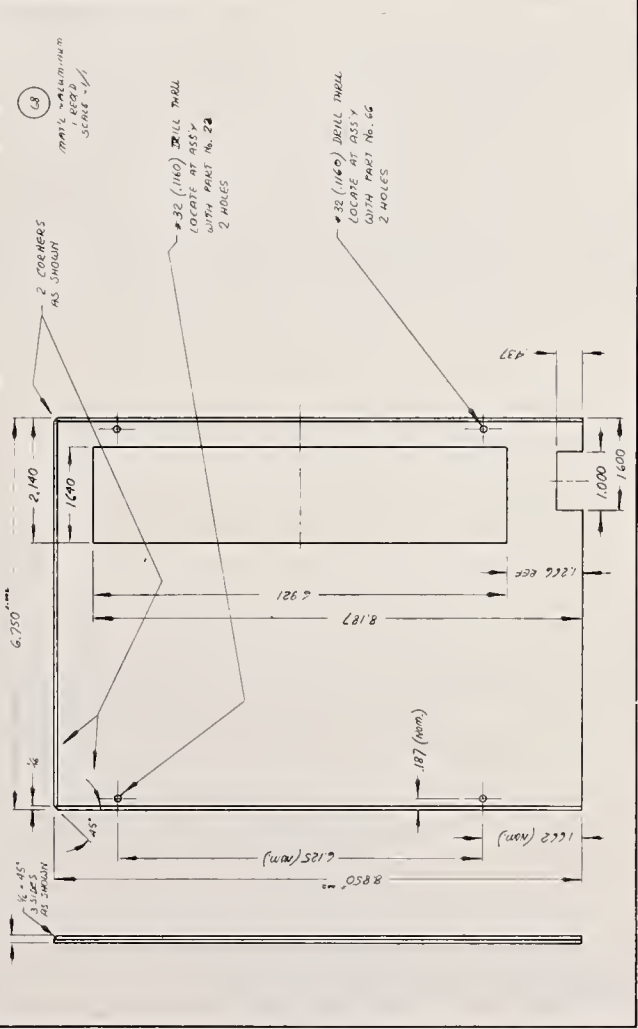
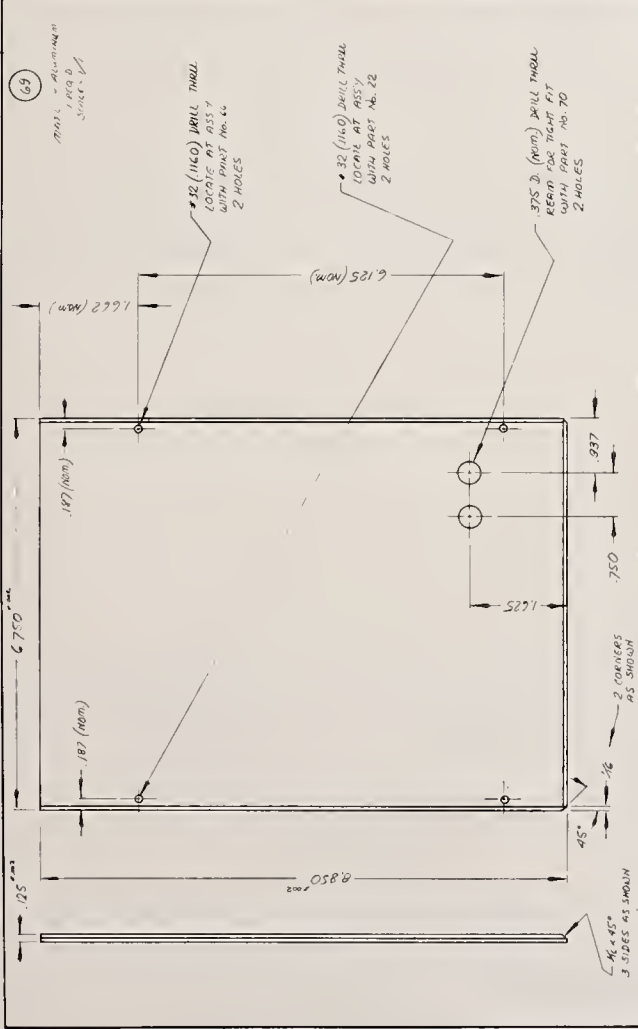
GENERAL DATA OF DRAWING			
DECEMBER 3, 1942			
NO.	1	2	3
DATE			
REVISION			
BY			
CHECKED			
APPROVED			

67  
MATERIAL - ALUMINUM  
1 REQ'D  
SCALE - 1/4"



NATIONAL BUREAU OF STANDARDS			
PRECISION ROTARY VANE ATTENUATOR			
NO.	118 80	118 80	118 80
DATE			
REVISION			
BY			
CHECKED			
APPROVED			

SHEET 10 OF 10





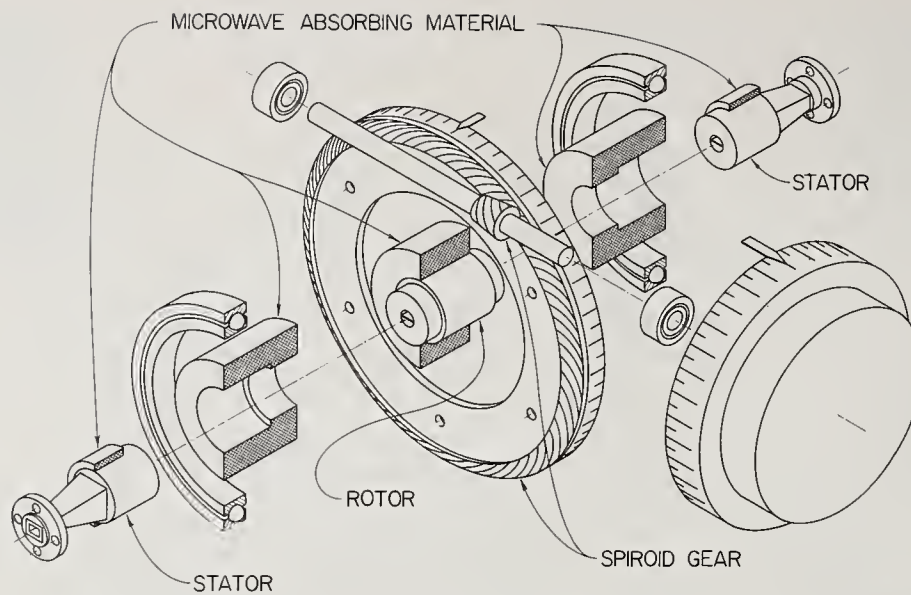


FIGURE 88. Exploded view of a rotary-vane attenuator utilizing a Spiroid gear set in WR15 waveguide.

U.S. DEPT. OF COMM. BIBLIOGRAPHIC DATA SHEET	1. PUBLICATION OR REPORT NO.  NBS-MN 144	2. Gov't Accession No.	3. Recipient's Accession No.
4. TITLE AND SUBTITLE  The Rotary-Vane Attenuator as an Interlaboratory Standard		5. Publication Date  October 1975	
		6. Performing Organization Code	
7. AUTHOR(S)  Wilbur Larson		8. Performing Organ. Report No.	
9. PERFORMING ORGANIZATION NAME AND ADDRESS  NATIONAL BUREAU OF STANDARDS DEPARTMENT OF COMMERCE WASHINGTON, D.C. 20234		10. Project/Task/Work Unit No.  2764460	
		11. Contract/Grant No.	
12. Sponsoring Organization Name and Complete Address (Street, City, State, ZIP)  Same as Item 9.		13. Type of Report & Period Covered  Final	
		14. Sponsoring Agency Code	
15. SUPPLEMENTARY NOTES  Library of Congress Catalogue Card Number: 75-619099			
16. ABSTRACT (A 200-word or less factual summary of most significant information. If document includes a significant bibliography or literature survey, mention it here.) This paper presents a comprehensive report on the measurement and the use of the rotary-vane attenuator as an interlaboratory standard.  Methods of attenuation measurement developed at NBS are used to supply data for the evaluation of the deviations from theoretical $\cos^2$ law due to rotor misalignment, gear eccentricity, resettability, resolution, and insufficient maximum attenuation.  A precision rotary-vane attenuator with an optical readout capable of 1 second of arc angular resolution has an effective attenuation resolution of 0.00005 dB at a 3-dB dial setting, and 0.0005 dB at a 30-dB dial setting. This type of precision attenuator is an effective standard for use in the dual detection microwave bridge measurement system.			
17. KEY WORDS (six to twelve entries; alphabetical order; capitalize only the first letter of the first key word unless a proper name; separated by semicolons) Attenuation; interlaboratory standard; measurement; rotary-vane attenuator.			
18. AVAILABILITY <input checked="" type="checkbox"/> Unlimited  <input type="checkbox"/> For Official Distribution. Do Not Release to NTIS  <input checked="" type="checkbox"/> Order From Sup. of Doc., U.S. Government Printing Office Washington, D.C. 20402, SD Cat. No. C13.44:144  <input type="checkbox"/> Order From National Technical Information Service (NTIS) Springfield, Virginia 22151		19. SECURITY CLASS (THIS REPORT)  UNCLASSIFIED	21. NO. OF PAGES  70
		20. SECURITY CLASS (THIS PAGE)  UNCLASSIFIED	22. Price  \$5.05













